Synthesis and Characterization of Wholly Aromatic, Water-Soluble Polyimides and Poly(amic acid)s Towards Fire Suppression Foams

Benjamin Joseph Stovall

Thesis submitted to the faculty of the Virginia Polytechnic Institute and State University in partial fulfillment of the requirements for the degree of

Master of Science

In

Chemistry

Timothy E. Long (Chair)

Paul A. Deck

Robert B. Moore

April 20, 2021

Blacksburg, Virginia

Keywords: polyimide, poly(amic acid), AFFF, fire suppression, phosphonium, siloxane, rheology, scaling, aqueous foam, high-performance

Synthesis and Characterization of Wholly Aromatic, Water-Soluble Polyimides and Poly(amic acid)s Towards Fire Suppression Foams

Benjamin Joseph Stovall

Abstract

Polyimides epitomize one of the most versatile high-performance engineering polymers. Polyimides are inherently mechanically robust, chemically inert, and thermooxidatively stable to 400+ °C depending on their chemical structure, enabling their function in numerous aerospace, electronic, medical, and flame-retardant applications. Polyimides can be highly modular even within synthetic limitations, which promotes and sustains innovative research. One recent interest concerns the innovation of fire suppression foams. Aqueous film-forming foams (AFFFs) are regularly sought when engaging liquid fuel (gasoline, jet fuel) fires. AFFFs utilize perfluorinated compounds (PFCs) like perfluorooctanesulfonic acid (PFOS) and perfluorooctanoic acid (PFOA), which exhibit toxicity, bioaccumulation, and persistence in the environment resulting in the presence of fluorosurfactant chemicals in environments either through direct or secondary exposure via chemical migration. Recently, the USEPA has even detected PFAS in drinking water at hundreds of military training facilities and civilian airports. While fluorinated compounds provide desirable thermooxidative stability and excellent fire retardancy, the environmental impact imposed by these chemicals strongly encourages research that targets the complete removal of PFCs in conventional formulations. This thesis focuses on the fundamental development of water-soluble sulfonated polyimide (sPI) and poly(amic acid) (sPAA) systems for next-generation polymer-based fire suppression foams. The use

of sulfonated monomers and poly(amic acid) salt formation enables tunable structures and water solubilities. The polymers maintain competitive thermal stabilities to conventional polyimides and, when combined with readily available, non-toxic surfactants (SDS), produce stable foams. The MIL-F-24385F performance requirement evaluates foam quality/stability, drainage time, and burnback resistance to access viability and provides comparison to other systems; preliminary testing shows that sPI/sPAA formulations perform well. Solution rheology offers insights into fundamental scaling relationships of specific viscosity vs. concentration in both salt and salt-free solution that are important to future foam development. Additionally, the structural nature of the sPIs/ sPAAs allows for their modification with phosphonium moieties or siloxanes, which are slated to have positive effects on performance. Overall, these sPIs and sPAAs provide a promising platform for the future direction of fire suppression foams.

Synthesis and Characterization of Wholly Aromatic, Water-Soluble Polyimides and Poly(amic acid)s Towards Fire Suppression Foams

Benjamin Joseph Stovall

General Audience Abstract

High-performance polymers are used in the most demanding of engineering applications. Polyimides represent one of the most versatile high-performance polymers. Polyimides are mechanically strong, chemically inert, and resistant to extreme temperatures depending on their chemical structure, allowing their use in numerous aerospace, electronic, medical, and flame-retardant applications. Polyimides are synthetically versatile, which enables the discovery of new uses after decades of research. One new targeted application is fire suppression foams. Aqueous film-forming foams (AFFFs) are the standard when battling liquid fuel (gasoline, jet fuel) fires. AFFFs contain perfluorinated compounds (PFCs), which are toxic and persist in the environment; they migrate easily to affect indirectly exposed ecosystems. Recently, the USEPA has even detected PFAS in drinking water at hundreds of military training facilities and civilian airports. While AFFFs with PFCs are highly effective, replacement materials are needed. This thesis focuses on the fundamental development of water-soluble sulfonated polyimide (sPI) and poly(amic acid) (sPAA) systems for fire suppression foams. The polymers remain thermally stable, and when combined with readily available surfactants (SDS), produce stable foams. Preliminary fire testing shows that sPI/sPAA formulations perform well against military specifications. Solution rheology (study of flow) explores the solution behavior of sPI, which offers insights into fundamental concentration-viscosity relationships that are important to future

foam development. Additionally, the structural nature of the sPIs/ sPAAs allows for their modification with phosphonium groups or siloxanes, which changes their characteristics. Overall, these sPIs and sPAAs are initially promising for the future direction of fire suppression foams.

Acknowledgments

There isn't enough space to begin thanking everyone that helped me through this stage of my graduate career, but I will give it my best attempt. First, I would like to thank Dr. Timothy Long for agreeing to be my advisor and graciously taking me into his group when I needed support the most. His guidance and encouragement were invaluable, and I am grateful for our relationship and the skills that I have learned. I am also grateful to my committee members Dr. Paul Deck and Dr. Robert Moore, for their continued support, insight, and advice. Additionally, I would like to thank Dr. Alan Esker, Dr. John Morris, and Joli Huynh for their guidance, support, and frequent chats.

A researcher is often only as successful as the team to which they belong, and the Long Group is stellar. Not only have I developed rewarding academic relationships with my fellow group members, but also some great friendships. I thank each and every one of them. I'd especially like to thank Clay Arrington, whom I collaborated closely with on the SERDP project, and Josh Wolfgang and Tyler White, who stuck it out with me at Virginia Tech. Furthermore, I'd like to thank all the amazing friends that I have made at Virginia Tech, at RPI and from home- Ryan Archer, Sam Scannelli, Rachael Bianculli, Sarah Swilley-Sanchez (and Mike), Brady Hall (and Katy), Dan Cairnie, Brittney Bonnett, Ophelia Wadsworth, Tiffany Thompson, Ryan Carrazone, Kearsley Dillon, Sarah Blosch, Joel Serrano, Ke Cao, Dong Guo, Xiaozhou Yang, Assad Khan, Christine Desplat, Anju Malhotra, Erika Nicholas, Jason Roman, Devin Glenn, Michael Ferrucci, Sean Gallagher, Kyle Rivers, Jordan Riesel and McLane Tyoe. The list goes on…

All of my friends in the local music community also deserve equal acknowledgment as my musical life has provided me with stability and release- The Woogemen (Jon Wooge,

Andrew Cook, Tim Parker, George Brooks, and Bruce Coluccio), Arthur Krieck, Dixon Smiley, Jeff Ritchie, Daniel MacPherson, Matt McHugh, Dan Weber, Ben Slaughter, Cristen Mitchell, Dwight Bigler, Annie Pearce, Mary-Denson Moore, Brenda van Gelder, Jason Crafton, Scott Malbon, Dave McKee, Lou Madsen, Paul Deck (again), Brian Peters, Justin Craig, Nick Romantini, the men of the Adhoctet, SME, the Sauerkraut Band, the Blacksburg Community Band, the Blacksburg Community Strings, the Blacksburg United Methodist Church, and the New River Blues Society.

A significant acknowledgment goes out to Mrs. Donna Fulmer, my seventh-grade science teacher and one of my mentors all throughout high school. Without her influence and encouragement, I would not have chosen this path. I remember quite clearly, however, that one day she briefly stated that I needed to go into science, and it was that one statement that just flipped a switch. The rest was history (well…it wasn't… because I decided not to go into history).

Last but not least, I would like to thank my incredible family. My parents have been my rock, and I absolutely could not have done a single thing without their unwavering support, endless love, thousands of phone calls, regular visits, and many beers. I cannot begin to express how much I owe to them for making me who I am today. My partner, Katherine, deserves endless praise for dealing with me as I navigate graduate school. Without her love, patience, and support, these last few months would have been much harder. I can't wait to see what the future holds for us, Langley and Sass, and I look forward to spending endless hours in random antique stores together.

Table of Contents

Chapter 1. Recent advances in halogen-free, additive-free polymers with inherent flame-retardant properties

Benjamin J. Stovall and Timothy E. Long

Department of Chemistry, Macromolecules Innovation Institute (MII),
Virginia Tech, Blacksburg, VA, 24061

1.1. Abstract

Modern society relies heavily on the production of commercial and industrial plastics. Fire risks threaten commercial operations where plastics are employed. Even though there are significant monitoring and reduction of commonly used halogenated flame retardants, their worldwide usage still poses environmental hazards. To address these issues, many non-halogenated flame-retardant additives have been developed as replacements to these plastics but result in reduced composite homogeneity and mechanical strength. This review introduces the use of reactive flame retardants and discusses the effect of polymer structure on flame retardant properties. The synthesis and characterization of polymer systems (polyurethanes, polyamides, polyimides, polyesters, and epoxy resins) are discussed concerning their synthesis, structure, and characterization via TGA, cone calorimetry, limiting oxygen index, the UL-94 test, and more. These polymer systems herein represent a broad chemical space with which new systems may be developed with increasing modularity, utilizing heteroatom synergy and combinations of gas- and condensed-phase mechanisms of flame retardance.

1.2. Introduction

Polymers are responsible for the growth and development of many electronics, transportation, and aerospace technologies. In each of these applications, the underlying properties (e.g., thermal stability and mechanical properties) dictate the function of these materials. Certain applications,

such as aerospace, require increasingly lightweight, strong, and thermally stable materials to replace cumbersome metals and ceramics. However, a significant challenge still lies in developing polymers for use in these high temperatures and oxidative environments.[1] Many commodity polymers are inherently more flammable and lack the thermomechanical properties to support these high-performance applications, such as in aerospace and transportation. At high temperatures, these commodity polymers will ignite, thereby propagating many fire incidents involving consumers. Every year, fires cause billions of dollars in damage and significant loss of life. Thus, the need for polymer flame-retardant technology is at the forefront of materials advancement.

1.2.1. Characteristics of flame retardant materials

Traditional flame proofing commonly used in construction, transportation, and aerospace applications includes ceramics, mineral coatings, or fiber composites. While many of these approaches are still employed today, they are not applicable to technological development due to processing challenges or poor material integrity. With the evolution of electronics in the industrial and consumer realms, the need for lightweight materials that can be molded and processed into small parts is growing. Although engineering allows many commodity polymers to be used in this capacity, they are more flammable and lack the thermo-mechanical properties to support high-performance applications.[2] In the middle of the last century, the synthesis of highly aromatic, stiff-chain polymers (e.g., polyimides, polybenzimidazoles, polybenzoxazoles, and polybenzthiazoles) developed into a new division of engineering plastics (**Figure 1**). The chain stiffness, aromaticity, and heteroatom content of these engineering polymers afford high thermal degradation temperatures, low burn rates, and the formation of char,[2] thereby reducing the amount of

flammable volatiles that are released. The above-mentioned metrics for gauging the efficacy of flame-retardant polymers (burn rate, formation of char, and degradation temperature) guide the development of polymers with these designated. Current research is focused on investigating other polymer systems to meet the flame retardant demands of various high-performance applications.

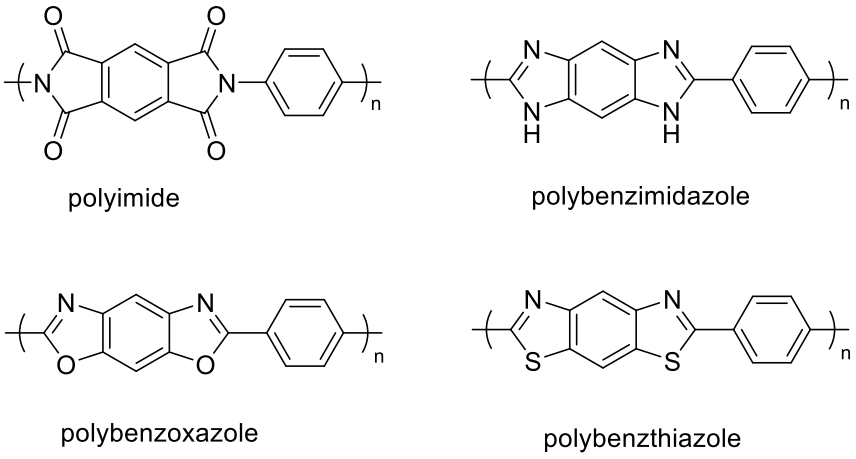

Figure 1. Structures of general classes of classic flame retardant/resistant polymers

1.2.2. Combustion and Flame Retardance

Organic polymers have a propensity to be fire epicenters due to structural degradation at high temperatures.[3-4] Thermal decomposition of polymers results in combustible volatiles in the form of small molecular species or radicals. With enough heating to promote further degradation or ignition or with an ignition event, the combustion of the volatile species will occur. Combustion of the volatiles proceeds in the gas phase (in the flame), while the bulk polymer is in the condensed phase. Combustion continues at the phase boundary—where the condensed and gas phases meet—as a self-sustaining reaction if there is sustained heating. Volatile products continue to evolve into the gas phase, while polymer degradation proceeds in the condensed phase, generally resulting in solid char (**Figure 2**).

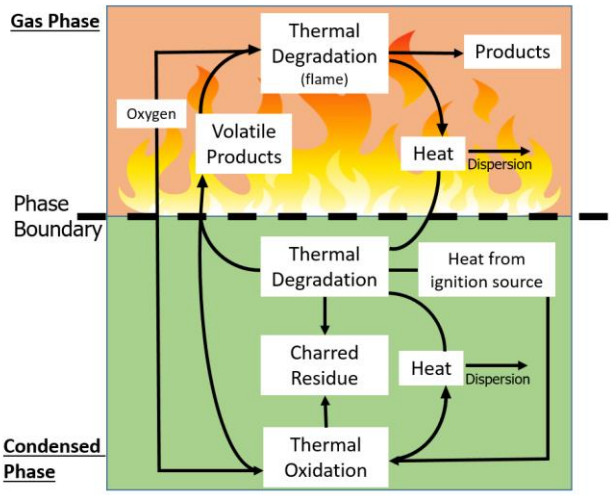

Figure 2. General schematic of polymer combustion.[3-4]

The focus of designing flame retardant polymer systems is to limit the release of volatile compounds, thereby quenching the combustion reactions and reducing heat at the phase boundary. Designing these materials takes involves several strategies: 1) promoting the formation of char, 2) scavenging radicals, and 3) diluting flammable volatiles. By including small molecule additives or modifying the polymer structure, one can enhance the flame retardancy of polymer systems.

1.2.2. Fire Testing Methods

Standard testing procedures, such as the UL94, are used to quantifying polymer flammability and determine the effectiveness of flame-retardant systems. In the UL94 test, a flame is applied to a polymer sample in the horizontal or vertical direction and subsequently removed after 30 seconds. UL94 assesses flammability with a series of ratings based on material response in terms of burning rate, specimen dripping, and propensity to transfer flame.[5] A schematic of the various tests and ratings is illustrated in **Figure 3a**.

The limiting oxygen index (LOI) quantifies the minimum oxygen concentration (in vol% oxygen/nitrogen) that supports the stable combustion of a polymer sample. Polymers with a high LOI value are less flammable and more stable in oxidative environments; a value > 21% is considered self-extinguishing. ASTM standards dictate testing parameters, and a typical experimental setup includes a vertical glass cylinder secured in a ring stand. A polymer strip is suspended inside of the cylinder that has a gas inlet at the bottom. A small flame ignites the top portion of the polymer sample, and the enflamed polymer extinguishes as the concentration of oxygen in the mixed gas stream is lowered below a critical level.[5] **Figure 3b** shows a representation of the LOI test.

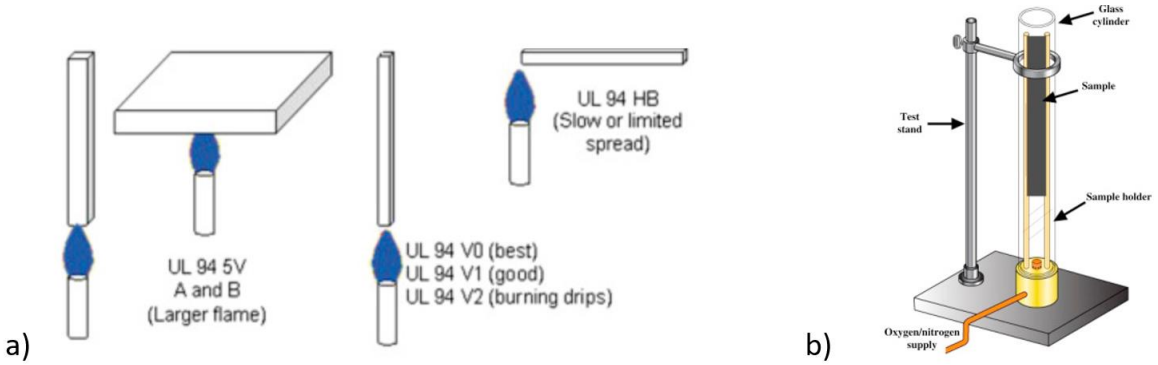

Figure 3. Schematic drawings of a) UL-94 rating test and b) limiting oxygen index (LOI) test.[5] Adapted from Shrivastava, A. 3 - Plastic Properties and Testing. In *Introduction to Plastics Engineering*, Shrivastava, A., Ed. William Andrew Publishing: 2018; pp 49-110, Copyright 2018, with permission from Elsevier.

Cone calorimetry (CC) is used to evaluate the flammability of polymers. CC, dictated by ASTM and ISO standards, is based on oxygen concentration regarding combustion gasses of a polymer exposed to variable heat flux. The heat release rate (HRR, kW/m^2) is calculated by measuring the changes in oxygen concentration and gas flow. The maximum and minimum HRR are generally used when assessing a polymer's fire behavior. HRR also provides information about the time of ignition and extinction, mass loss, O_2/CO_2 concentration, and total smoke release.

Integration of HRR versus time quantifies total heat release (THR) in kJ/m^2.[6] In the schematic representation depicted in **Figure 4**, a polymer sample is placed on a load cell under a cone heater. An electrical spark induces combustion, and off-gases are collected and analyzed via sensors in the exhaust duct.

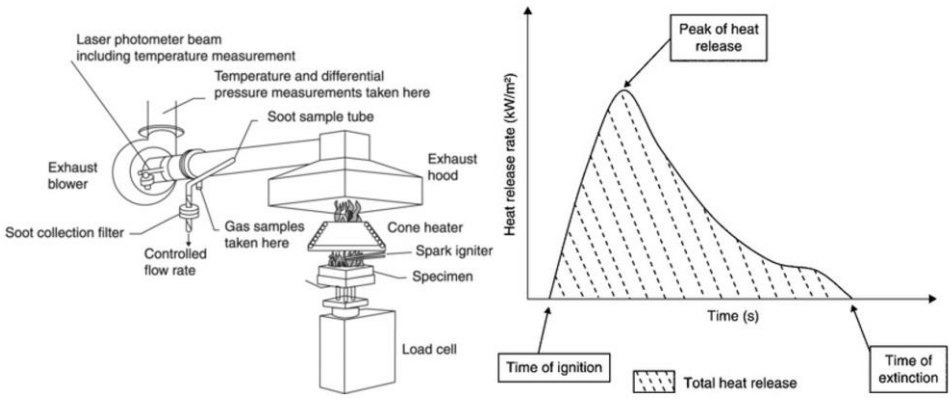

Figure 4. Schematic of a cone calorimeter and representative calorimetry plot.[6] Reprinted from Dewaghe, C.; Lew, C. Y.; Claes, M.; Belgium, S. A.; Dubois, P. 23 - Fire-retardant applications of polymer–carbon nanotubes composites: improved barrier effect and synergism. In *Polymer–Carbon Nanotube Composites*, McNally, T.; Pötschke, P., Eds. Woodhead Publishing: 2011; pp 718-745, Copyright 2011, with permission from Elsevier.

1.2.4. Benefits of halogen- and additive-free

HFRs belong to a broad chemical space comprising many structural architectures and substituents. Among these are tetrabromobisphenol A (TBBPA), hexabromocyclododecane (HBCD), and mixtures of polybrominated diphenyl ethers (PBDEs), though these have either been banned or almost completely phased out. The US, however, still uses many chlorinated flame retardants in the form of various chlorinated phosphates and chlorinated paraffins, all of which still pose considerable health risks.[8-9] Thus, it is of the utmost importance that HFRs are phased out and replaced by more sustainable means.

Many HFRs used in commercial or industrial products serve as additives in polymeric materials. These are referred to as "additive" type flame retardants. While many researchers are developing non-halogenated additives for various polymer systems, including polyurethanes and epoxy resins,[10-11] additives are still associated with many problems. The main concern for researchers working to develop flame-retardant polymeric systems is compatibility. If the miscibility of the additive phase and the polymer phase is low, material properties will suffer. If the mechanical integrity is limited, then thermal properties will be poor. As a result, additives will still migrate and leach from such systems. While additive flame retardants are still the most common due to their cost-effectiveness and availability in industry, polymers from "reactive" flame retardant monomers that possess inherent structural-based flame retardancy are gathering momentum toward commercial realization.[12] Developing inherently flame-retardant materials without additives can lead to significant improvements in material development for aerospace technologies and additive manufacturing as the problems associated with additives are removed. A review published in 2002 by Lu and Hamerton[13] describes many inherently flame retardant systems or blends that demonstrate the growing efforts to expand the range of applicable chemistries.

Herein, we present recent developments of halogen-free, inherently flame-retardant polymers from the past ten years. The polymers and polymer systems discussed do not possess additives and are not composites. We wish to focus on polymer structure of those materials that can be independently used. We do this to focus on the fundamental aspects of what is successful in designing new flame-retardant materials and developing new approaches.

1.3. Polymer Systems

1.3.1. Polyurethanes, Polyamides, Polyimides

Polyurethanes (PU) are a class of thermoplastics that are extremely useful in many applications, including textiles, adhesives, and biomaterials. In general, polyurethanes lack adequate heat resistance and thermo-oxidative stability. However, with clever and informed design, polyurethanes can be tailored to have outstanding fire-resistant and thermal properties. Suen et al.[14] synthesized a novel reactive flame retardant, 5-hydroxy-3-(2-hydroxyethyl)-3-methylpentyl-3-[2-carboxyethylphenylphosphine]propanoate (HMCPP, **Compound 1**, **Table S1**) to prepare polyurethanes (HMCPP/PU). HMCPP and polycaprolactone diol were used as soft segments, 4,4′-diphenylmethane diisocyanate (MDI) as a hard segment and 1,4-butanediol as a chain extender, affording the incorporation of pendant phosphorous moieties. While T_g and $T_{d,5\%}$ of the virgin PU were slightly higher than the phosphorus-containing polymers, HMCPP/PUs all achieved UL94 V-0 ratings with a maximum LOI of 31.8 for the PU containing 4.2 wt% phosphorous.

In a similar manner, Sarwar et al.[15] describe the synthesis of a novel thiourea- and pyridine-based aromatic diol, isophthaloyl bis(3-(3-hydroxopyridyl)thiourea) (IBHPT, **Compound 2, Table S1**), which was subsequently converted to the diisocyanate using 1,4-phenylene diisocyanate (PDI) to give isophthaloyl bis(3-((4-isocyanatophenylcarbamoyloxy)pyridyl) thiourea) (IBPCOT, **Figure 5**). This diisocyanate monomer with 2,7-dihydroxynaphthalene (DHN) as chain extender (hard segment) and varying mol% of polyethylene glycol (PEG, soft segment) form segmented poly(urethane-thiourea)s (PUTs) via a one-pot reaction (**Figure 5**). The PUTs with the lowest 20 mol% PEG exhibited the highest $T_{d,10\%}$ of 524 °C via thermogravimetric analysis (TGA), and the highest T_g of 278 °C, due to the nature and content of the hard segment.

LOI value for the 20mol% PEG PUTs was 44, higher than other reported polyurethanes and commercial polyimides, and scored a V-0 UL 94 rating.

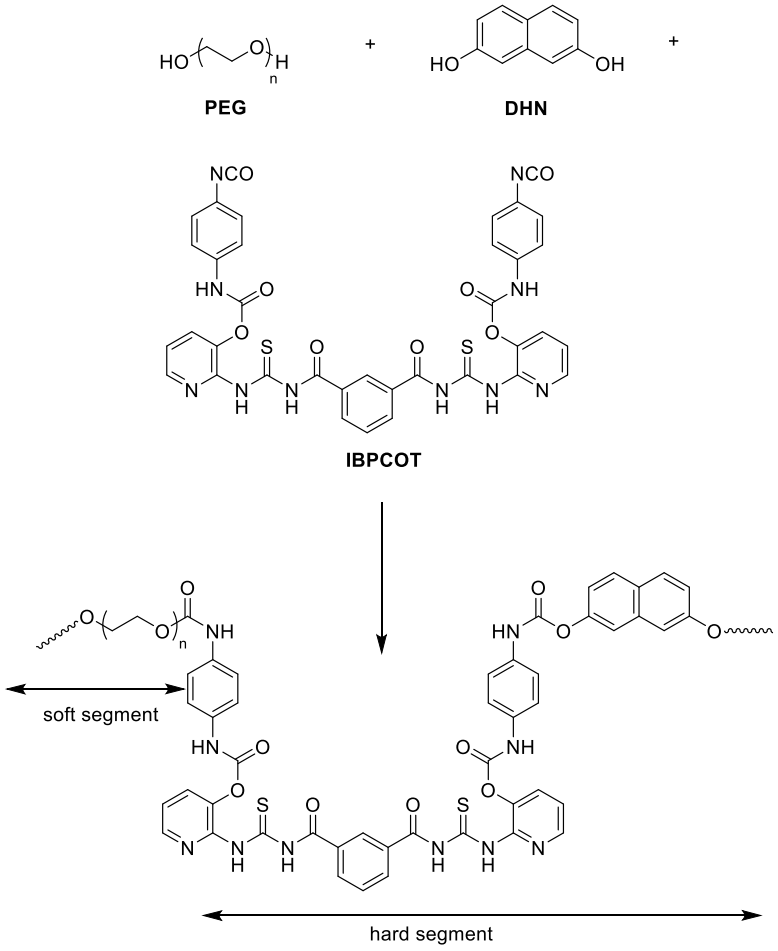

Figure 5. Synthesis of novel poly(urethane-thiourea) (PUT).[15] Adapted from Kausar, A.; Zulfiqar, S.; Sarwar, M. I. *Polym. Degrad. Stab.* **2013**, *98*, 368-376, Copyright 2013, with permission from Elsevier.

Sarwar et al.[16] have also used the thiourea moiety to synthesize novel poly(thiourea-ether-imide)s (PTEIs). They prepared an aromatic diamine monomer 4,4′-oxydiphenyl-bis(thiourea) (ODPBT, **Figure 6**), which reacted with various dianhydrides via a two-step chemical imidization (**Figure 6**). Those polymers made with pyromellitic dianhydride (PMDA) not only had the highest $T_{d,10\%}$ at 530 °C, and highest char yields at around 54% (at 700 °C) but also had the highest LOI value, an incredible 55 (**Figure 7**). This study's LOI values were all above 50, making these

polymers incredibly well-performing, surpassing similarly reported phosphorous-containing and other flame-retardant polyimides. The thiourea functionality is linked to the enhanced flame retardancy, though the authors have not performed additional char or off-gassing analysis.

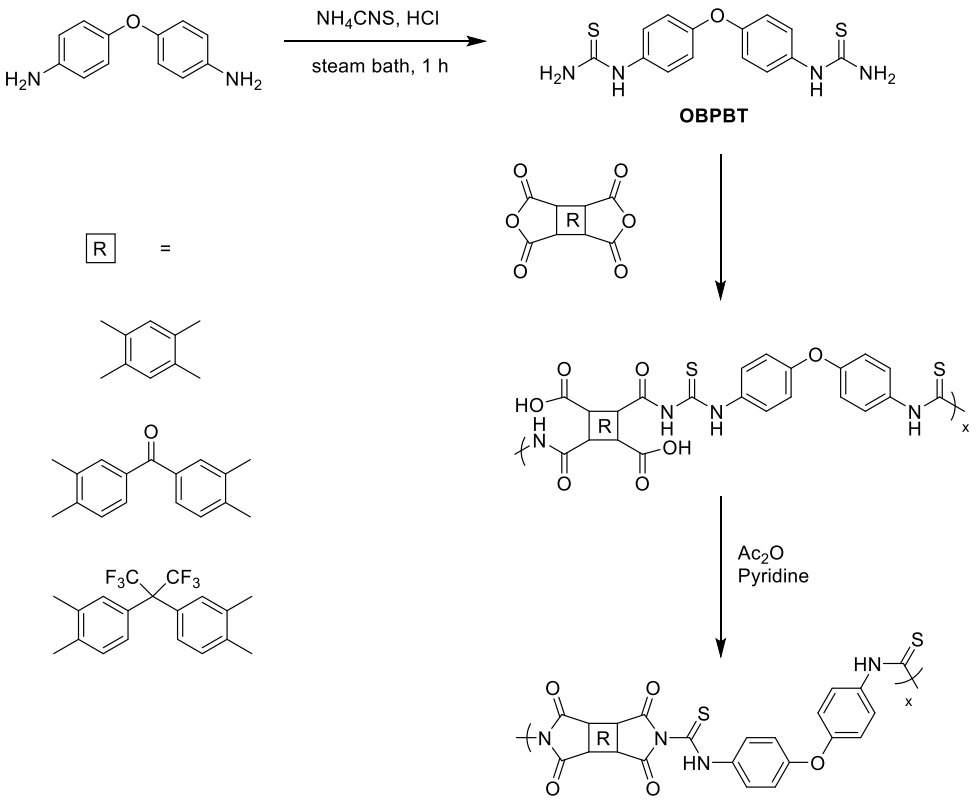

Figure 6. Synthesis of new aromatic monomer, 4,4'-oxydiphenylbis(thiourea) (ODPBT) and subsequent poly(imide-thiourea).[16] Copyright 2011Wiley. Adapted with permission from Kausar, A.; Zulfiqar, S.; Ali, L.; Ishaq, M.; Sarwar, M. I. *Polym. Int.* **2011**, *60*, 564-570.

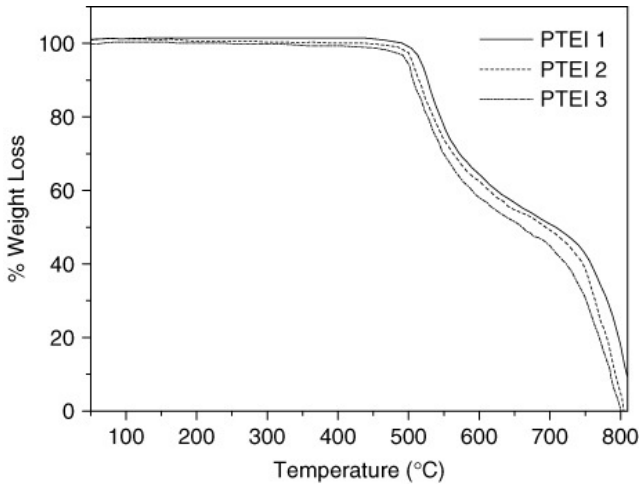

Figure 7. TGA traces of the poly(imide-thiourea)s in Figure 9,[16] with the polymers showing char yields above 50% at 700 °C. Copyright 2011Wiley. Used with permission from Kausar, A.; Zulfiqar, S.; Ali, L.; Ishaq, M.; Sarwar, M. I. *Polym. Int.* **2011**, *60*, 564-570.

Poly(imide-urethane) copolymers have been more popular in recent literature[17-18], though little research has characterized flame retardant characteristics. He et al.[19] described a series of thermoplastic (polyimide-urethane)s (TPIUs) that are inherently flame retardant. From pyromellitic dianhydride (PMDA) and 4,4′-diphenylmethane diisocyanate (MDI) (hard segment) and poly(tetrahydrofuran) (PTMG), the mechanically robust TPIUs performed best with the most hard segment content (37 %). They showed improved properties over a conventional TPU in all characterization methods, including metrics determined by cone calorimetry. Though these TIPUs showed no dripping behaviors and enhanced char formation, they do not qualify in the UL 94 test and exhibit much lower LOI values (21 at highest) compared to the aforementioned PUTs. He et al. [20] proceeded to study the same TPIU system with the incorporation of PDMS, which lowered the HRR and the THR substantially. This observation was attributed to the increased charring of the surface-active PDMS.

Waterborne polyurethanes are known for their versatility as various adhesives and coatings.[21-23] Water-soluble Pus are attractive alternatives to organic solvent-based lacquers and varnishes due to the use of water as the primary solvent, thereby limiting the use of harmful organic solvents and hazardous pollutants. Many researchers have investigated the synthesis of flame-retardant waterborne PUs, which continue to broaden their usefulness. Among the many other inherently flame retardant polymers, one of the most common methods is to increase the content of heteroatoms in the polyurethane structure, especially phosphorous and nitrogen, by using reactive-type monomers (covalently incorporated) that mimic small molecule flame retardants.[24-32]

Yan et al.[25] described a novel flame retardant waterborne polyurethane by chain-extending the PU with a cyclic phosphoramidate diol, 2-(5,5-dimethyl-2-oxo-2λ^5-1,3,2-dioxaphosphinan-2-ylamino)-2-methyl-propane-1,3-diol (PNMPD, **Compound 3**, **Table S1**) and silane coupling agent. Previous studies have shown that the pendant phosphoramidate groups are more hydrolytically stable as opposed to those incorporated into the main chain of the polymer.[26-27] In this case, the silane coupling agent employed for post-chain extension was crosslinked, giving Si–O–Si linkages. This exhibited improvement in the mechanical strength of films and $T_{d,5\%}$ compared to those polymers without (though slightly less than the pure WPU). With 12wt% of PNMPD and a post chain extension ratio of 6 for the silane coupling agent, the FRWPU obtained a UL 94 rating of V0 with an LOI of 27.7. This rating was an increase from that without the silane agent. The same FRWPU sample showed an HRR of 715 kWm^{-2} and a THR of 42.8 MJm^{-2}, which was also an improvement over that without the silane linkage and a 43% reduction compared to the pure WPU. By utilizing residual char analysis, the authors suggested a synergistic effect between the phosphorus and silicon in the condensed phase to explain improvement, citing the formation of –P(=O)–O–Si– linkages in a more stable, compact char.

Du et al.[29] employed a phosphorous- and nitrogen-containing diol monomer (lateral in contrast to the above report) and a multifunctional phosphorous-nitrogen-containing monomer to impart crosslinking in the polyurethane system. Novel tri(N,N-bis-(2-hydroxy-ethyl)acyloxoethyl) phosphate (TNAP, **Compound 4**, **Table S1**) was synthesized as the crosslinker for an FRWPU containing a novel diol (3% in the polymer), pentaerythritol di-N-hydroxyethyl phosphamide (PDNP, **Compound 5**, **Table S1**), reported in an earlier work reported by the authors.[33] The addition of 4% of the crosslinker TNAP increased the LOI to 25.5 from 19 and 21 for the pure WPU and 3% PDNP WPU respectively, while only 2% TNAP incorporation decreased the HRR and THR by 15% and 38% respectively over the pure WPU. The authors' char analysis, which included SEM-EDS, elucidated that the action of TNAP works in both the gas and condensed phases due to its contributions to porous char formation and release of non-volatile gaseous bi-products. Most notable from their work is that the flame retardant crosslinker significant improvement in mechanical properties in the WPU systems.

Polyurethane foams are an additional class of polyurethanes that are highly versatile and widely used for commercial and industrial applications, from seating cushions and insulation to automotive and electrical components.[34-35] As with most polyurethanes, these foam versions are also highly flammable but are perhaps even more dangerous due to the volume in which they are utilized. Polyurethane foams are among the most cited materials that are responsible for devastating fires.[36] Naturally, there have been ongoing efforts to formulate flame retardants into these systems. In this regard, PUFs can be made increasingly flame retardant with various phosphorous moieties by modifying the polyol or by adding additional phosphorous-containing crosslinkers or chain extenders.[37-41] Many of these studies have also utilized biomaterials and bioinspired chemistries with castor oil and cyclodextrin derivatives.[41-43] Additionally, many

FRPUF studies have used phosphorous modified 1,3,5-triazole derivatives as chain extenders that take advantage of the P-N synergistic effects.[41, 44-45]

A handful of studies on flame-retardant polyurethane sealants have also taken advantage of combinations of bio-based and phosphorous-nitrogen-based chemistries.[46-47] Wang et al.[45] describe the synthesis of a novel phosphorous-containing triazole- based triol, 2,4,6-triphosphoric acid diethyl ester hydroxymethyl phenoxy-phosphonate (TDHTPP, **Figure 8**), to be combined with a commercial polyether polyol, a PEG chain extender, and pMDI as the hard segment to give a rigid FRPUF (DI water as the blowing agent). The TDHTPP was incorporated in 5, 10, and 15 wt%, steadily increasing compressive strength while maintaining low thermal conductivities similar to the neat rigid PUF, approximately 0.030 W/(mK) (**Figure 8**). Although the TDHTPP decreased the thermal stability slightly, the rigid FRPUFs passed a UL-94 V-0 rating with an LOI of 25.5%, readily surpassing a FRPUF with a similar small molecule additive. Cone calorimetry experiments also showed notable improvements with THR as low as 11.1 MJ/m^2. Char and volatile analysis via methods such as XPS, SEM-EDX, TGA-IR, and Py-GCMS elucidated that the mode of flame-retardant action is primarily in the vapor phase due to the dilution of combustible gases by phosphorous-containing volatiles. Simultaneously, a small percentage remained in the condensed phase from the formation of crosslinked structures of nitrogen-containing products and polyphosphoric acid within a carbonaceous char.

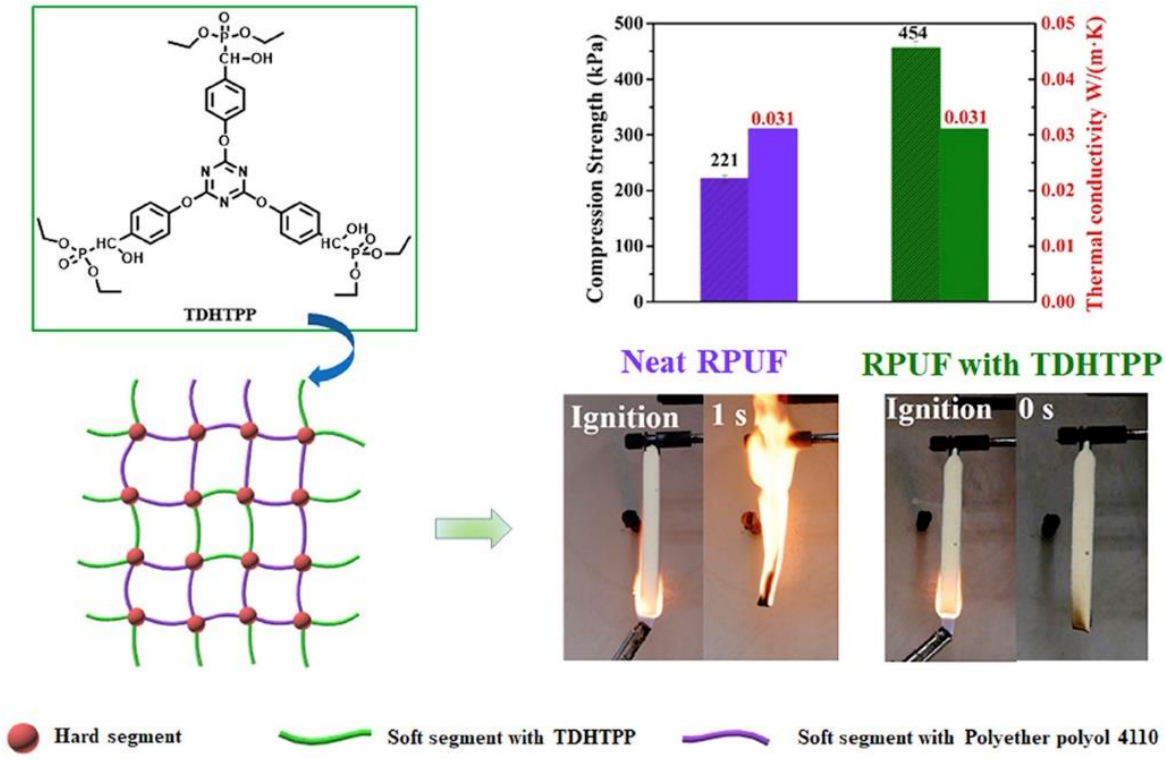

Figure 8. TDHTPP reactive flame retardant triol monomer used in rigid polyurethane foam that shows improvement not only in flame retardancy compared to neat RPUF but also in compressive strength while maintaining thermal conductivity.[45] Reprinted from Wang, S.-X.; Zhao, H.-B.; Rao, W.-H.; Huang, S.-C.; Wang, T.; Liao, W.; Wang, Y.-Z. *Polymer* **2018**, *153*, 616-625, Copyright 2018, with permission from Elsevier.

Polyamides are used in many industrial and consumer goods, mainly in the form of textiles such as fully aliphatic Nylon to fully aromatic Nomex and Kevlar. However, they are also used in the solid form for the automotive industry as molded parts. Although aromatic high-performance polyamides such as Nomex and Kevlar, poly(*m*-phenylene terephthalamide) and poly(*p*-phenylene terephthalamide), respectively, are inherently flame-resistant due to their structure, there is a need for alternative and more cost-effective solutions for consumer-grade, flame-retardant polyamides. Polyamide systems have been modified by the incorporation of flame-retardant phosphorous moieties into the structure of the monomers, usually the diacid or diacid chloride, and most commonly in aliphatic polyamide systems.[48-54]

A report by Hu et al.[48] describes the conversion of a diacid monomer containing a pendant phosphorous unit, 9,10-dihydro-10-[2,3-di(hydroxycarbonyl)propyl]-10-phosphaphenanthrene-10-oxide, (DDP, **Compound 6**, **Table S1**) a 9,10-dihydro-9-oxa-10-phosphaphenanthrene-10-oxide derivative (DOPO, **Compound 7**, **Table S1**), to the acyl chloride form (DPP-COCl) for use in an interfacial copolymerization with adipoyl chloride and hexamethylene diamine, with varying mol% of the different acyl chlorides (**Figure 9**).

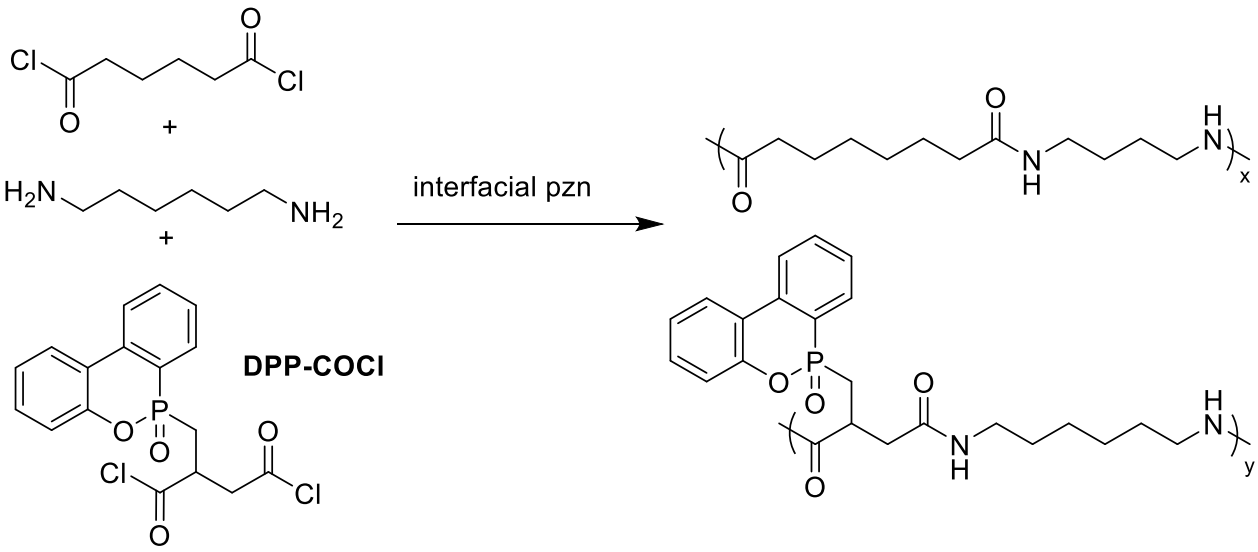

Figure 9. Synthesis of inherently flame retardant polyamide copolymers using DDP.[48] Adapted from Ge, H.; Wang, W.; Pan, Y.; Yu, X.; Hu, W.; Hu, Y. *RSC Advances* **2016**, *6*, 81802-81808 with permission from The Royal Society of Chemistry.

At a maximum of 10 mol% DPP-COCl incorporation, $T_{d,5\%}$ was at a minimum of 319 °C but had the highest char yield (**Figure 10**) due to DDP promoting carbonization. Although the polyamide with the highest DDP-COCl incorporation had the lowest $T_{d,5\%}$, its LOI was at a maximum of 29.5% and scored a UL-94 V1 rating, while also reducing the peak HRR almost 50% from the virgin polyamide. The authors attribute the increase in performance to DPP

decomposition to PO radicals that work in the gas phase to capture free radicals and quench radical chain reactions while also promoting carbonization through phosphoric acid formation.

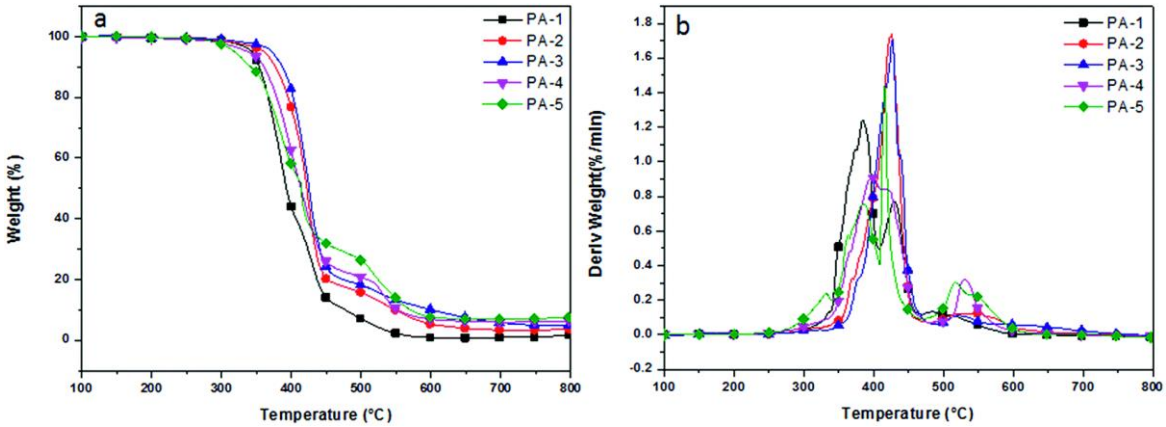

Figure 10. TGA and derivative weight loss plots for inherently flame retardant polyamide copolymers shown in Figure 7.[48] Reproduced from Ge, H.; Wang, W.; Pan, Y.; Yu, X.; Hu, W.; Hu, Y. *RSC Advances* **2016**, *6*, 81802-81808 with permission from The Royal Society of Chemistry.

Historically, poly(amide-imide)s are also used in high-performance applications where flame retardance is necessary. As with the aramids, these polymers are challenging to process. Abouzari-Lotf et al.[55] describe the synthesis of poly(amide-ether-imide) with a novel nicotinic-based diamine containing amide, ether, and pyridine moieties. The monomer was prepared via nucleophilic substitution of 2,6-diaminopyridine with 6-chloronicotinoyl chloride to give a dichloro-diamide compound that was subsequently converted to a diamine with 5-amino-1-naphthol. Polycondensation reaction with various dianhydrides afforded the poly(amide-ether-imide) (**Figure 11**). The polymers synthesized with pyromellitic dianhydride (PMDA) gave the highest LOI values at 41% while maintaining the highest $T_{d,5\%}$ at 428 °C, and char yields around 60%, remaining competitive with commercial standards.

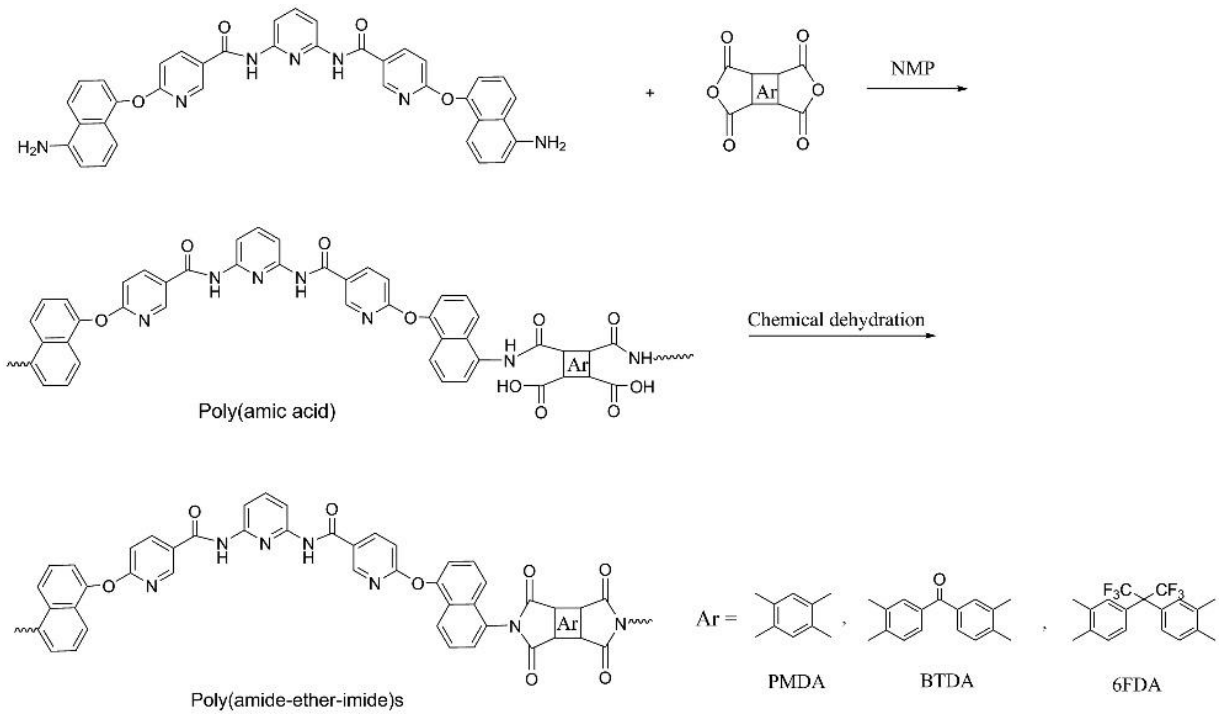

Figure 11. Polycondensation reaction of the nicotinic-based diamine with different dianhydrides, including PMDA and BTDA. The resulting poly(amide-ether-imide)s exhibited high LOI values.[55] Adapted from Mehdipour-Ataei, S.; Babanzadeh, S.; Abouzari-Lotf, E. *Des. Monomers Polym.* **2015**, *18*, 451-459 with permission from Taylor & Francis.

1.3.2. Polyesters/ copolymers

Like polyamides, polyesters make up a large share of polymers produced in fibrous form for various textiles, food and beverage packaging, films, and some electrical engineering capacities. As with many commodity polymers, polyesters are combustible, while fire retardant additives or coatings are detrimental to mechanical performance and environmentally hazardous. These reasons catalyze the ongoing research to incorporate flame retardant units into the main polymer structure. As with polyamides, many works have investigated the effects of using modified monomers with pendant phosphorous-containing groups, usually in the form of a phosphaphenanthrene-containing derivative, such as 9,10-dihydro-10-[2,3-

di(hydroxycarbony)propyl]-10-phosphaphenanthrene-10-oxide (DDP, **Compound 6**, **Table S1**) for example.[56-62] Incorporation of phosphates, phosphinates, phosphine oxide, and their derivatives directly into the main chain of polyesters and in unsaturated polyester resins have also been continuously investigated.[63-71]

Wang et al.[65-66] synthesized a novel bifunctional phosphinate monomer, the sodium salt of 10H-phenoxaphosphine-2,8-dicarboxylic acid,10-hydroxy-2,8-dihydroxyethyl ester,10-oxide (DHPPO-Na), and studied its incorporation into polyethylene terephthalate (PET) (**Figure 12**). Although PET ionomers (PETIs) with 10 mol% DHPPO-Na incorporation show a $T_{d,5\%}$ of 384 °C under nitrogen atmosphere, which is only 10 °C lower than the virgin PET, its $T_{d,5\%}$ under air, was approximately 50 degrees higher and char residue was significantly higher in both instances. Additionally, these PETIs exhibited a significantly lower HRR, down to 259 kW/m^2 from 897 kW/m^2 of virgin PET, with a THR and LOI of 43 MJ/m^2 and 31, respectively. The authors also investigated the effects of changing the counterion from sodium to potassium (DHPPO-K) and a non-ionic, covalently bound phenyl group (DHPPO-Ph). By changing the counterion to potassium, the LOI increased slightly while cone calorimetry stayed marginally the same, attributed to a similar ionization pathway. Furthermore, while the non-ionic polymers that incorporated DHPPO-Ph performed only slightly worse than the ionomers, they suffer from less restricted melt dripping and high smoke release during combustion due to the absence of ionic aggregates. The authors also point out via Py-GCMS, Raman spectroscopy, and ICP-AES, the pyrolysis and flame-retardant behavior of the ionic and non-ionic phosphorus-containing PETs are different. The PETIs act mostly in the condensed phase due to ionization and ionic aggregates in contrast to the non-ionomers that mainly act in the gas phase while promoting some carbonization. It is worth noting

that although these PETIs exhibited enhanced anti-dripping compared to PET, there was still significant enough dripping not to be evaluated in a UL-94 test.

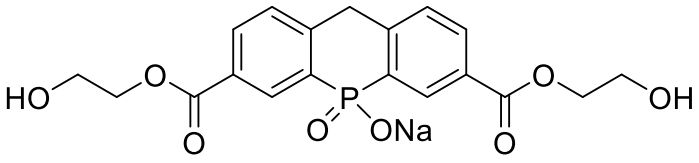

DHPPO-Na

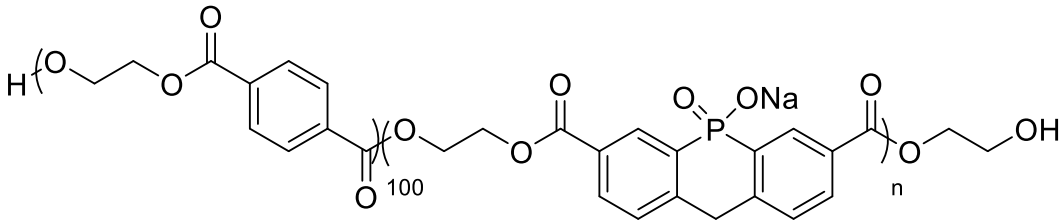

PETIs

Figure 12. Novel bifunctional phosphinate monomer, DHPPO-Na, and copolyester ionomer. Though the incorporation of this moiety improved LOI and anti-dripping performance, these copolyesters failed UL-94 due to a vertical dripping phenomenon. Wang et al. go on to propose many successful polyester systems.[69] Copyright 2017 Wiley. Used with permission from Zhao, H.-B.; Wang, Y.-Z. *Macromol. Rapid Commun.* **2017**, *38*, 1700451.

Hu et al.[67] reported the synthesis of an unsaturated polyester resin system that used a phosphine oxide monomer as a co-curing agent (**Figure 13**). This tris (allyloxymethyl) phosphine oxide (TAOPO) was incorporated into the UPR up to 25 wt% (3% P incorporation), which yielded the lowest $T_{d,5\%}$ in both air and nitrogen atmosphere while giving the highest char yields facilitated by the presence of the phosphorous moieties promoting char formation. CC experiments revealed that HRR (**Figure 14a**) and THR (**Figure 14b**) were reduced by approximately 50 % by incorporating 25% TAOPO. The LOI was also notably increased from 20 of the virgin UPR to 27.

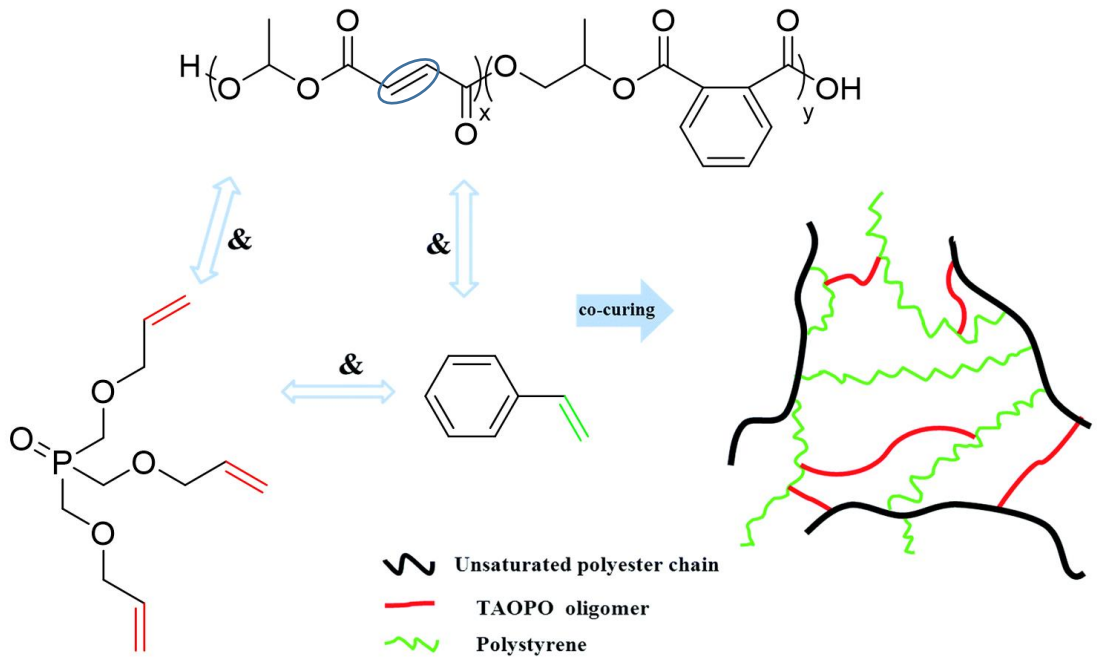

Figure 13. The curing process of flame retardant UPR samples using novel TAOPO monomer.[67] Adapted from Lin, Y.; Yu, B.; Jin, X.; Song, L.; Hu, Y. *RSC Advances* **2016**, *6*, 49633-49642 with permission from The Royal Society of Chemistry.

In a similar vein, Sabnis et al.[72] describe the use of allyl phosphates as reactive flame retardants in commercial UPRs. Two novel phosphates were synthesized from phosphorous oxychloride and allyl alcohol; triallyl phosphate (TAP, **Compound 8**, **Table S1**) and a diethylene glycol (DEG) bridged tetraallyl diphosphate (D-TAP, **Compound 9**, **Table S1**), which were each separately incorporated at 5, 10, and 15 phr (per hundred resin). Following a similar trend to many of the previously discussed systems, these modified UPRs exhibited lower $T_{d,5\%}$, due to the phosphorous content but greater char yields up to 14%. LOI showed increases above 30 as TAP or D-TAP content increased, and all modified UPRs with 10 and 15 phr were rated UL-94 V-0 with no dripping. Overall, those D-TAP modified polymers performed slightly better than those with TAP.

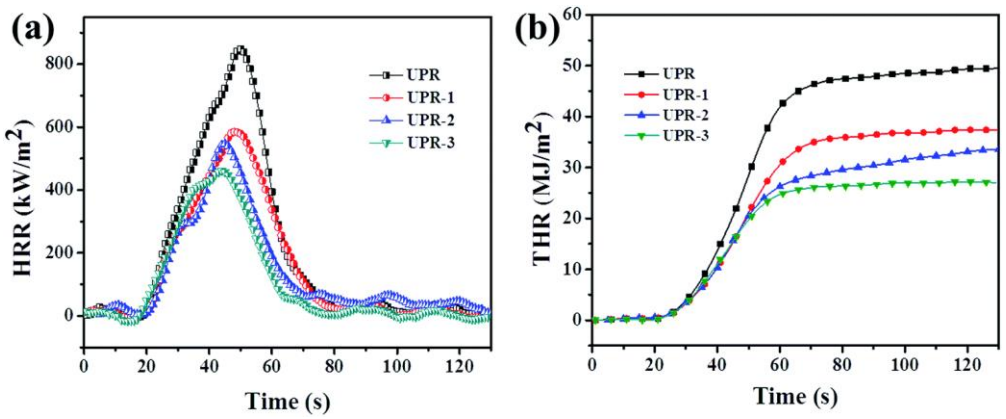

Figure 14. (a) HRR and (b) THR curves of UPR and FR-UPR samples under a 35 kW m^{-2} heat flux.[67] Reproduced from Lin, Y.; Yu, B.; Jin, X.; Song, L.; Hu, Y. *RSC Advances* **2016**, *6*, 49633-49642 with permission from The Royal Society of Chemistry.

The literature also highlights self-crosslinking polyesters and polyesters that undergo inter- and intramolecular chemistries upon thermal exposure.[73-74] Crosslinked polyesters utilize the phenylethynyl group, familiar from the high-performance polymer literature, especially that of polyimides.[75-76] At elevated temperatures (before the onset and through the duration burning), the phenylethynyl groups crosslink the polyester system to create a network and inhibit melt dripping while still allowing regular synthetic and processing conditions. Schiff base[77] and azobenzene moieties[78] have also been used for self-crosslinking polyesters to improve charring and reduce melt dripping. Additionally, phenylmaleimide groups incorporated into polyesters enable crosslinking through a $2\pi + \pi$ cycloaddition mechanism, which effectively improves flame retardancy.[79] Aside from crosslinking polyesters, thermally triggered rearrangement chemistries can also be incorporated into polyesters. Arylene-ether units copolymerized in polyesters have been shown to increase the thermal stability and char yields significantly via rearrangement reactions to form conjugated heteroaromatic structures.[80] Hydroxy-containing phthalimide groups have been used in copolyesters to rearrange into benzoxazole structures that can "capture"

fragments of the thermally degrading polyester, thereby enhancing residue in the condensed phase.[81]

1.3.3. Epoxy Resin Systems

Epoxy resins, or polyepoxides, are a thermosetting material characterized by multiple epoxide moieties that allow for curing with a proton donor. The uses for epoxy resin systems are quite vast. From the most common adhesives and paints to specialized coatings for tanker ships and airplanes, epoxy resins are just as universal as any of the polymers discussed so far. [82-83] Aside from their inherent flammability, epoxy resins have an additional fire hazard if mixed incorrectly as the curing reaction can be greatly exothermic that may ignite nearby materials. In order to combat these issues, many researchers have turned to the popular DOPO (**Compound 7**, **Table S1**) and its derivatives to modify the structure of epoxy resin components or give additional co-curing agents.[84-88] The use of DOPO in combination with heterocycles and other heteroatom moieties has garnered attention due to the various synergistic effects of phosphorous combined with nitrogen and sulfur, etcetera. These types of DOPO-containing systems include functional groups of triazines,[89] triazoles,[90] tetrazoles,[91] and isocyanurates,[92] imidazoles[93-94], and thiazoles.[95-96]

Epoxy resin systems have utilized additional phosphorous functionalities to improve flame retardancy and performance in the form of phosphine oxides,[97] phosphinamides,[98] phosphates,[99] phosphinates,[100-101], and phosphonates[102-104], among others. These systems often employ various forms of heteroatom-containing structures or heterocycles. Lin et al.[97] synthesized a novel phosphine oxide diamine curing agent containing thiophene functional groups, bis(3-amino-2-thienyl) phenylphosphine oxide (ABTPPO, **Compound 10**, **Table S1**), that was shown to improve LOI, HRR, and THR significantly. However, the phosphine oxide only managed to score UL-94 rating of V-2 and V-1 at its best compositions. Wang et al.[100] and Yang et al.[101] developed reactive

phosphinate salts as latent hardeners using nitrogen heterocycles of imidazolium and melaminium, respectively. Using similar epoxy resin systems and a low percentage of phosphorous incorporation, both systems achieved a UL-94 V-0 rating and LOIs above 35. Chen et al.[99] simply modified bisphenol A epoxy resin with phosphoric acid to give phosphate modified resins (**Figure 15**). When these modified resins are primarily used in the cured systems, they achieve UL-94 V-0 ratings and LOI over 30, with the flame-retardant mechanism of action largely in the condensed phase due to the nature of the phosphate groups to decompose at lower temperatures and form a stable char layer.

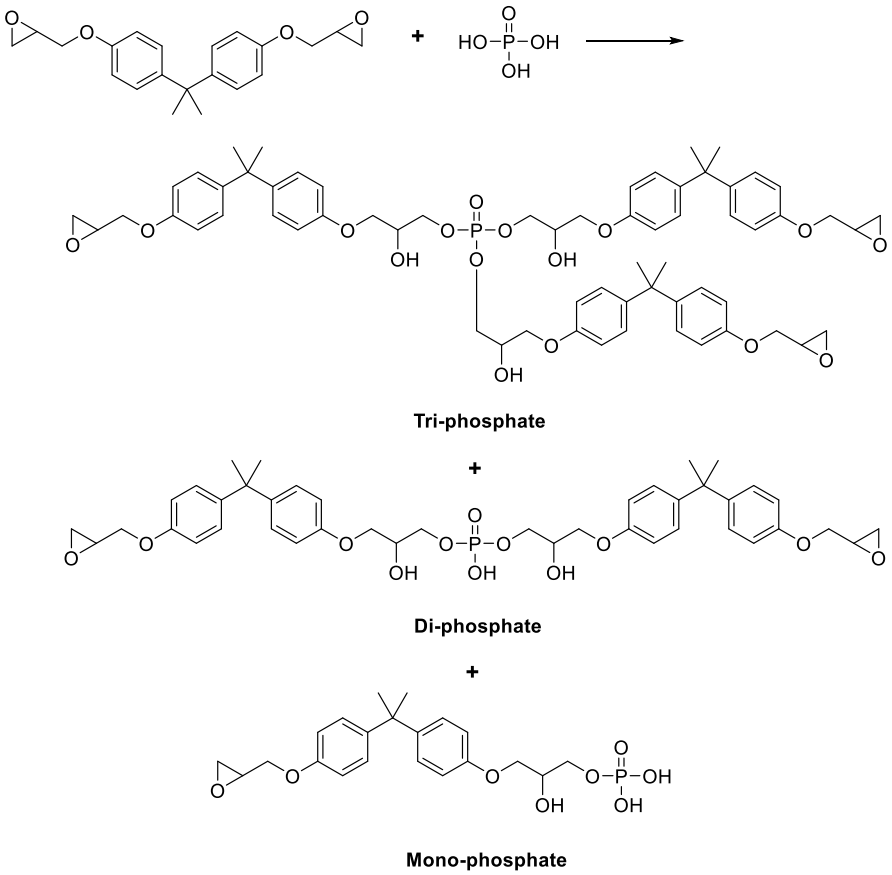

Figure 15. Bisphenol A epoxy resin modified by phosphoric acid to afford variations of phosphate-modified resins.[99] Adapted by permission from Springer Nature: Jiao, C.; Zhuo, J.; Chen, X.; Li, S.; Wang, H. *J. Therm. Anal. Calorim.* **2013**, *114*, 253-259, Copyright 2013.

Phosphorus-containing macromolecular curing agents have been used to impart epoxy resin systems with improved flame retardancy. Narula et al.[105] prepared poly(amide-imide)s (PAI)s containing phosphine/ phosphine oxide groups and free amines to act as a co-curing agent for cycloaliphatic epoxy resin. The PAIs were synthesized from PMDA and L-tryptophan to give a diacid-diimide that was subsequently reacted with phosphorus-containing triamines (**Figure 16**). The free amine groups co-cure the epoxy resin with 4,4′-diaminodiphenylmethane (DDM) or *p*-phenylenediamine (*p*PD). All the system combinations (of equal molar ratios to epoxy) tested had char yields (via TGA in nitrogen atmosphere) between approximately 30–44 %. Each resin displayed decreased $T_{d,\,5\%}$, when compared to resins cured just with *p*PD or DDM. However, the epoxy resin system from DDM and the phosphine oxide-containing PAI exhibited the highest $T_{d,\,5\%}$ at 488 °C, and char yield at approximately 44%. All the phosphorous-containing systems achieved LOIs between 31–38 and UL-94 V-0 ratings with no dripping. The authors did not report cone calorimetry experiments.

Li et al.[106] reported a phosphorous-containing poly(ethyleneimine-thiourea) macromolecular curing agent. The polymer's main chain was synthesized using a reaction of a branched polyethyleneimine, and thiourea then subsequently reacted with diphenylphosphinyl chloride to give phoshinamide groups at approximately 30% functionalization. The system was cured with a commercial epoxy resin and forms optically clear and robust films. Systems containing between 25–35wt% of the macromolecular curing agent obtained LOIs of between 28–32 and UL-94 V-0 ratings. Cone calorimetry elucidated that HRR and THR decreased by 61% and 58% for 30wt% systems. Using FTIR, XPS, and py-GCMS, the authors concluded the flame-retardant mechanism was a joint combination of gas and condensed phase activity due to the formation of cyclized and

aromatic structures and release of sulfur and phosphorous structure into the gas phase to either act as diluents or radical capturing moieties.

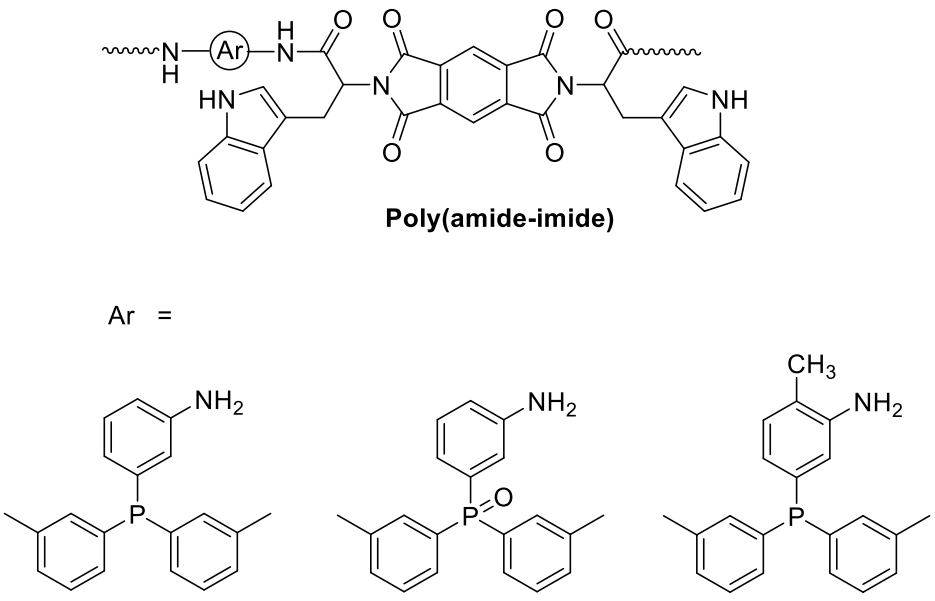

Figure 16. Phosphorus-containing poly(amide-imide)s with free amine groups used in the curing of epoxy resin.[105] Adapted by permission from Springer Nature: Agrawal, S.; Narula, A. K. *J. Therm. Anal. Calorim.* **2014**, *115*, 1693-1703, Copyright 2014.

Linear or cyclic phosphazenes have been of interest as flame retardant materials, not only as the central matrix component,[107-108] but also as additions or modifications to other matrix polymers, especially epoxy resin systems.[109-114] The attraction to phospazines lies in their chemical space; the combination of phosphorous and nitrogen, as has been discussed above, behave synergistically to promote flame retardancy.[115]

Wu et al.[111] described the synthesis and use of a novel linear polyphosphazene-based epoxy resin (LPN-EP) with diglycidyl ether of bisphenol A (DGEBA) and DDM as a hardener (**Figure 17**). Although the synthetic route to the LPN-EP required six steps, the co-cured epoxy resin

system results were promising. Despite expected decreases in $T_{d,\,5\%}$ with increasing phosphorous content, char yields showed significant increases with increasing phosphorous content. The system with 30wt% LPN-EP incorporation (phosphorous content of 2.63wt%) scored a UL-94 rating of V-0 and LOI value of approximately 32. Systems containing 10 and 20 wt% scored V-1 classifications.

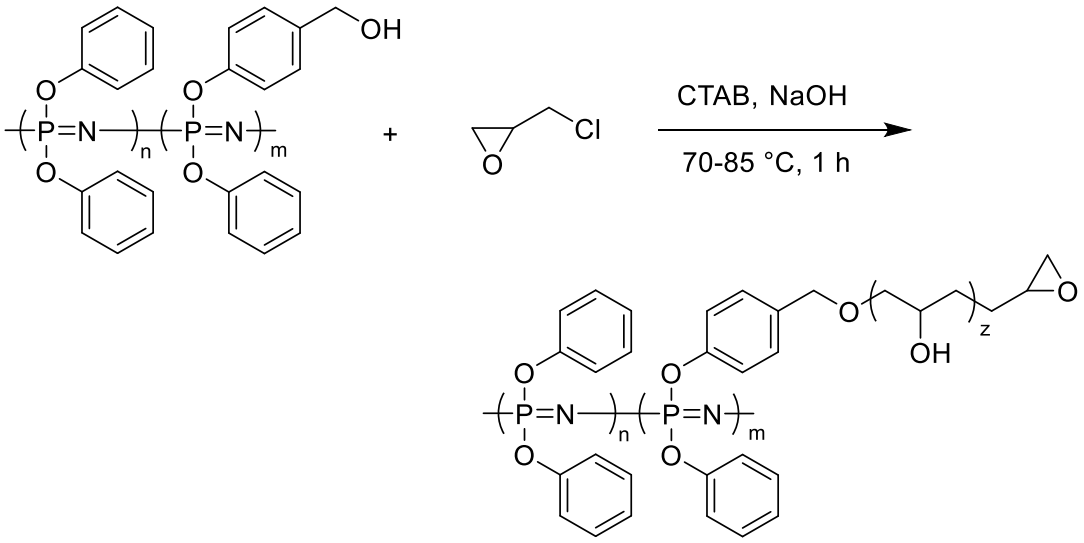

Figure 17. Last step in the synthetic pathway to a novel linear phosphazene epoxy resin.[111] Adapted from Liu, H.; Wang, X.; Wu, D. *Polym. Degrad. Stab.* **2015**, *118*, 45-58, Copyright 2015, with permission from Elsevier.

Char residue analysis via SEM, EDX, FTIR, and solid-state ^{13}C NMR illuminate the flame-retardant mechanism to act in both gas and condensed phases. Nitrogen-containing nonflammable gasses and volatile moieties released by the polyphosphazenes during combustion act as nonreactive diluents while phosphoric and polyphosphoric acid promotes phosphorous-rich carbonaceous char formation. The FTIR in **Figure 18**, for instance, shows characteristic absorption bands for P–O–P and P–O–Ph indicating the presence of phosphate/phosphorous oxides as well as heteroaromatic and polyaromatic structures.

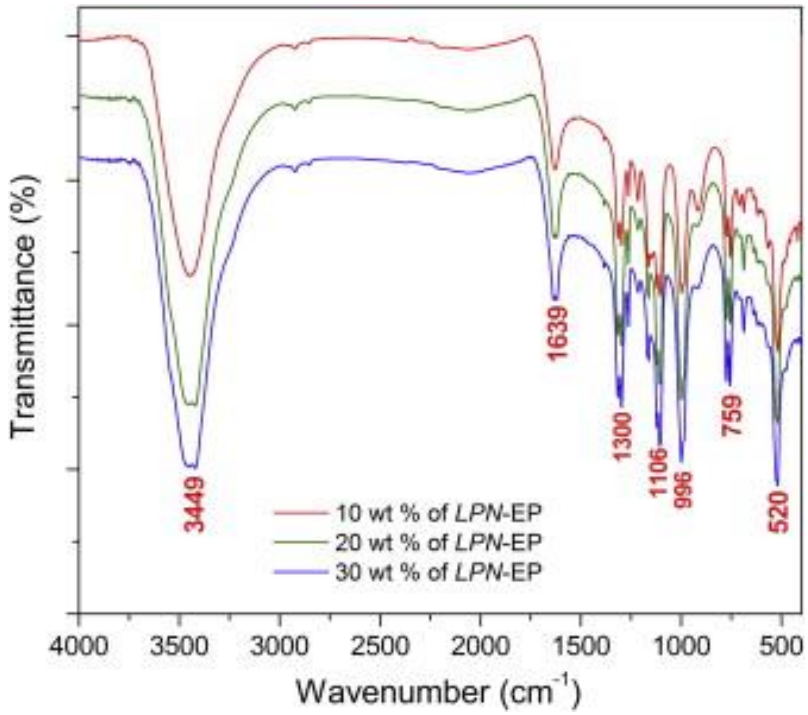

Figure 18. FTIR of the residual char from the LOI test of linear phosphazene EP depicted in Figure 17.[111] Reprinted from Liu, H.; Wang, X.; Wu, D. *Polym. Degrad. Stab.* **2015**, *118*, 45-58, Copyright 2015, with permission from Elsevier.

Ding et al.[114] describe the fabrication of a one-component epoxy resin system that uses a benzimidazolyl-substituted cyclotriphosphazine as a latent curing agent. Synthesized from benzimidazole and hexachlorocyclotriohosphazene, the benzimidazolyl-substituted cyclotriphosphazene (BICP) was cured with a commercial BPA epoxy resin up to about 14 wt% (~1.4 wt% phosphorous) and maintained competitive mechanical properties (**Figure 19**). For systems with 10, 12, and 14 wt%, BCIP incorporation nearly gave the same $T_{d,\,5\%}$, char yields, LOIs (approximately 33), and UL-94 V-0 ratings, within acceptable error. HRR and THR were also approximately equal at ~140 kW/m^2 and 63 MJ/m^2, respectively, a reduction of about 30% compared to the system cured with just benzimidazole. Av-EHC, FTIR, and EDX revealed that the primary mechanism of flame retardancy is in the condensed phase and its contents.

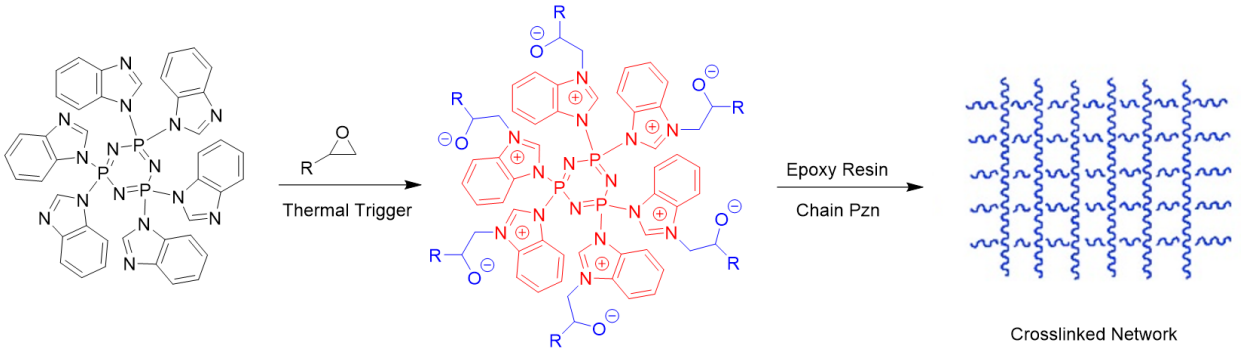

Figure 19. The curing process of benximidazolyl-substituted cyclotriphosphazene epoxy resin system.[114] Adapted from Cheng, J.; Wang, J.; Yang, S.; Zhang, Q.; Huo, S.; Zhang, Q.; Hu, Y.; Ding, G. *Compos. B Eng.* **2019**, *177*, 107440, Copyright 2019, with permission from Elsevier.

Additional studies on flame-retardant epoxy resin systems contain no phosphorous but instead rely on other structures and mechanisms to impart flame retardancy. In one instance, Wang et al.[116] designed a novel thermally co-crosslinking epoxy resin system containing phenylethynyl (phenylacetylene) and azobenzene groups, the curing process with DGEBA of which can be seen below in **Figure 20**. All system combinations were in a 1:1 ratio of epoxy to anhydride. The azo-epoxy resin system cured with phenylethynyl phthalic anhydride (PEPA) was the most noteworthy in its flame-retardant performance. Despite having lower $T_{d,5\%}$ than DGEBA cured resins, the azo-EP cured with PEPA exhibited an increase in $T_{d,5\%}$ of about 35 °C (296 °C), and the highest char yield at 48%. The LOI in this system was also the highest at 27.5%. Continuing this trend, the HRR and THR were 289 kW/m^2 and 24.9 MJ/m^2, respectively. From py-GCMS, XPS, and Raman spectroscopy, the authors concluded that incorporating the phenylethynyl and azobenzene groups allowed for co-crosslinking that promoted the formation of a stable, compact char layer, with minimal action in the gas phase.

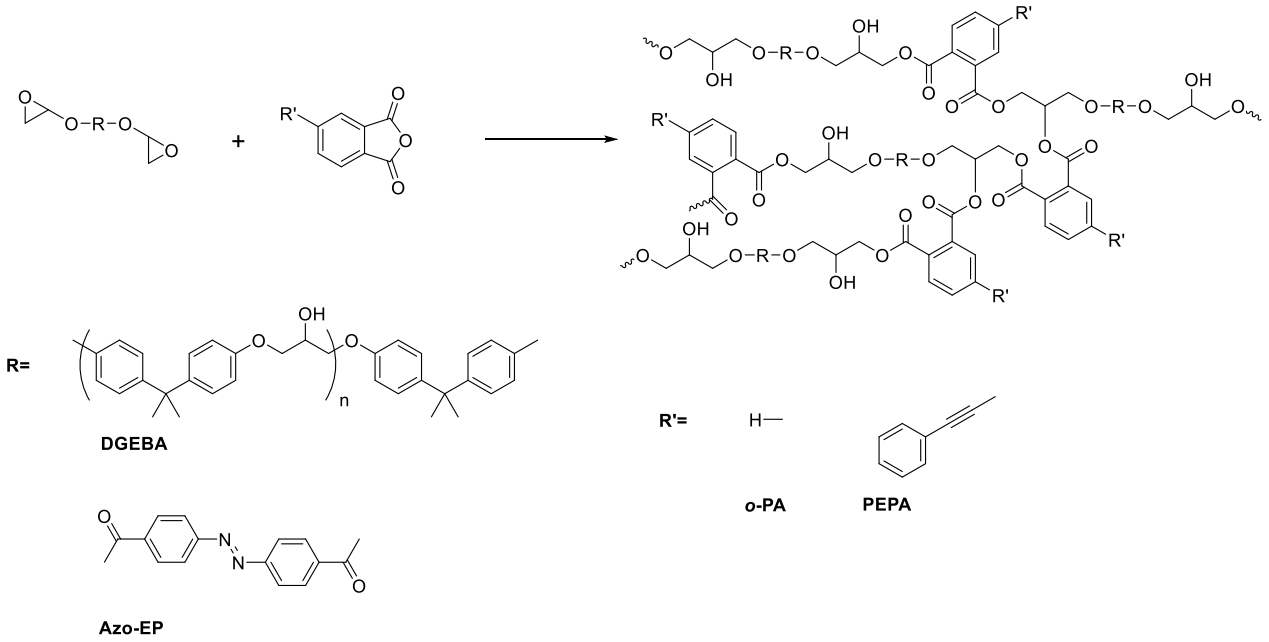

Figure 20. Curing process of epoxy resin system with variations containing phenylethynyl and azobenzene groups with DGEBA. [116] Adapted from Liu, B.-W.; Zhao, H.-B.; Tan, Y.; Chen, L.; Wang, Y.-Z. *Polym. Degrad. Stab.* **2015**, *122*, 66-76. Copyright 2015, with permission from Elsevier.

In a very recent, particularly exciting case, Goh et al.[117] describe the preparation of a hexahydrotriazine derivative containing imidazole, 1,3,5-tris[4′-(1H-imidazol-1-yl)-(1,1′-biphenyl)-4-yl]-1,3,5-triazinane (HIM) to be used as a co-curing agent with 4,4′-oxydianiline (ODA) in a commercial BPA based epoxy resin. **Figure 21** shows this synthetic process. DGEBA and ODA were added in a 1:1 molar ratio, and HIM was added up to 20 phr. The incorporation of HIM notably improves mechanical properties. Similar weight loss behavior is shown in the TGA analysis, while char yields steadily increase to a maximum of 36%. Microcone calorimetry results also displayed a steady decrease to a minimum HRR and THR of 236.4 kW/m^2 and 19.6 MJ/m^2, respectively. They did not report on LOI or VL-94 testing.

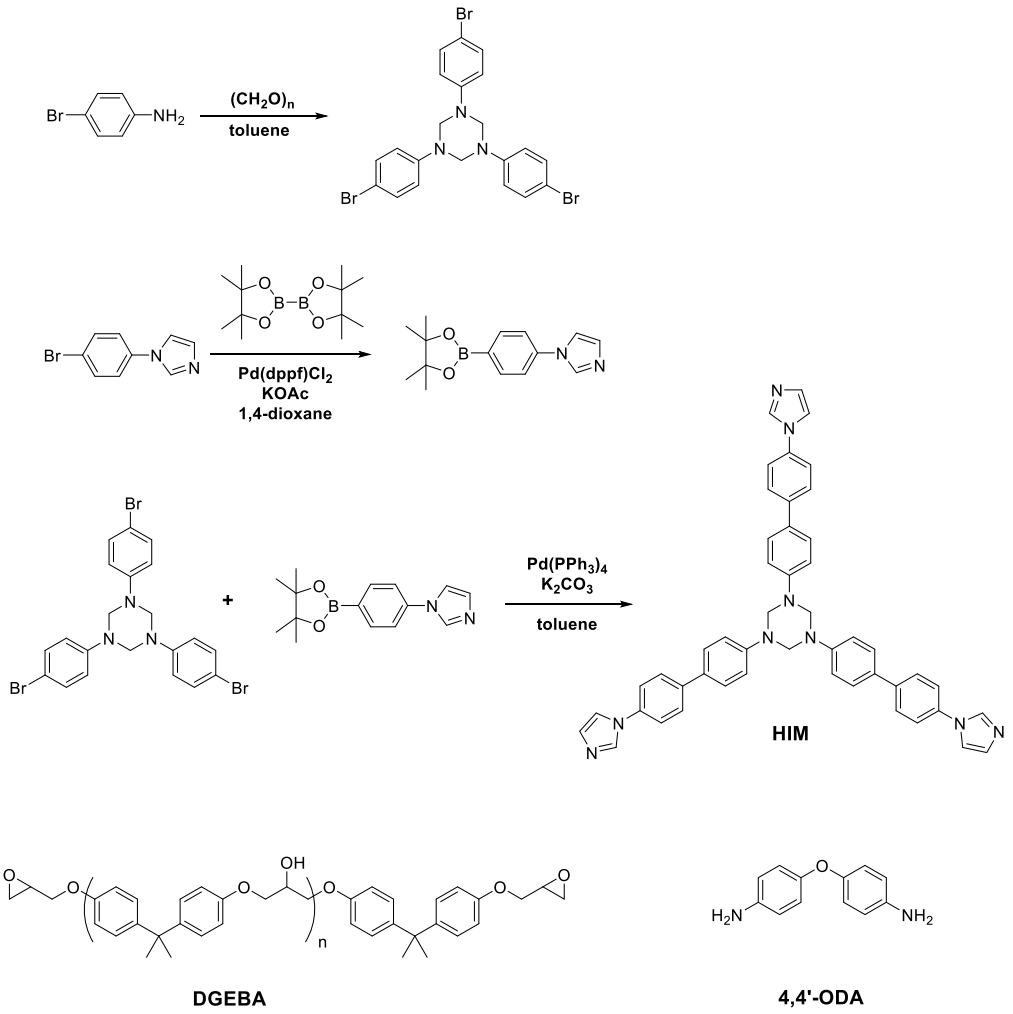

Figure 21. The synthesis of HIM represented with the additional components of the epoxy resin system- DGEBA and ODA.[117] Copyright 2017 Wiley. Adapted with permission from Kim, D. H.; Kim, Y.; Goh, M. *J. Appl. Polym. Sci.* **2020**, *n/a*, 49422.

There has been much interest in developing sustainable polymer and using bio-sourced material to replace petroleum feedstocks. Many flame-retardant epoxy resin systems seem to be highlighting these principles.[118-119] Some bio-sourced materials have been used for their inherent flame retardant properties, while others have been combined with flame retardant moieties, most commonly those containing phosphorous (DOPO, etc.). Examples of these bio-based, sustainable resources from which reactive materials are derivatized include lignin/vanillin,[103] furan,[120-121] eugenol/isoeugenol,[120, 122] daidzein,[123] diphenolic acid,[124,] and itaconic acid.[125-126]

1.3.4. Additional Systems of Interest

There are a handful of other flame retardant polymer systems that have been studied over the last decade. Poly(lactic acid) (PLA) has attracted much interest due to its biodegradability and production from renewable resources while maintaining competitive properties compared to other commodity polymers. Researchers have investigated the effects of putting phosphorous moieties in the backbone **(Figure 22**),[127] as pendant groups like DOPO,[128] and using non-phosphorous containing heterocyclic units, like benzoxazole.[129-130]

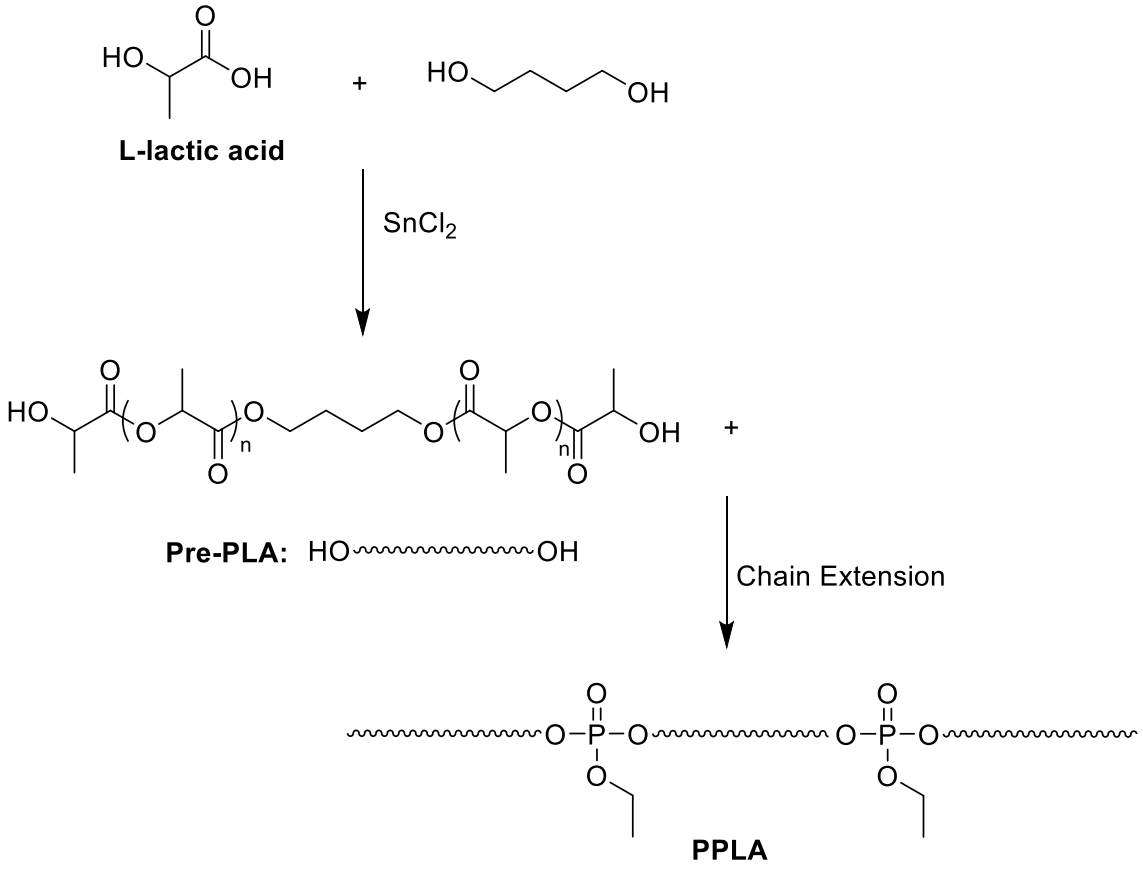

Figure 22. Phosphorous-containing PLA synthesis and chain extension with ethyl phosphorodichloride for an inherently flame retardant PLA. [127] Adapted from Wang, D.-Y.; Song, Y.-P.; Lin, L.; Wang, X.-L.; Wang, Y.-Z. *Polymer* **2011**, *52*, 233-238. Copyright 2011, with permission from Elsevier.

An additional class of high-performance polymer, the relatively new polyoxadiazole, has been researched in efforts further to boost flame retardancy via phosphorous-containing and non-phosphorous-containing methods. Xu et al.[131] reported novel polyoxadiazoles containing triphenylphosphine oxide units. This synthetic pathway can be seen in **Figure 23a**. Up to 20 mol% of the phosphine oxide unit was incorporated, although this led to a notable reduction of mechanical properties. No significant changes in thermal stability were seen, but char yields were increased by about 22%. **Figure 23b** shows significant increases in LOI (up to 35) as phosphorous content increases and the gross heat of combustion (GHC) steadily decreases. Xu et al.[132] in an earlier study, reported on sulfonated polyoxadiazoles by incorporating 4,4′-oxybisbenzoic acid (OBBA) (up to 15 mol %) into the main backbone using a similar synthetic methodology to that seen in Figure 21. In this case, above 10 wt%, the sPOD polymers achieved a UL-94 V-0 rating with a maximum LOI of approximately 39. Furthermore, diluent SO_2 gasses released during combustion help to enhance flame retardancy in the gas phase.

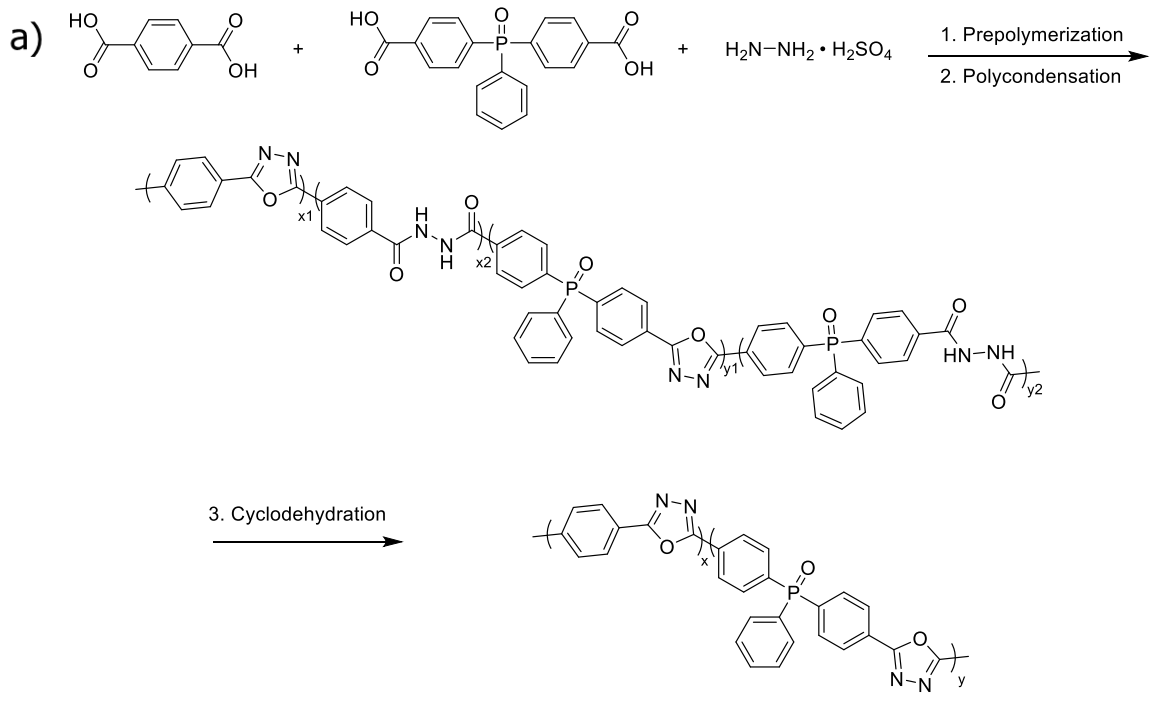

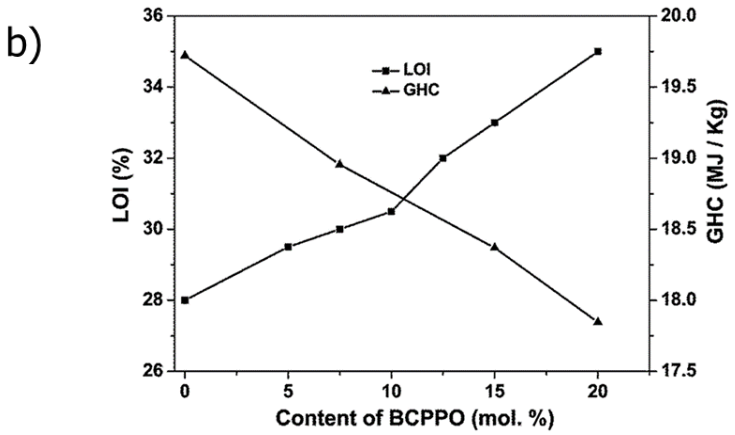

Figure 23. a) Synthetic route to phosphine oxide containing poly(oxadiazole)s b) LOI and gross heat of combustion (GHC) as a function of bis(4-carboxyphenyl)phenyl phosphine oxide content for the poly(oxadiazoles)s.[131] Adapted from Liu, P.; Dong, L.; Wu, L.; Zeng, L.; Xu, J. *RSC Advances* **2019**, *9*, 7147-7155 with permission from The Royal Society of Chemistry.

Due to their versatility, widespread usage, and biocompatibility, siloxanes have been candidates for flame retardant improvement. While many studies focus on incorporating heteroatoms like P, N, or B,[133-136] others have addressed the structural possibilities of siloxane-based flame retardant systems. In a more recent study, Gouri et al.[137] describe a novel hyperbranched polysiloxane curable network. As seen in **Figure 24**, vinyltriethoxysilane (VTES), diphenyldimethoxysilane (DPDMS), and dimethyldiethoxysilane (DMDES) are prepared into branched terpolymer through hydrolysis and condensation. The terpolymer is then cured into a network via Si-O-Si bonds with the aid of a tin catalyst. The network with the greatest content of vinyl groups (~53 mol%) has an astounding $T_{d,5\%}$ at 541 °C with a char residue at 900 °C of 86%. This system shows negligible signs of "unzipping,"- the evolution of D_3 and D_4 cyclomers, with decomposition. This system also affords an LOI of 37 with a UL-94 V-0 rating. Py-GCMS, Raman, and SEM elucidated that the high performance can be attributed to the thermal rearrangement and carbonization of the vinyl moieties as they give rise to higher-order aromatic structures.

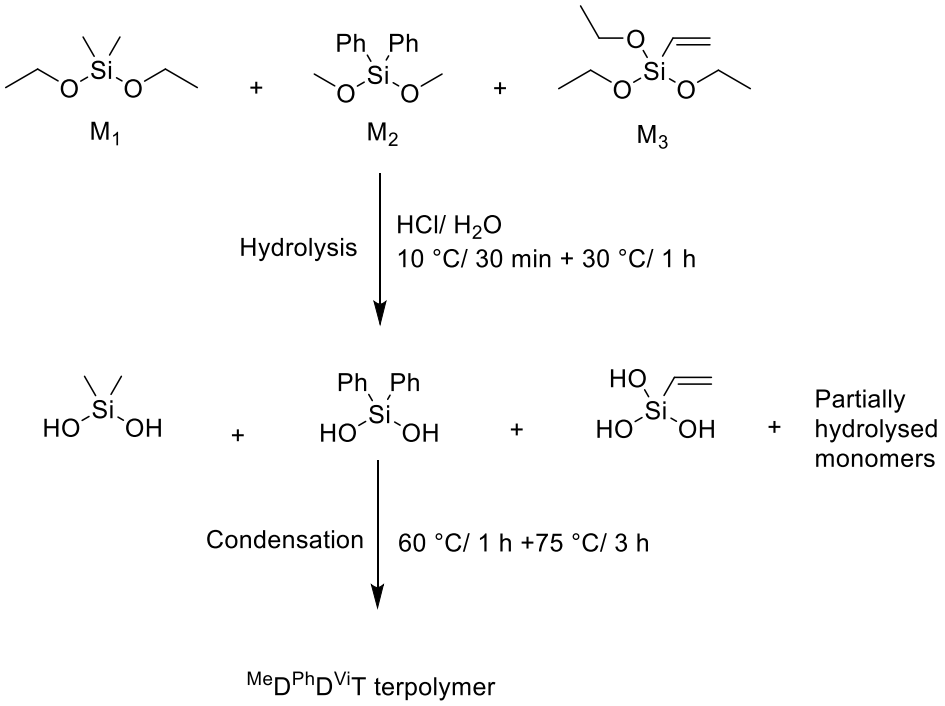

Figure 24. Synthesis of vinyl-containing hyperbranched polysiloxanes that are cured into networks with high LOI and V-0 rating.[137] Adapted from Indulekha, K.; Thomas, D.; Supriya, N.; Rajeev, R. S.; Mathew, D.; Ninan, K. N.; Gouri, C. *Polym. Degrad. Stab.* **2018**, *147*, 12-24, Copyright 2011, with permission from Elsevier.

1.4. Conclusions and Outlook

In the past decade, there has been much effort to research and develop polymer systems with flame retardant properties. Materials that incorporate reactive flame retardants or utilize inherent chemical structure to impart flame retardance often circumvent issues associated with additives and composites, such as reduced mechanical integrity and chemical leaching, which can pose many environmental problems. The most successful systems are those that use a combination of aromatic, heteroatom/ heterocyclic structures with phosphorous-containing groups such as DOPO and phosphine oxides. The synergistic effect between phosphorous and elements such as nitrogen, silicon, sulfur, etc., allows for effective combinations of gas and condensed phase fire suppression mechanisms. There also have been many systems that have built upon the principles of green and

sustainable chemistry. The next generations of flame retardant polymers have much to build from when designing structures with complementary features to increase LOI, increase UL-94 ratings, and lower combustion/ heat release kinetics.

Additionally, as shown in this review, the chemical space of flame retardancy inherent and integral to polymer structure spans across the polymer spectrum and continues to expand; there is an element of modularity. This review has highlighted the synthesis, structure, and fire properties of such recent polymer systems. Fire will not cease to be a continuous threat to society and technological advancement. Concurrently, scientists must take steps to reduce the environmental impacts associated with halogenated and composite materials. Therefore, research done in this light is of great value with high potential impact.

1.5. References

1. Bhat, G.; Kandagor, V. 1 - Synthetic polymer fibers and their processing requirements. In *Advances in Filament Yarn Spinning of Textiles and Polymers*, Zhang, D., Ed. Woodhead Publishing: 2014; pp 3-30.

2. Lyon, R. E.; Janssens, M. L. *Polymer Flammmibility*; Federal Aviation Administration: Washington, D. C., 2005.

3. Camino, G.; Costa, L.; Luda di Cortemiglia, M. P. *Polym. Degrad. Stab.* **1991**, *33*, 131-154.

4. Holder, K. M.; Smith, R. J.; Grunlan, J. C. *J. Mater. Sci.* **2017**, *52*, 12923-12959.

5. Shrivastava, A. 3 - Plastic Properties and Testing. In *Introduction to Plastics Engineering*, Shrivastava, A., Ed. William Andrew Publishing: 2018; pp 49-110.

6. Dewaghe, C.; Lew, C. Y.; Claes, M.; Belgium, S. A.; Dubois, P., 23 - Fire-retardant applications of polymer–carbon nanotubes composites: improved barrier effect and synergism. In *Polymer–*

Carbon Nanotube Composites, McNally, T.; Pötschke, P., Eds. Woodhead Publishing: 2011; pp 718-745.

7. Zaikov, G. E.; Lomakin, S. M. *J. Appl. Polym. Sci.* **2002**, *86*, 2449-2462.

8. Shaw, S. D. *Rev. Environ. Health* **2010**, *25*, 261 - 306.

9. Council, N. R. *Toxicological Risks of Selected Flame-Retardant Chemicals*. The National Academies Press: Washington, DC, 2000; p 534.

10. Xu, W.; Wang, G.; Zheng, X. *Polym. Degrad. Stab.* **2015**, *111*, 142-150.

11. Battig, A.; Markwart, J. C.; Wurm, F. R.; Schartel, B. *Polym. Chem.* **2019**, *10*, 4346-4358.

12. Morgan, A. B. *Polym. Rev.* **2019**, *59*, 25-54.

13. Lu, S. Y.; Hamerton, I. *Prog. Polym. Sci.* **2002**, *27*, 166-1712.

14. Chiu, S.-H.; Wu, C.-L.; Lee, H.-T.; Gu, J.-H.; Suen, M.-C. *J. Polym. Res.* **2016**, *23*, 205.

15. Kausar, A.; Zulfiqar, S.; Sarwar, M. I. *Polym. Degrad. Stab.* **2013**, *98*, 368-376.

16. Kausar, A.; Zulfiqar, S.; Ali, L.; Ishaq, M.; Sarwar, M. I. *Polym. Int.* **2011**, *60*, 564-570.

17. Ben Youssef, I.; Alem, H.; Sarry, F.; Elmazria, O.; Jimenez Rioboo, R.; Arnal-Hérault, C.; Jonquières, A. *Sens. Actuators B Chem.* **2013**, *185*, 309-320.

18. Ma, R.; Zhao, T.; Pu, H.; Sun, M.; Cui, Y.; Xie, X. *ACS Omega* **2020**, *5*, 6911-6918.

19. Tang, Q.; Song, Y.; He, J.; Yang, R. *J. Appl. Polym. Sci.* **2014**, *131*.

20. Tang, Q.; Yang, R.; He, J. *Ind. Eng. Chem. Res.* **2014**, *53*, 9714-9720.

21. Choi, S. H.; Kim, D. H.; Raghu, A. V.; Reddy, K. R.; Lee, H.-I.; Yoon, K. S.; Jeong, H. M.; Kim, B. K. *J. Macromol. Sci. B* **2012**, *51*, 197-207.

22. Xu, H.; Qiu, F.; Wang, Y.; Wu, W.; Yang, D.; Guo, Q. *Prog. Org. Coat.* **2012**, *73*, 47-53.

23. Lei, L.; Zhong, L.; Lin, X.; Li, Y.; Xia, Z. *Chem. Eng.* **2014**, *253*, 518-525.

24. Wu, G.; Li, J.; Luo, Y. *Polym. Degrad. Stab.* **2016**, *123*, 36-46.

25. Zhang, P.; Fan, H.; Tian, S.; Chen, Y.; Yan, J. *RSC Advances* **2016**, *6*, 72409-72422.

26. Zhang, P.; Zhang, Z.; Fan, H.; Tian, S.; Chen, Y.; Yan, J. *RSC Advances* **2016**, *6*, 56610-56622.

27. Zhang, P.; Tian, S.; Fan, H.; Chen, Y.; Yan, J. *Prog. Org. Coat.* **2015**, *89*, 170-180.

28. Niu, X.; Nie, Z.; Wang, G. *Fire Mater.* **2018**, *42*, 933-945.

29. Wang, S.; Du, X.; Jiang, Y.; Xu, J.; Zhou, M.; Wang, H.; Cheng, X.; Du, Z. *J. Colloid Interface Sci.* **2019**, *537*, 197-205.

30. Wang, H.; Du, X.; Wang, S.; Du, Z.; Wang, H.; Cheng, X. *RSC Advances* **2020**, *10*, 12078-12088.

31. Wang, S.; Du, X.; Fu, X.; Du, Z.; Wang, H.; Cheng, X. *J. Appl. Polym. Sci.* **2020**, *137*, 48444.

32. Wang, H.; Wang, S.; Du, X.; Du, Z.; Wang, H.; Cheng, X. *J. Appl. Polym. Sci. n/a*, 49368.

33. Wang, S.; Du, Z.; Cheng, X.; Liu, Y.; Wang, H. *J. Appl. Polym. Sci.* **2018**, *135*, 46093.

34. Gama, N. V.; Ferreira, A.; Barros-Timmons, A. *Materials* **2018**, *11*, 1841.

35. Troitzsc, J. H. *Int. Polym. Sci. Technol.* **2013**, *40*, 1-6.

36. McKenna, S. T.; Hull, T. R. *Fire Sci. Rev.* **2016**, *5*, 3.

37. Chen, M.-J.; Chen, C.-R.; Tan, Y.; Huang, J.-Q.; Wang, X.-L.; Chen, L.; Wang, Y.-Z. *Ind. Eng. Chem. Res.* **2014**, *53*, 1160-1171.

38. Rao, W.-H.; Liao, W.; Wang, H.; Zhao, H.-B.; Wang, Y.-Z. *J. Hazard. Mater.* **2018**, *360*, 651-660.

39. Rao, W.-H.; Xu, H.-X.; Xu, Y.-J.; Qi, M.; Liao, W.; Xu, S.; Wang, Y.-Z. *Chem. Eng.* **2018**, *343*, 198-206.

40. Rao, W.-H.; Zhu, Z.-M.; Wang, S.-X.; Wang, T.; Tan, Y.; Liao, W.; Zhao, H.-B.; Wang, Y.-Z. *Polym. Degrad. Stab.* **2018**, *153*, 192-200.

41. Sykam, K.; Meka, K. K. R.; Donempudi, S. *ACS Omega* **2019**, *4*, 1086-1094.

42. Zhang, L.; Zhang, M.; Hu, L.; Zhou, Y. *Ind. Crops Prod.* **2014**, *52*, 380-388.

43. Zeng, S.-L.; Xing, C.-Y.; Chen, L.; Xu, L.; Li, B.-J.; Zhang, S. *Polym. Degrad. Stab.* **2020**, *178*, 109171.

44. Rao, W.-H.; Hu, Z.-Y.; Xu, H.-X.; Xu, Y.-J.; Qi, M.; Liao, W.; Xu, S.; Wang, Y.-Z. *Ind. Eng. Chem. Res.* **2017**, *56*, 7112-7119.

45. Wang, S.-X.; Zhao, H.-B.; Rao, W.-H.; Huang, S.-C.; Wang, T.; Liao, W.; Wang, Y.-Z. *Polymer* **2018**, *153*, 616-625.

46. Ding, H.; Wang, J.; Wang, C.; Chu, F. *Polym. Degrad. Stab.* **2016**, *124*, 43-50.

47. Ding, H.; Xia, C.; Wang, J.; Wang, C.; Chu, F. *J. Mater. Sci* **2016**, *51*, 5008-5018.

48. Ge, H.; Wang, W.; Pan, Y.; Yu, X.; Hu, W.; Hu, Y. *RSC Advances* **2016**, *6*, 81802-81808.

49. Li, Y.; Liu, K.; Zhang, J.; Xiao, R. **2018**, *29*, 951-960.

50. Liu, K.; Li, Y.; Tao, L.; Xiao, R. *RSC Advances* **2018**, *8*, 9261-9271.

51. Zhang, X.; Tang, X.; Wang, R.; Wang, R.; Yan, X.; Shi, M. *Text. Res. J.* **2018**, *88*, 1299--1307.

52. Liu, K.; Li, Y.; Tao, L.; Liu, C.; Xiao, R. *Polym. Degrad. Stab.* **2019**, *163*, 151-160.

53. Mourgas, G.; Giebel, E.; Bauch, V.; Schneck, T.; Unold, J.; Buchmeiser, M. R. *Polym. Adv. Technol.* **2019**, *30*, 2872-2882.

54. Lu, P.; Zhao, Z.-Y.; Xu, B.-R.; Li, Y.-M.; Deng, C.; Wang, Y.-Z. *Chem. Eng.* **2020**, *379*, 122278.

55. Mehdipour-Ataei, S.; Babanzadeh, S.; Abouzari-Lotf, E. *Des. Monomers Polym.* **2015**, *18*, 451-459.

56. Chen, H.-B.; Zhang, Y.; Chen, L.; Shao, Z.-B.; Liu, Y.; Wang, Y.-Z. *Ind. Eng. Chem. Res.* **2010**, *49*, 7052-7059.

57. Bai, Z.; Song, L.; Hu, Y.; Yuen, R. K. K. *Ind. Eng. Chem. Res.* **2013**, *52*, 12855-12864.

58. Zhang, J.-B.; Wang, X.-L.; He, Q.-X.; Zhao, H.-B.; Wang, Y.-Z. *Polym. Degrad. Stab.* **2014**, *108*, 12-22.

59. Wei, Z.; Zhou, C.; Yu, Y.; Li, Y. *Polymer* **2015**, *71*, 31-42.

60. Zhou, C.; Wei, Z.; Yu, Y.; Li, Y. *J. Therm. Anal. Calorim.* **2015**, *120*, 1799-1810.

61. Zhang, C.; Huang, J. Y.; Liu, S. M.; Zhao, J. Q. *Polym. Adv. Technol.* **2011**, *22*, 1768-1777.

62. Lin, Y.; Jiang, S.; Gui, Z.; Li, G.; Shi, X.; Chen, G.; Peng, X. *RSC Advances* **2016**, *6*, 86632-86639.

63. Wang, J.-S.; Zhao, H.-B.; Ge, X.-G.; Liu, Y.; Chen, L.; Wang, D.-Y.; Wang, Y.-Z. *Ind. Eng. Chem. Res.* **2010**, *49*, 4190-4196.

64. Chen, H.-B.; Zhang, Y.; Chen, L.; Wang, W.; Zhao, B.; Wang, Y.-Z. *Polym. Adv. Technol.* **2012**, *23*, 1276-1282.

65. Zhang, Y.; Ni, Y.-P.; He, M.-X.; Wang, X.-L.; Chen, L.; Wang, Y.-Z. *Polymer* **2015**, *60*, 50-61.

66. Zhang, Y.; Chen, L.; Zhao, J.-J.; Chen, H.-B.; He, M.-X.; Ni, Y.-P.; Zhai, J.-Q.; Wang, X.-L.; Wang, Y.-Z. *Polym. Chem.* **2014**, *5*, 1982-1991.

67. Lin, Y.; Yu, B.; Jin, X.; Song, L.; Hu, Y. *RSC Advances* **2016**, *6*, 49633-49642.

68. Kim, S.; Linh, P. T. T.; Kang, J.; Kim, I. *J. Appl. Polym. Sci.* **2017**, *134*, 45478.

69. Zhao, H.-B.; Wang, Y.-Z. *Macromol. Rapid Commun.* **2017**, *38*, 1700451.

70. Dai, K.; Deng, Z.; Liu, G.; Wu, Y.; Xu, W.; Hu, Y. *Polymers* **2020**, *12*, 1441.

71. Dai, K.; Song, L.; Jiang, S.; Yu, B.; Yang, W.; Yuen, R. K. K.; Hu, Y. *Polym. Degrad. Stab.* **2013**, *98*, 2033-2040.

72. Wazarkar, K.; Kathalewar, M.; Sabnis, A. *Polym. Compos.* **2017**, *38*, 1483-1491.

73. Bicak, N.; Karagoz, B.; Tunca, U. *J. Polym Sci. A Polym. Chem.* **2003**, *41*, 2549-2555.

74. Alemdar, N.; Karagoz, B.; Erciyes, A. T.; Bicak, N. *Prog. Org. Coat.* **2007**, *60*, 69-74.

75. Zhao, H.-B.; Chen, L.; Yang, J.-C.; Ge, X.-G.; Wang, Y.-Z. *J. Mater. Chem.* **2012**, *22*, 19849-19857.

76. Zhao, H.-B.; Liu, B.-W.; Wang, X.-L.; Chen, L.; Wang, X.-L.; Wang, Y.-Z. *Polymer* **2014**, *55*, 2394-2403.

77. Wu, J.-N.; Chen, L.; Fu, T.; Zhao, H.-B.; Guo, D.-M.; Wang, X.-L.; Wang, Y.-Z. *Chem. Eng.* **2018**, *336*, 622-632.

78. Jing, X.-K.; Wang, X.-S.; Guo, D.-M.; Zhang, Y.; Zhai, F.-Y.; Wang, X.-L.; Chen, L.; Wang, Y.-Z. *J. Mater. Chem. A* **2013**, *1*, 9264-9272.

79. Dong, X.; Chen, L.; Duan, R.-T.; Wang, Y.-Z. *Polym. Chem.* **2016**, *7*, 2698-2708.

80. Guo, D.-M.; Fu, T.; Ruan, C.; Wang, X.-L.; Chen, L.; Wang, Y.-Z. *Polymer* **2015**, *77*, 21-31.

81. Liu, B.-W.; Chen, L.; Guo, D.-M.; Liu, X.-F.; Lei, Y.-F.; Ding, X.-M.; Wang, Y.-Z. *Angew. Chem. Int. Ed.* **2019**, *58*, 9188-9193.

82. Brydson, J. A. 26 - Epoxide Resins. In *Plastics Materials (Seventh Edition)*, Brydson, J. A., Ed. Butterworth-Heinemann: Oxford, 1999; pp 744-777.

83. Oldring, P. K. T., Coatings, Colorants, and Paints. In *Encyclopedia of Physical Science and Technology (Third Edition)*, Meyers, R. A., Ed. Academic Press: New York, 2003; pp 175-190.

84. Hu, J.; Shan, J.; Wen, D.; Liu, X.; Zhao, J.; Tong, Z. *Polym. Degrad. Stab.* **2014**, *109*, 218-225.

85. Xu, W.; Wirasaputra, A.; Liu, S.; Yuan, Y.; Zhao, J. *Polym. Degrad. Stab.* **2015**, *122*, 44-51.

86. Yang, J.-W.; Wang, Z.-Z.; Liu, L. *J. Appl. Polym. Sci.* **2017**, *134*.

87. Chen, T.; Chen, X.; Wang, M.; Hou, P.; Jie, C.; Li, J.; Xu, Y.; Zeng, B.; Dai, L. *Polym. Adv. Technol.* **2018**, *29*, 603-611.

88. Howell, B. A.; Lienhart, G. W.; Livingstone, V. J.; Aulakh, D. *Polym. Degrad. Stab.* **2020**, *175*, 109110.

89. Wirasaputra, A.; Yao, X.; Zhu, Y.; Liu, S.; Yuan, Y.; Zhao, J.; Fu, Y. *Macromol. Mater. Eng.* **2016**, *301*, 982-991.

90. Wang, P.; Cai, Z. *Polym. Degrad. Stab.* **2017**, *137*, 138-150.

91. Wang, P.; Chen, L.; Xiao, H. *J. Anal. Appl. Pyrolysis* **2019**, *139*, 104-113.

92. Huo, S.; Liu, Z.; Wang, J. *J. Therm. Anal. Calorim.* **2020**, *139*, 1099-1110.

93. Huo, S.; Wang, J.; Yang, S.; Li, C.; Wang, X.; Cai, H. *Polym. Degrad. Stab.* **2019**, *159*, 79-89.

94. Zhang, Q.; Wang, J.; Yang, S.; Cheng, J.; Ding, G.; Huo, S. *Compos. B Eng.* **2019**, *177*, 107380.

95. Huo, S.; Wang, J.; Yang, S.; Chen, X.; Zhang, B.; Wu, Q.; Zhang, B. *Polym. Adv. Technol.* **2018**, *29*, 497-506.

96. Wang, P.; Xiao, H.; Duan, C.; Wen, B.; Li, Z. *Polym. Degrad. Stab.* **2020**, *173*, 109078.

97. Xu, M.; Zhao, W.; Li, B.; Yang, K.; Lin, L. *Fire Mater.* **2015**, *39*, 518-532.

98. Huo, S.; Yang, S.; Wang, J.; Cheng, J.; Zhang, Q.; Hu, Y.; Ding, G.; Zhang, Q.; Song, P. *J. Hazard. Mater.* **2020**, *386*, 121984.

99. Jiao, C.; Zhuo, J.; Chen, X.; Li, S.; Wang, H. *J. Therm. Anal. Calorim.* **2013**, *114*, 253-259.

100. Xu, Y.-J.; Shi, X.-H.; Lu, J.-H.; Qi, M.; Guo, D.-M.; Chen, L.; Wang, Y.-Z. *Compos. B Eng.* **2020**, *184*, 107673.

101. Zhu, Z.; Lin, P.; Wang, H.; Wang, L.; Yu, B.; Yang, F. *J. Mater. Sci.* **2020**, *55*, 12836-12847.

102. Wang, G.; Nie, Z. *Polym. Degrad. Stab.* **2016**, *130*, 143-154.

103. Wang, S.; Ma, S.; Xu, C.; Liu, Y.; Dai, J.; Wang, Z.; Liu, X.; Chen, J.; Shen, X.; Wei, J.; Zhu, J. *Macromolecules* **2017**, *50*, 1892-1901.

104. Toan, M.; Park, J.-W.; Kim, H.-J.; Shin, S. *Fire Mater.* **2019**, *43*, 717-724.

105. Agrawal, S.; Narula, A. K. *J. Therm. Anal. Calorim.* **2014**, *115*, 1693-1703.

106. Shao, Z.-B.; Tang, Z.-C.; Lin, X.-Z.; Jin, J.; Li, Z.-Y.; Deng, C. *Mater. Des.* **2020**, *187*, 108417.

107. Sun, J.; Yu, Z.; Wang, X.; Wu, D. *ACS Sustain. Chem. Eng.* **2014**, *2*, 231-238.

108. Amarnath, N.; Appavoo, D.; Lochab, B. *ACS Sustain. Chem. Eng.* **2018**, *6*, 389-402.

109. Liu, F.; Wei, H.; Huang, X.; Zhang, J.; Zhou, Y.; Tang, X. *J. Macromol. Sci. B* **2010**, *49*, 1002-1011.

110. Liu, H.; Wang, X.; Wu, D. *Polym. Degrad. Stab.* **2014**, *103*, 96-112.

111. Liu, H.; Wang, X.; Wu, D. *Polym. Degrad. Stab.* **2015**, *118*, 45-58.

112. Zhou, L.; Zhang, G.; Li, J.; Jing, Z.; Qin, J.; Feng, Y. *J. Therm. Anal. Calorim.* **2017**, *129*, 1667-1678.

113. Zhou, L.; Zhang, G.; Feng, Y.; Zhang, H.; Li, J.; Shi, X. *J. Mater. Sci.* **2018**, *53*, 7030-7047.

114. Cheng, J.; Wang, J.; Yang, S.; Zhang, Q.; Huo, S.; Zhang, Q.; Hu, Y.; Ding, G. *Compos. B Eng.* **2019**, *177*, 107440.

115. Allen, C. W. *J. Fire Sci.* **1993**, *11*, 320-328.

116. Liu, B.-W.; Zhao, H.-B.; Tan, Y.; Chen, L.; Wang, Y.-Z. *Polym. Degrad. Stab.* **2015**, *122*, 66-76.

117. Kim, D. H.; Kim, Y.; Goh, M. *J. Appl. Polym. Sci.* **2020**, *n/a*, 49422.

118. Rad, E. R.; Vahabi, H.; de Anda, A. R.; Saeb, M. R.; Thomas, S. *Prog. Org. Coat.* **2019**, *135*, 608-612.

119. Wang, X.; Guo, W.; Song, L.; Hu, Y. *Compos. B Eng.* **2019**, *179*, 107487.

120. Miao, J.-T.; Yuan, L.; Guan, Q.; Liang, G.; Gu, A. *ACS Sustain. Chem. Eng.* **2017**, *5*, 7003-7011.

121. Meng, J.; Zeng, Y.; Zhu, G.; Zhang, J.; Chen, P.; Cheng, Y.; Fang, Z.; Guo, K. *Polym. Chem.* **2019**, *10*, 2370-2375.

122. Pourchet, S.; Sonnier, R.; Ben-Abdelkader, M.; Gaillard, Y.; Ruiz, Q.; Placet, V.; Plasseraud, L.; Boni, G. *ACS Sustain. Chem. Eng.* **2019**, *7*, 14074-14088.

123. Dai, J.; Peng, Y.; Teng, N.; Liu, Y.; Liu, C.; Shen, X.; Mahmud, S.; Zhu, J.; Liu, X. *ACS Sustain. Chem. Eng.* **2018**, *6*, 7589-7599.

124. Chi, Z.; Guo, Z.; Xu, Z.; Zhang, M.; Li, M.; Shang, L.; Ao, Y. *Polym. Degrad. Stab.* **2020**, *176*, 109151.

125. Ma, S.; Liu, X.; Jiang, Y.; Fan, L.; Feng, J.; Zhu, J. *Sci. China Chem.* **2014**, *57*, 379-388.

126. Zhang, J.; Mi, X.; Chen, S.; Xu, Z.; Zhang, D.; Miao, M.; Wang, J. *Chem. Eng.* **2020**, *381*, 122719.

127. Wang, D.-Y.; Song, Y.-P.; Lin, L.; Wang, X.-L.; Wang, Y.-Z. *Polymer* **2011**, *52*, 233-238.

128. Yuan, X.-Y.; Wang, D.-Y.; Chen, L.; Wang, X.-L.; Wang, Y.-Z. *Polym. Degrad. Stab.* **2011**, *96*, 1669-1675.

129. Xiong, J.-F.; Luo, S.-H.; Wang, Q.-F.; Wang, Z.-Y.; Qi, J. *Des. Monomers Polym.* **2013**, *16*, 389-397.

130. Xiong, J.-F.; Wang, Q.-F.; Peng, P.; Shi, J.; Wang, Z.-Y.; Yang, C.-l. *J. Appl. Polym. Sci.* **2014**, *131*.

131. Liu, P.; Dong, L.; Wu, L.; Zeng, L.; Xu, J. *RSC Advances* **2019**, *9*, 7147-7155.

132. Yan, X.; Li, Z.; Zhou, W.; Jiang, M.; Liu, P.; Xu, J. *J. Therm. Anal. Calorim.* **2016**, *126*, 1301-1311.

133. Mosurkal, R.; Kirby, R.; Muller, W. S.; Soares, J. W.; Kumar, J. *Green Chem.* **2011**, *13*, 659-665.

134. Hsieh, C.-Y.; Su, W.-C.; Wu, C.-S.; Lin, L.-K.; Hsu, K.-Y.; Liu, Y.-L. *Polymer* **2013**, *54*, 2945-2951.

135. Hsu, C.-Y.; Han, W.-G.; Chiang, S.-J.; Su, W.-C.; Liu, Y.-L. *RSC Advances* **2016**, *6*, 4377-4381.

136. Gao, S.; Liu, Y.; Feng, S.; Lu, Z. *J. Polym Sci. A Polym. Chem.* **2017**, *55*, 2390-2396.

137. Indulekha, K.; Thomas, D.; Supriya, N.; Rajeev, R. S.; Mathew, D.; Ninan, K. N.; Gouri, C. *Polym. Degrad. Stab.* **2018**, *147*, 12-24.

1.6. Supporting Information

Table S1. Reference Table of Compounds

Compound	Name	Abbrv.	Ref.
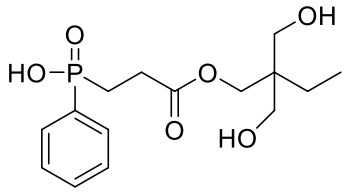 **1**	5-hydroxy-3-(2-hydroxyethyl)-3-methylpentyl-3-[2-carboxyethylphenylphosphine]propanoate	HMCPP	14
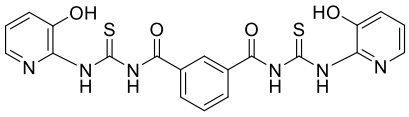 **2**	isophthaloyl bis(3-(3-hydroxopyridyl)thiourea)	IBHPT	15
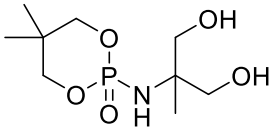 **3**	2-(5,5-dimethyl-2-oxo-2λ^5-1,3,2-dioxaphosphinan-2-ylamino)-2-methyl-propane-1,3-diol	PNMPD	25, 26
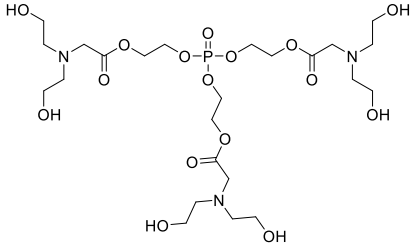 **4**	tri(N,N-bis-(2-hydroxy-ethyl)acyloxoethyl) phosphate	TNAP	29
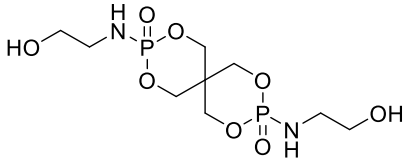 **5**	pentaerythritol di-N-hydroxyethyl phosphamide	PDNP	29, 33

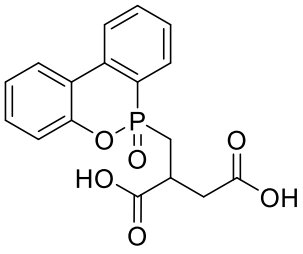 **6**	9,10-dihydro-10-[2,3-di(hydroxycarbonyl)propyl]-10-phosphaphenanthrene-10-oxide	DPP	48
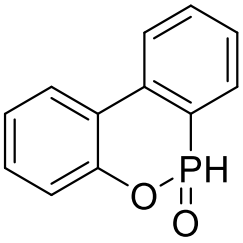 **7**	9,10-dihydro-9-oxa-10-phosphaphenanthrene-10-oxide	DOPO	Mlt.
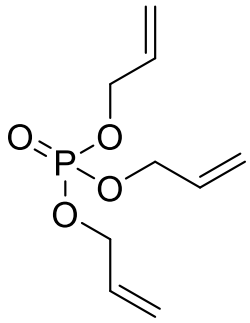 **8**	triallyl phosphate	TAP	72
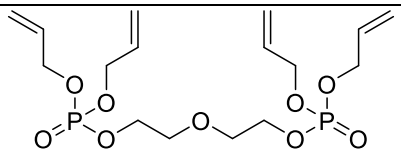 **9**	diethylene glycol (DEG) bridged tetraallyl diphosphate	D-TAP	72
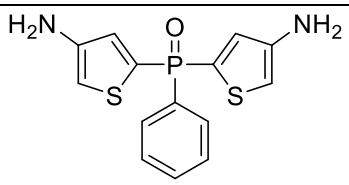 **10**	bis(3-amino-2-thienyl)phenylphosphine oxide	ABTPPO	97

Chapter 2. Synthesis, characterization, and foamability of wholly aromatic, water-soluble sulfonated polyimides

Benjamin J. Stovall*, Clay B Arrington*, Johanna Vandenbrande*, Joshua B. Dinaburg[1], Gerard G. Back[1], and Bran Y. Lattimer[1] and Timothy E. Long*

*Department of Chemistry, Macromolecules Innovation Institute (MII), Virginia Tech, Blacksburg, VA, 24061
[1]Jensen Hughes, Baltimore, MD 21227

2.1. Abstract

Traditionally, polyimides like Kapton™ are thought of as rugged, unprocessable polymers due to their high glass transition temperatures and insolubilities. A limited number of "water-soluble" polyimides and polyimide precursors have been reported previously. However, due to more complicated synthetic steps, incorporation of alkyl linkers and halogenated substituents, or additional chemical modification, this may not be as desirable for certain applications and green chemistry considerations, especially when looking to reduce adverse effects on the environment. In the current work, sulfonated polyimides (sPI, Kapton™ derivatives) with wholly aromatic backbones from pyromellitic dianhydride (PMDA), the sodium salt of 4,4'-diaminodiphenyl-2,2'-disulphonic acid (BDSA-Na), and 4,4'-oxydianiline (ODA) are made from a facile 2-step synthetic method using just dimethyl sulfoxide (DMSO) as the reaction solvent followed by subsequent thermal imidization. These copolymers exhibit high thermal stability (> 450 °C) and produce free-standing films with varying flexibility and water solubility depending on the diamine monomer ratio. Polyimides of this type are promising for use in coatings and adhesives as well as electronic components, medical devices, and fluorine-free fire-fighting foams.

2.2. Introduction

Aromatic polymers exhibit excellent thermal stability, chemical resistance, insulating behavior, and thermomechanical performance, which enables their wide application in the fields of aerospace and microelectronics.[1-5] Polyimides especially have been at the forefront of these applications.[6-9] Conversely, synthetic challenges limit the development of highly aromatic polyimides for aqueous applications. There have been numerous examples of water-soluble polyimide precursors, utilizing such techniques as the versatile poly(amic acid) (PAA) salt method. This method employs a suitable base to neutralize the carboxylic acid groups of the PAA.[10-11] Neutralization of the acid groups to form a salt imparts water solubility at a high enough degree. While this method has many practical advantages, after imidization, the resulting polyimides are insoluble in water. In a similar vein, Saadeh et al.[12] used various synthetic methods to give aromatic diamines with carboxylic acid moieties, either pendent or linked with an alkyl spacer to the phenyl rings. Following polymerization and imidization, these polyimide carboxylic acids are converted to carboxylate ammonium salts, which impart water solubility to the polyimide. Carboxylic acid and carboxylate moieties generally exhibit low thermal stability, which ultimately affects the operating temperature of the corresponding polyimides. Additionally, the synthesis of aromatic diamine carboxylic acid monomers requires harsh reaction conditions, metal catalysts, multiple reaction steps, and gives low yields.

Another standard method to impart water solubility in polymers is to utilize sulfonate or sulfonic acid groups. Sulfonated cellulose derivatives and sulfonated polystyrene are notable examples. Although many high-performance aromatic polymers such as poly(ether ether ketone),[13-14] polysulfone,[15-16] and polyimide[17-18] are used in their sulfonic acid forms for fuel cell applications and are not readily soluble in aqueous media, these polymers may become water-

soluble with high enough degrees of sulfonation. Synthetic techniques of these polymers, especially polyimides, can be challenging, requiring disagreeable solvents such as m-cresol to adjust for monomer solubility or various post-polymerization sulfonation methods, which make it challenging to control precision and degree of sulfonation.[15, 17]

However, the continual development of the disulfonic acid-containing diamine monomers enables facile production of readily water-soluble, wholly aromatic polyamides.[19-20] In light of recent advances, we present the design and facile synthesis of a family of sulfonated aromatic polyimides to explore their intrinsic properties and potential applications. The polymers are synthesized using the classic two-step polymerization of polyimides in dimethyl sulfoxide, a relatively benign and green solvent. Use of the sodium salt of 4,4'-diaminodiphenyl-2,2'-disulfonic acid (BDSA) imparted water solubility to the aromatic, rigid backbone while maintaining highly thermally stabile moieties. Modification of the polymer backbone through copolymerization with non-sulfonated monomers (4,4'-oxydianiline, ODA) permitted facile modularity.

These polymers can be useful in several applications for adhesion and coatings. However, an area of research in replacing water-based fluorinated surfactant formulations that combat liquid fuel (gasoline, jet fuel) fires has been gathering significant traction due to interest from the U.S. Congress and the Department of Defense. Perfluoroalkyl substances (PFAS) such as perfluorooctanoic acid (PFOA) and perfluorosulfonic acid (PFSA) are the main ingredients in aqueous film-forming foams (AFFF) used by military and civilian airports to fight fuel fires. However, they pose many environmental hazards, including persistence, bioaccumulation, and toxicity (PBT). These PFAS easily migrate to affect populations not directly exposed to PFAS/ AFFFs. A recent report by Harvard and the USEPA detected PFAS in drinking water at 664

military training facilities and 533 civilian airports.[21] Currently, there are many remedial studies (DOD, proprietary, academic) that explore polymers, proteins, and siloxanes for surfactant roles for fluorine-free foams. These generally fall short of attaining the performance of AFFF and satisfying the requirements of the U.S. Military for fire-fighting foams, however.[22-24] Thusly, the development of a modular family of water-soluble polyimides can facilitate the exploration of the use of high-performance aromatic polymers as replacements for PFAS in fire-fighting foams.

2.3. Experimental

Materials: Sodium dodecyl sulfate (SDS) (Sigma Aldrich, 98%), hydrochloric acid (Fisher Chemical, certified ACS), deuterated chloroform (CIL, 99.8%), deuterated dimethyl sulfoxide (DMSO- d_6) (CIL, 99. %) were used as received. Dimethyl sulfoxide anhydrous (Acros Organics, 99.5%) and N-methyl-2-pyrrolidone anhydrous (NMP) (Acros Organics, 99.5%) were stored over activated molecular sieves. Pyromellitic dianhydride (PMDA) (Acros Organics, > 98%), and 4, 4'-oxydianiline (ODA) (Acros Organics, 98%) were sublimed before use. 2,2'-Benzidinedisulfonic acid (BDSA) (TCI, > 70 %) was titrated with NaOH and stored in a vacuum oven at 150 °C before use.

Analytical Methods: ^{1}H nuclear magnetic resonance (NMR) spectroscopy was performed using a Varian Unity U4-DD2 400 (400 MHz) at 25 °C. $CDCl_3$ or DMSO-d_6 was used as the solvent for NMR analysis. Thermogravimetric analysis (TGA) was performed on a T.A. Instruments Q500 with a 10 °C/min heating rate from 25 °C to 600 °C/1000 °C under N_2 or air. Differential scanning calorimetry (DSC) was conducted using a T.A. Instruments Q2000 DSC coupled with an RCS90 cooling system, utilizing a heat/cool/heat cycle with a 30 °C/min rate and N_2 cell purge. Glass transition (T_g) values (if present) were determined from the midpoint of the thermal transition in

the second heat cycle using T.A. Universal Analysis software. Dynamic mechanical analysis (DMA) was performed on a T.A. Instruments Q800 in tension mode at a frequency of 1Hz with an oscillatory amplitude of 5 μm, a static force of 0.01 N, and a force track of 125%. Samples were heated at 3 °C/min to 400 °C. FTIR analysis was performed using a Nicolet iS5 equipped with an iD7 ATR stage at room temperature. Water uptake/ sorption was analyzed with a T.A. Instruments Q5000 (TGA-SA) via an isohume experiment. Sample films were subject to a 1 h pre-dry at 60 °C. When the temperature was reduced to 25 °C and humidity increased to 95%, the experiment was initiated. The experiment was terminated if the sample reached an equilibrium state (<0.01% of weight change within 10 min). Water uptake was determined relative to film pre-dried weight. Optical microscopy was performed on a Nikon LV100.

Representative poly(amic acid) synthesis (50 mol% BDSA-Na). A two-neck round bottom flask equipped with a magnetic stir bar and nitrogen inlet was charged with BDSA-Na (0.4451 g, 1.146 mmol) and ODA (0.2295 g, 1.146 mmol). The flask was evacuated and refilled with N_2 three times before the addition of 8-10 mL of anhydrous DMSO. Following complete dissolution of the amines, PMDA (0.5000 g, 2.292 mmol) was added to the solution with an additional 2-3 mL of DMSO. The resultant viscous solution was allowed to stir under nitrogen for 12 h before being stored in a refrigerator at 8 °C until ready to use.

Film fabrication. The poly(amic acid) solution was allowed to warm to room temperature and was bladed onto a glass slide on a level surface (additional DMSO or NMP added if necessary). The slide was then placed into a vacuum oven and kept at room temperature for 1 hour before being slowly ramped to 200 °C. The film was then held at 200 °C for 0.5 h and then transferred to a vacuum chamber residing in a metal bath. The chamber was then heated slowly (approximately 2 °C/min) to 400 °C and held at that temperature for 1 h. Films were then cooled slowly to room

temperature and delaminated using acetone (if needed) and then dried at 60 °C overnight and stored in a desiccator before analysis. Film thickness approximately ranged between 0.003 mm and 0.006 mm for TGA and 0.008-0.010 mm for FTIR.

Foam formulation and testing. sPI in powdered form (100 mol% BDSA-Na) was dissolved in water at 3 %(w/v) and 6 %(w/v) at 80 °C. Following full dissolution, SDS was then added at a concentration of 0.15 %(w/v). At Jensen Hughes, these were mixed on the gallon scale, sprayed onto a foam drainage board through a Mil-SPEC (MIL-F-24385F) regulation nozzle with an application rate of 2 gal/ min. The resultant foam was drained into a 1 L graduated cylinder, and drainage time was calculated when 25% fluid of the total foam volume had drained. The expansion ratio was calculated by dividing the total volume of foam by the total volume solution dispensed.

2.4. Results and Discussion

Synthesis of BDSA-Na/PMDA sulfonated polyimides and copolymers with ODA

Previous work performed by joint efforts of the Long group and others at Virginia Tech elucidated that telechelically sulfonated polyimide ionomers are not soluble or dispersible in water.[25-27] This prompted the exploration of polyimides with pendant sulfonate groups to promote water solubility. Because of its recent use in polyimide and polyamide literature, the diamine monomer BDSA was chosen to impart a high degree of sulfonation. **Scheme 1** shows the synthesis and copolymerization with ODA of wholly aromatic sulfonated polyimides via the classic two-step route to polyimide formation.

Polar aprotic solvents such as NMP or DMAc are conventionally used to facilitate poly(amic acid) (PAA) reactions.[28] DMSO, however, was needed to dissolve BDSA-Na as BDSA-Na is not soluble in any other typical organic solvents, including m-cresol. The classical two-step

polyimidization facilitated successful polymerization as opposed to the one-step method due to the instability of DMSO at temperatures around 180 °C as well as concerns over the final polyimide solubility in the reaction solvent. Later testing showed that the synthesized polyimides had a reduced solubility in DMSO. Various copolyimide compositions from 100% to 0% BDSA-Na: ODA were synthesized and discussed.

Scheme 1. Synthesis of PMDA/BDSA-Na sulfonated polyimide (sPI) and copolymers with ODA

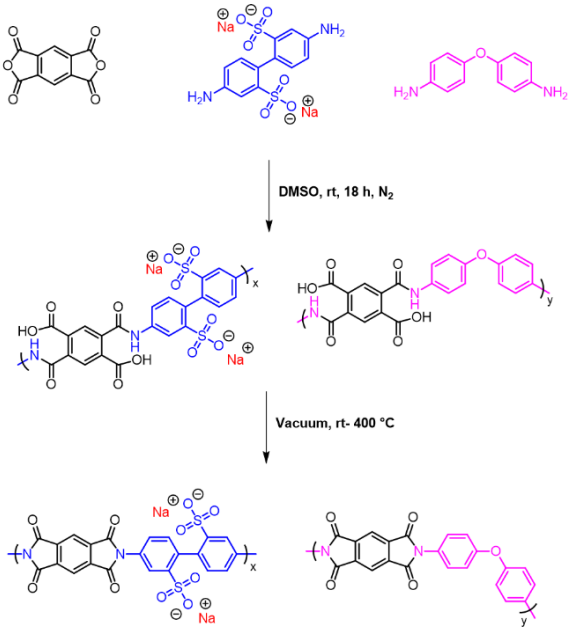

Initially, the polyimides were heated on a schedule to 350 °C to facilitate imidization. However, ^{1}H NMR and IR spectroscopy revealed residual amide groups, suggesting incomplete imidization. Analysis of the polymers heated to 400 °C still revealed residual amide signals. **Figure 1** depicts the ^{1}H NMR spectrum of the fully sulfonated PI, imidized up to 400 °C. At approximately 10.8 ppm, a small peak corresponding to the amide moiety of un-imidized amic acids was seen despite having raised the imidization temperature.

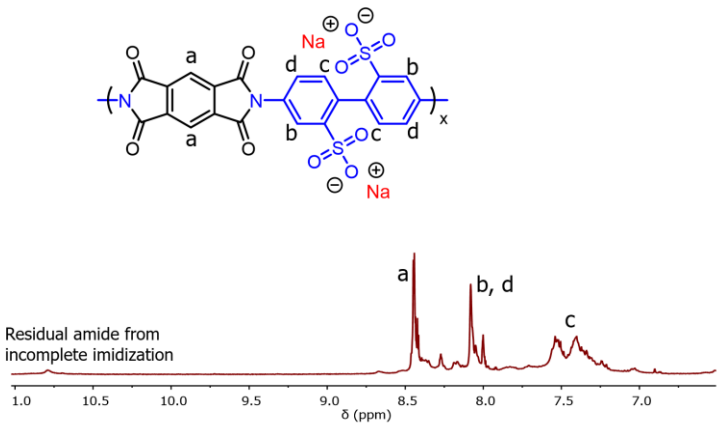

Figure 1. NMR spectrum of PMDA/BDSA-Na sPI. The residual amide peak is present at approximately 10.8 ppm (DMSO-d_6, 400 MHz)

IR spectroscopy further confirmed incomplete imidization. **Figure 2** shows an IR spectrum of the fully sulfonated PI imidized up to 400 °C. Despite the intense signal at 1750 cm^{-1} corresponding to the imide carbonyl stretch and the imide C-N stretch at 1380 cm^{-1}, the presence of the amic acid carbonyl stretch at approximately 1660 cm^{-1} indicates some degree of incomplete imidization. **Equation (1)**, where A is the area of the IR bands, enabled the comparison of the polyimides prepared at different temperatures. The C=C stretch at 1500 cm^{-1} corresponding to the para-substituted benzene rings in the backbone was the internal standard, while the C-N imide stretch at 1380 cm^{-1} quantified imidization (degree of imidization, DOI) as it is least hindered by other bands.[29]

$$DOI\% = \frac{(A_{1380}/A_{1500})_{350°}}{(A_{1380}/A_{1500})_{400°}} \times 100 \quad \textbf{(1)}$$

The comparison of samples heated to 200 °C to 400 °C revealed differences in the degrees of imidization **(Figure 3**). From between 300 °C to 400 °C, there is less than a 5% change in DOI, and above 350 °C, differences were negligible. This suggested a kinetic stop in the process of

imidization. A kinetic stop describes the retardation of imide cyclization in the late stages of the imidization procedure at higher temperatures. Cyclization at temperatures of approximately 180-250 °C is relatively fast but quickly slows down. At higher temperatures, the imidization rate is rapidly decreased as the reaction is limited by amic acid diffusion rate to the activated from the inactive state. Glass transition temperature (T_g) greatly influences imidization kinetics due to its effect on the entropy of poly(amic acid); a higher T_g restricts molecular motion and hence decreases the entropy of amic acid groups at high levels of imidization.[30-31] The T_gs of the sPIs were undiscernible from DSC or DMA, which supports the conclusion of a kinetic stop, the limit of attainable degree of imidization. Samples for the remainder of the study were imidized up to 400 °C to ensure as complete imide formation as possible while not exceeding the limits of our equipment and, more importantly, the thermal stability of the polymer samples themselves.

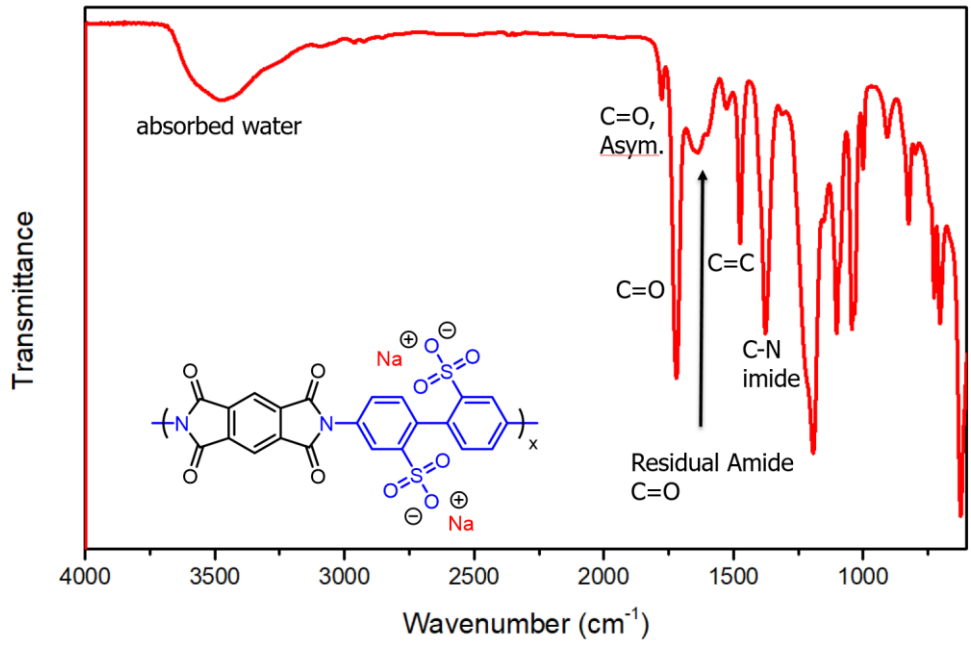

Figure 2. IR spectrum of PMDA/BDSA-Na sPI

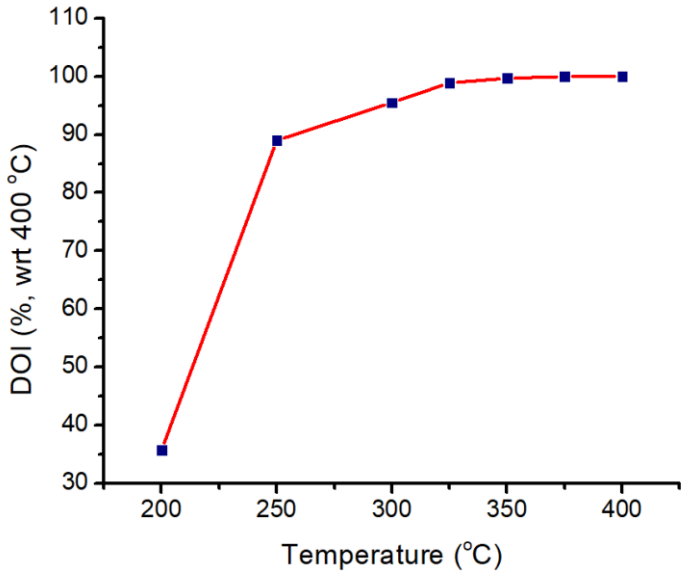

Figure 3. Degree of imidization of films heated at different temperatures for 1 h. With respect to films heated at 400 °C, DOI starts to plateau at approximately 350 °C.

Film Formation and Water Solubility of sPIs

All compositions of the sPIs produced free-standing films of varying mechanical robustness. As the content of ODA increased, the cast polymer films became increasingly more robust and creasible. Copolyimides containing 100 mol% and 75 mol% BDSA gave very brittle and increasable films; however, thoroughly dried thin films of the sPIs exhibited flexibility and moderate creasibility. Following water uptake, films with high degrees of sulfonation (≥50%) began to lose mechanical integrity, becoming softer and breaking up even more easily. This is attributed to the hydrophilic nature of the sulfonate groups, which allowed water to act as a plasticizer.[32]

TGA-SA at 95 % RH enabled a more quantitative study of water uptake of the sPI films (**Figure 4**). Unsurprisingly, the 100 mol% BDSA-Na sPI exhibited the most significant water sorption at approximately 50 wt% after 300 min. As the mol% of the hygroscopic BDSA-Na monomer (content of the sulfonate groups) increases, the hygroscopic nature of the sPI polymers

increases thusly, along with water uptake. A trend is linear across all compositions within the testing parameters, and the maximum water uptake/ wt% increase of the polymer films can be determined. The data can also inform correlations to water solubility through compositional behavior.

Loading of the copolyimides at 3 wt% in DI water ascertained their water solubility (**Table 1**) while also providing a metric to compare with typical fire-fighting foam concentrates. Polymers with above 75 mol% BDSA-Na content exhibited excellent solubility in aqueous solution, even at much higher wt% loadings. Over a few days, however, the 75 mol% polymers became less stable in solution, as evidenced by the crashing out of solids. 0 mol% and 25 mol% polymers were not water-soluble in either their PI or PAA (non-neutralized) forms. While the PAA of the 50 mol% BDSA-Na polymer was water-soluble, the PI was less so; it only appeared to swell. Replacement of the BDSA-Na with *p*-phenylene diamine (PPD) enabled water solubility 50 mol%, however. This can be attributed to a reduction in the weight percent of the non-sulfonated aromatic content (**Figure S4**).

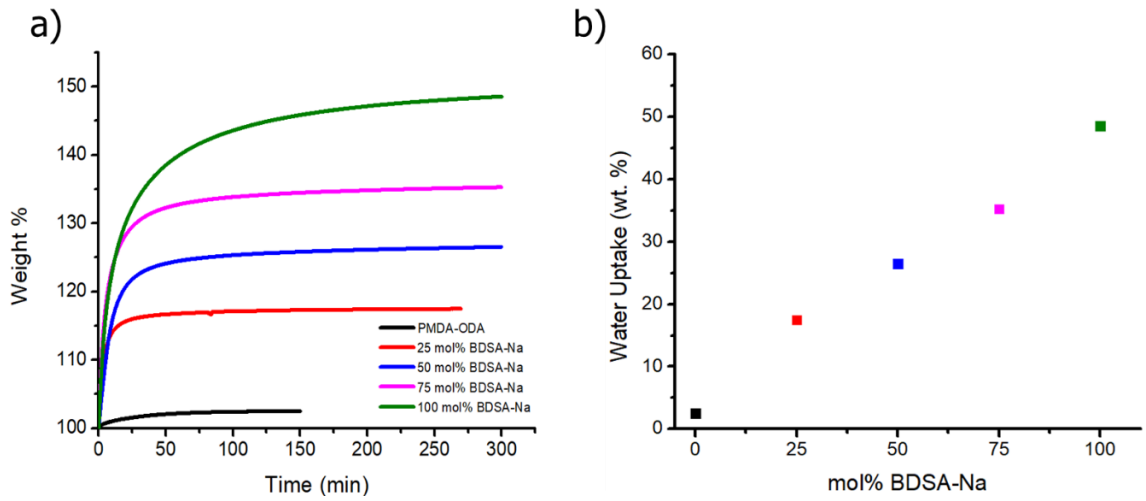

Figure 4. a) A plot of wt% increase vs. time for various sPI compositions. b) Plot of water uptake vs. composition in mol% BDSA-Na. As the mol% of BDSA-Na increases in the polymer composition, water uptake increases linearly

Table 1. Water solubility and creasability of sPI series of PMDA-BDSA-Na/ PMDA-ODA

BDSA-Na mol%	Polyamic acid solubility	Polyimide solubility	Dry polyimide Creasability
0	-	-	++
25	-	-	++
50	+	-	+
75	++	+	-
100	++	++	-

Thermal analysis of sPIs

TGA elucidated the weight loss profiles of the varying sPI compositions. $T_{d,5\%}$ of all compositions was reduced relative to the PMDA-ODA polyimide. Desulfonation, occurring at around 450 °C for the fully sulfonated PI, is responsible for reducing the weight loss temperatures of the PIs (**Figure 5a**). As the content of BDSA-Na is increased from 50 mol% to 100 mol% and thusly the degree of sulfonation, the $T_{d,5\%}$ decreased quite linearly (**Figure 5b**). Despite decreases in weight loss across compositions, char yields at 600 °C (under N_2) stayed relatively the same, between approximately 65-70%, which indicated the efficient formation of carbonaceous material during degradation. Such high char yields can be expedient if paired with flame suppression applications, potentially reducing the production of toxic degradation products. The $T_{d,5\%,}$ and char yields at 600 °C (for sPIs with greater than 50 mol% BDSA-Na incorporation) under air did not change drastically from those polymers under nitrogen atmosphere (**Figure S6** and **Table S1**). This showed that the polymers are equally stable under atmospheric conditions at elevated temperatures up to their initial weight-loss temperatures. There seems to be a possible char insulating phenomenon related to sulfonate content occurring for these polymers above 600 °C, but this will require further systematic investigation. However, it is of note that all sPIs have higher char yields than PMDA-ODA under air at 1000 °C.

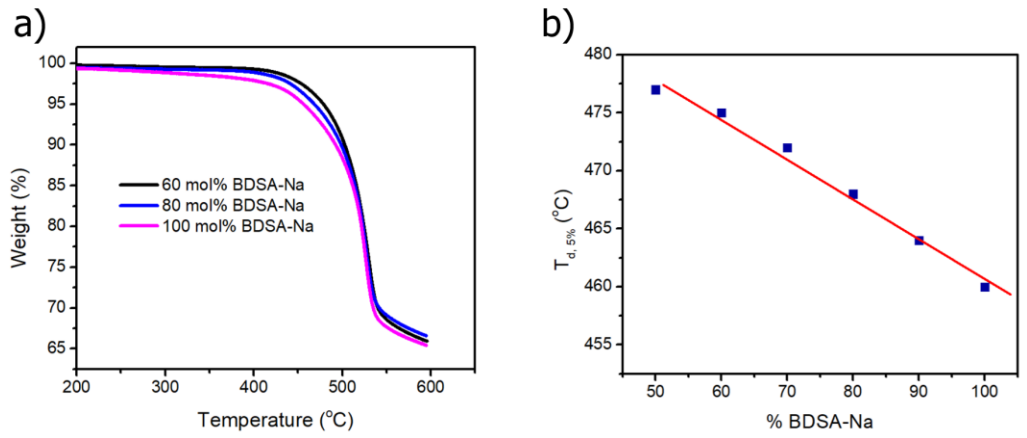

Figure 5. a) Representative weight loss profiles for sPI. b) Plot of $T_{d,5\%}$ vs. BDSA-Na content (10 °C/min ramp, N_2)

DSC did not discern any transitions for sPIs up to 400 °C. This observation was validated by the glass transition temperature of the 0 mol% BDSA-Na polymer (PMDA-ODA) being approximately 430 °C. Incorporating the BDSA-Na moiety was expected to increase the glass transition due to its highly rigid nature; the position of the sulfonate groups hinders the rotation of the phenyl groups along their axis.[17] Additionally, the incorporation of sulfonate groups invokes ionic interactions like aggregation, which also hinder internal movement.[14, 33] To further this conclusion, DMA yielded no observable transitions. While 100 mol% and 75 mol% BDSA-Na polymers were mostly too brittle to give adequate data, a 50 mol% polymer only showed slight relaxations in modulus, passing through no transitions (**Figure 6**). This is in contrast to PMDA-ODA, where the glass transition initiates at around 365 °C. The higher storage modulus is again related to the incorporation of the highly rigid BDSA-Na moieties. At a high level of incorporation, the films become very brittle.

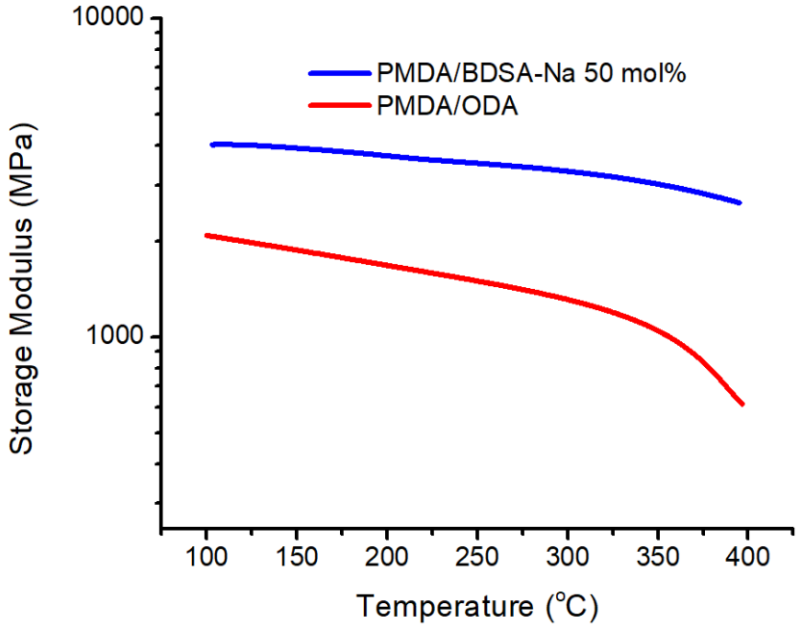

Figure 6. DMA of an sPI copolymer and pure PMDA/ODA. Notice the lower modulus and the beginning of a thermal transition (glass transition) of the PMDA/ODA at around 365 °C. Transitions for all polymers by DSC are unobservable (0.1% strain, 3 °C/min)

Foaming behavior of sPI in Aqueous Media

To initiate screening of the sPI for potential use in fluorine-free fire-fighting foams, we needed to qualify its foamability. Use of 100 mol% sPI assessed foaming formulations due to its excellent solubility and stability in aqueous solution. At 3 wt.% loading in DI water, minimal foaming was observed following agitation. Upon addition of 0.15 wt % sodium dodecyl sulfate, a well-studied, common commercial surfactant, stable foams were produced, which could persist upwards of thirty minutes in the vial and on a petri dish. SDS foams in the absence of polymer displayed markedly more deficient foaming and foam stability. **Figure 7** shows the differences in foaming. This is likely because the surfactant was loaded below its reported critical micelle concentration (CMC) of about 8 mM.[34] The synergistic effect seen in the mixture of the polymer and surfactant is likely attributed to the introduction of a critical aggregation concentration (CAC), or the point

of measurable association between polyelectrolyte and surfactant, which occurs at concentrations below the CMC of surfactant.[35]

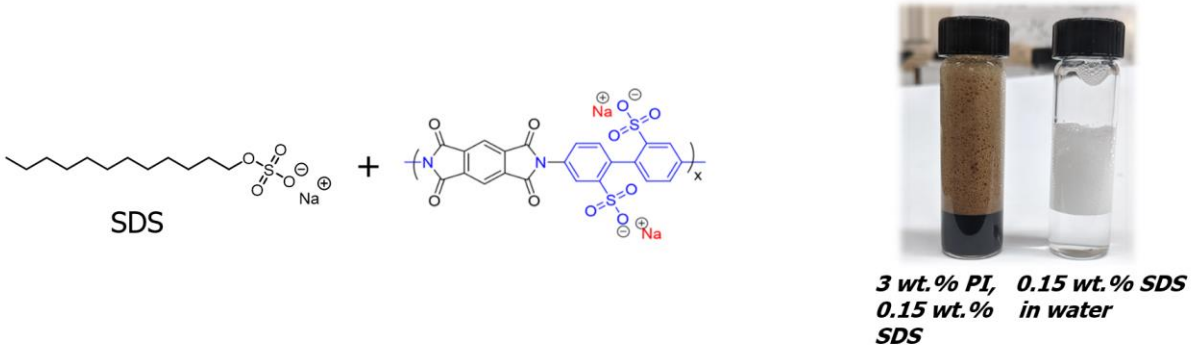

Figure 7. Formulation of polyimide foam. The addition of SDS enables polyimide to produce stable foams. Note the increase in foaming with agitation of polymer and surfactant over just the surfactant solution.

Initial production of the stable formulation enabled a large-scale synthesis (~300 g of dried sPI) to produce a usable amount of polymer for industrial foam testing. Material was sent to our collaborators at Jensen Hughes and tested against the Mil-SPEC (MIL-F-24385F) requirements for drainage time (DT) and expansion ratio (ER). For a foam formulation to be successful, DT cannot be less than 2.5 min for 25% of the initial foam volume, and ER cannot be lower than 5. As many commercial fire-fighting foam agents, solutions containing 3 wt% and 6 wt% of polymer were tested. The formulation of 3 wt% sPI and 0.15 wt% SDS in water exceeded the Mil-SPEC benchmark and exhibited drainage times of 3.80±0.08 min and an average expansion ratio of 6.93±0.16. Increasing the concentration of the sPI to 6%(w/v) yielded a drainage time of 4.24 ±0.03 min and expansion of 6.19±0.09, also exceeding the Mil-SPEC benchmark. The DT and ER increased and decreased, respectively, due to a perceivable increase in foam density resulting from a viscosity increase of the 6 wt% solution (**Figure S7)**.

Compared to the DT and ER of commercial AFFFs (BCI, Phoschek, Foamtec), the 3% and 6% sPI formulations fell below their target ER while maintaining competitive DT (**Figure 8**). Despite this, the correlations between ER/ DT and Mil-SPEC fire test success are hard to determine. Our collaborators at Jensen Hughes have been working very hard on correlation studies. Some commercial AFFFs are more successful than others, and many remain available despite failure to satisfy the Mil-SPEC. An in-depth discussion of formulation fire testing and other SERDP efforts can be found in the Addendum to this chapter.

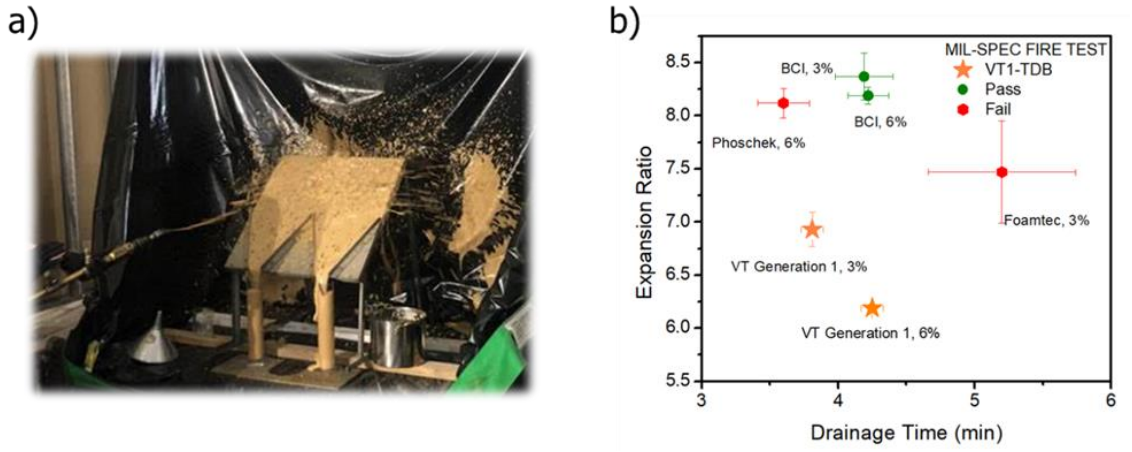

Figure 8. a) testing of polyimide foam at Jensen Hughes for drainage time and expansion ratio. b) Comparison of ER/DT for polyimide foams at 3 and 6 wt% concentrations compared to other commercial fire-fighting foams. There is an unclear correlation to fire test success.

2.5. Conclusions

Sulfonated polymers have been a topic of interest in polymer science for decades. Researchers have studied sulfonated polyimides extensively, and yet there are still many fundamentals to be explored and applications to be considered. In this study, sodiosulfonated polyimides were synthesized via a facile 2-step synthetic route, characterized for their intrinsic properties, and preliminarily gauged their promise for AFFF replacement. sPIs at sulfonation degrees of less than

or equal to 50% formed robust and creasible films. All sPIs had competitive thermal stability compared to their non-sulfonated analogs, with weight loss temperatures over 460 °C and char yields above 60%. BDSA-Na content dictated polymer water sorption, and above 70% sulfonation (BDSA-Na content), sPIs were fully water-soluble. At 100% sulfonation, sPIs were evaluated for their foaming behavior. The addition of a surfactant sodium dodecyl sulfate (SDS) facilitated enhanced foaming behavior of the polymer solution and allowed for large-scale foam testing at Jensen Hughes. Compared to the Mil-SPEC benchmarks for ER and DT, 3 wt% and 6 wt% solutions of sPI and SDS exceeded the benchmarks, though they fell below other commercial AFFFs in terms of ER. These metrics have yet to be explicitly linked to Mil-SPEC fire test success. This study shows that these wholly aromatic, sulfonated polyimides can provide a promising platform in the efforts towards AFFF replacement.

2.6. Addendum

Table A1. Summary of Polymer Foam Generations and Revisions

Polymer Formulation	Description
Generation 1	**3 wt% sPI, 0.15 wt% SDS**
Generation 1, revision 1	**6 wt% sPI, 0.15 wt% SDS**
Generation 2	**3 wt% sPAAS with DMAEMA, 0.3 wt% SDS**
Generation 3	**3 wt% sPI, 0.15 wt% SDS, 0.3 wt% MTPP-Br, 0.3 wt%NaCl**
Generation 4	**3 wt% sPAAS with DMAE, 0.15 wt% SDS**
Generation 5	**3 wt% sPAAS with DMAE, 0.15 wt% SDS, 1 wt% MTPP-Br**
Generation 6	**3 wt% 40:60 sPI (Gen1): sPAAS with DMAE (Gen4), 0.15wt% SDS**
Generation 7	**3wt% 50:50 sPAAS with DMAEMA (Gen2): sPAAS with DMAE (Gen4), 0.3 wt% SDS**

Formulation of sulfonated poly(amic acid) salts (sPAAS)

Investigation of sulfonated poly(amic acid) salts aimed to provide a less time-consuming, synthetic route for polymeric surfactant production, affording a second major pathway. The sPAAS utilize the same synthetic procedure as the sPI without requiring the second thermal imidization step. Following PAA formation, amine-containing dimethylaminoethyl methacrylate (DMAEMA) facilitated neutralization to form the PAA salt (**Scheme A1**). Neutralization imparts two attributes to the PAA: increased hydrolytic and time stability via reduced intramolecular depolymerization,[16] and improved water solubility via further inclusion of polar interaction along the backbone. Likewise, by tethering methacrylate functionality, the sPAAS are cross-linkable via radical polymerization.

The sPAAS display improved water solubility (50 mol% BDSA-Na readily dissolve at over 30 wt.% loadings in water) relative to the imidized sPIs. Due to this, the 50 mol% BDSA-Na copoly(amic acid) was utilized for initial foam testing. Solutions of the sPAAS in water at 3 wt.%

produced modest foaming; however, incorporation of low wt.% (~ 0.3 wt.%) SDS yielded stable foams, which persisted in Petri dishes for ~ 25 min (**Figure A1**). Likewise, the addition of glycolic ethers and small molecular inorganic salts (i.e., NaCl) improved foam performance.

Scheme A1. Poly(amic acid) salt production using DMAEMA.

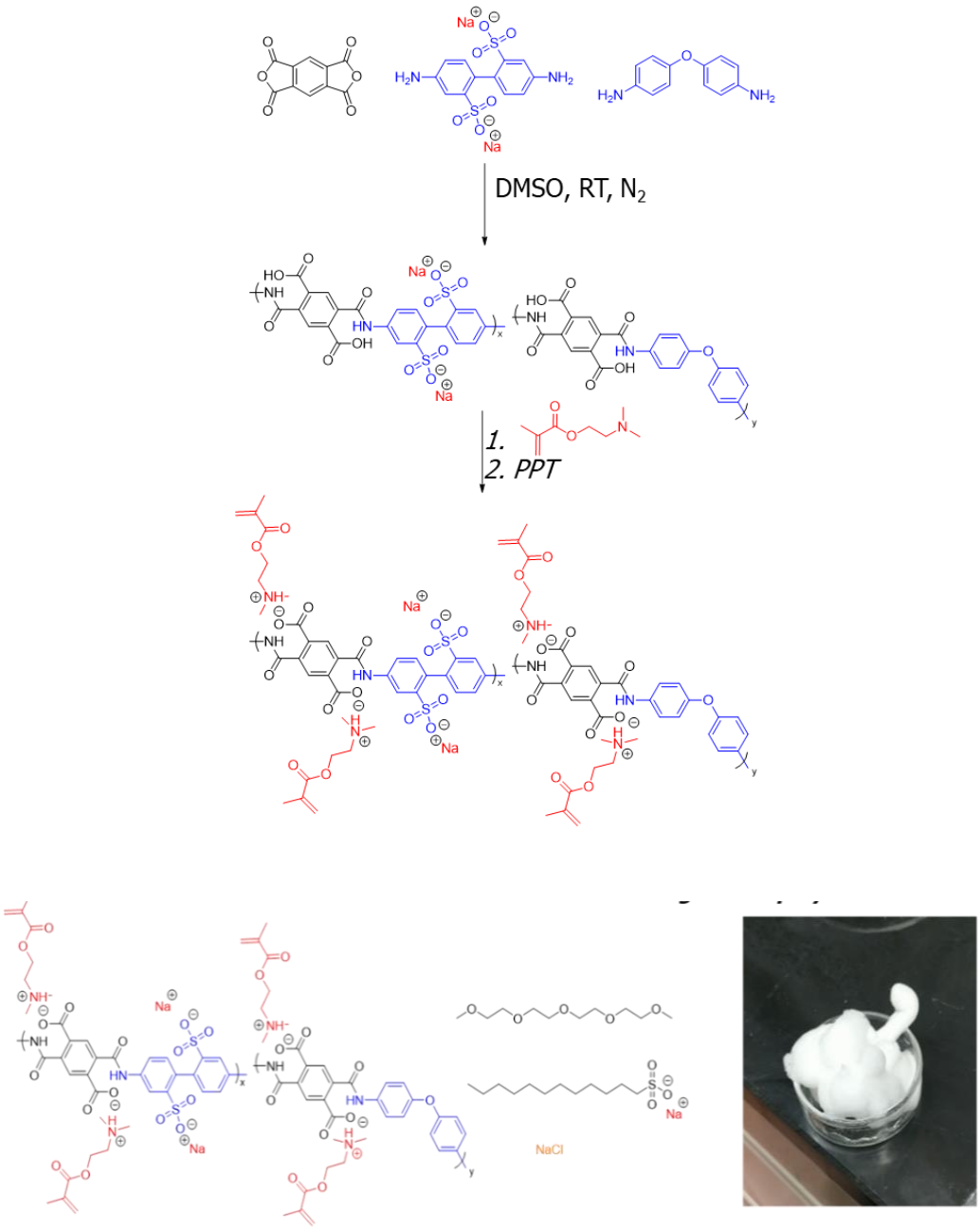

Figure A1. Aqueous sPAAS formulation components and foam. Amino acrylate units aim to provide crosslinking during flame suppression, combating migration of foams.

Inclusion of DMAEMA was hypothesized to improve charring through in-*situ* crosslinking during flame suppression. When coupled with a photoinitiator, sPAAS exhibit rapid photocrosslinking and produce high strength hydrogels at 20 wt.% loadings in water (**Figure A2**). From the photorheology, the sPAAS may be suitable for additive manufacturing using vat photopolymerization in water. Water-soluble, aromatic polyimide precursors for 3D printing would enable freeze-drying of printed hydrogels, permitting the formation of aerogel materials for potential insulating applications.

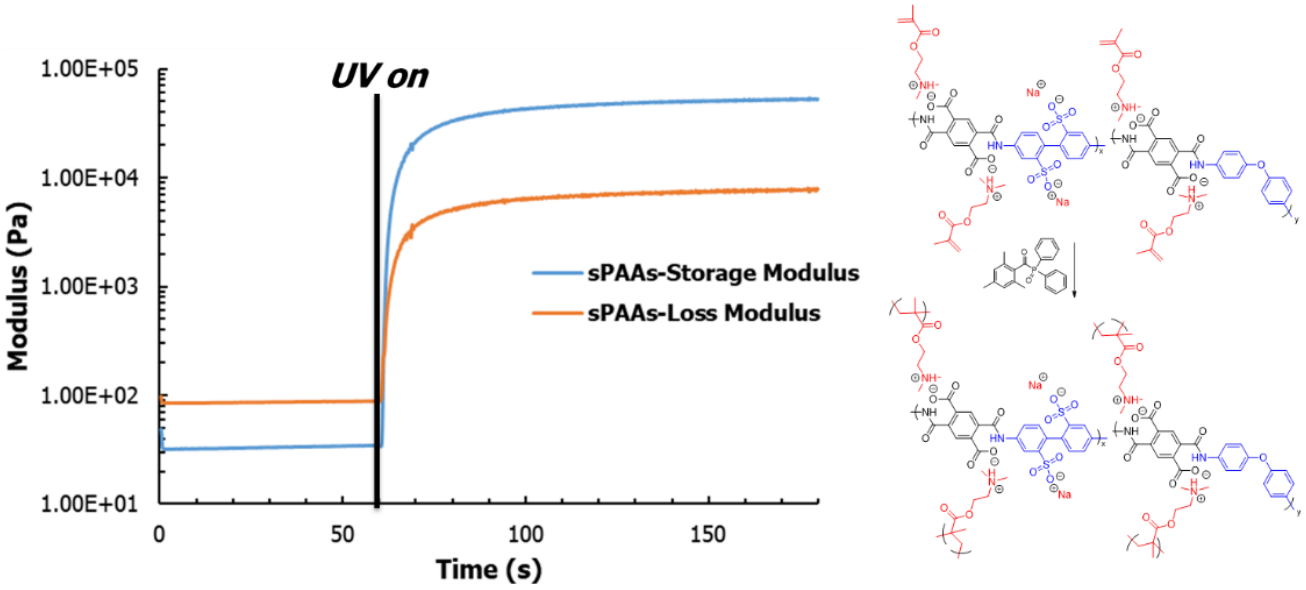

Figure A2. Photorheology of 20 wt.% sPAAS in water. Solutions produce rapid cross-over times and high moduli plateaus.

Efforts toward fire suppression of sPI and sPAAS formulations

During initial flame suppression and burnback testing of the 3 wt.% (Generation 1) and 6 wt.% (Generation 1, Revision 1) formulations on a 6" square pan containing hexane fuel, both formulations extinguished all but one corner of the pan, establishing suppression. The corner then

reignited the rest of the pan by 70 s for both loadings of the sPI. Foam stability tests were not conducted.

sPAAS based formulation (3 wt.% PAAs, 0.3 wt.% SDS, Generation 2) produced similar expansion and drainage to previous formulations (6.5 and 7 min). For a 1 x 1 ft gasoline fire involving a 10 s pre-burn and application of 405 g of expanded foam, the formulation was unable to extinguish the fire, hindering obtaining a burnback value, though it exhibited rapid fire control. Only small flamelets existed on the foam surface and edges after application. The ignition resistance of this formulation is greatly increased, however, attributed to chemical structure. Under higher radiant heating, 40 kW/m^2, thermal crosslinking of the polymer's acrylate sites delayed ignition by several minutes, with intermittent flashing and sustained flame (114 sec to flash, 134 sec to sustained ignition).

A similar poly(amic acid) salt, neutralized with dimethylaminoethanol (DMAE), was synthesized using the same synthetic methodology. The structure can be seen in **Figure A3.** The incorporation of DMAE instead of DMAEMA ascertained the ability of the sPAAS system to be modified. The addition of DMAE not only improved solubility but allowed for the controlling of the methacrylate concentration, which may affect fire control as C=C may react uncontrollably within a combustion environment, producing many radical species.

As a control, a formulation of sPAAS neutralized with DMAE (0.15 wt% SDS in 3 wt% solution, Generation 4) gave an average expansion ratio of 7.14 and drainage time of 3.00 min, comparable to the previous test. 405 g of foam (approximately equal to 90 seconds of spray from the MILSPEC nozzle onto a 28 ft² MILSPEC fire) almost extinguished a 1x1 ft gasoline fire apart from one corner and spread back to 25% in an additional 35 seconds. It prevented ignition on heated fuel for about 1 minute, and under 20kW/m^2, for about 2 minutes, both with flashing

intermittently. This is quite promising as the performance was not hindered by the modifications and may help to act synergistically with Generation 2.

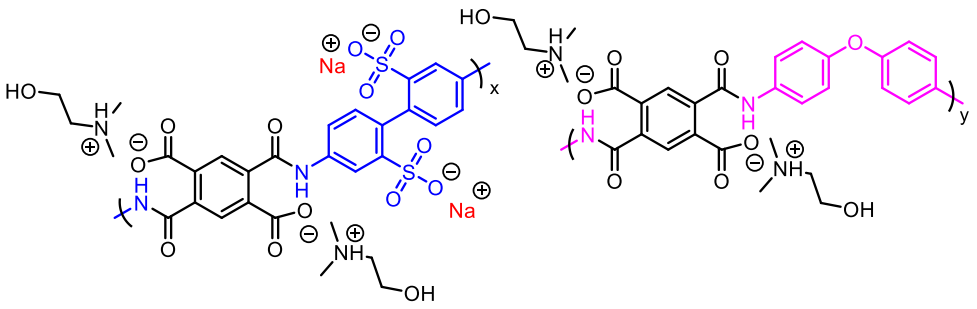

Figure A3. Structure of sPAAs neutralized with DMAE, Generation 4

Mixtures of various generations investigated any effects of mixing structure. First, a mixture of Generation 1 and Generation 4 material (Generation 6) was mixed in an approximate 40:60 ratio (0.15wt% SDS, 3wt% solution), achieving an ER of 7.25 drainage time of 3.02 min. Using the same testing protocol, this formulation (Generation 6) successfully extinguished a 1x1 gasoline pan fire in approximately 25 seconds, which none of the other generations achieved (**Figure A4)** Burnback, however, was deficient, as evidenced after the addition of the burnback pan the fire spread to 25% coverage within 20 seconds. This is a similar performance as compared to other FFFs. In terms of foam stability on fuel surface, under 0 kW/m^2, the first ignition sustained at 1min 33 sec after adding the foam to the fuel, and under 20 kW/m2, it was 1 min 13 sec after heat added to flash ignition and 1 min 20 sec until sustained ignition.

Figure A4. Progression of extinguishment for Generation 6, from pre-burn to suppression/control to extinguishment

A mixture of Generation 2 and Generation 4 (0.3wt% SDS, 3wt% solution) attempted to elucidate effects of controlling acrylate concentration when exposed to a combustion environment (to reduce uncontrolled radical reactions in flame, allowing crosslinking due to heat boosting sealability, while other component helps in flame knockdown). The formulation, Generation 7, achieved an expansion ration of 6.73 and a drainage time of 3.73 min. as well as an extinguishment of a 1x1 ft. gasoline pan fire. It exceeded the Mil-SPEC control of 30 seconds. However, extinguishing the fire in approximately 55 seconds and burnback performance was more deficient; the pan was reignited almost immediately and reached 25% burnback in approximately 15 seconds. Stability on fuel surface was approximately the same at 0 kW/m^2 compared to Generation 6 and about 25 seconds less for time to ignition under 20 kW/m^2.

Based on all of the figures and statistics gathered for all formulations, we developed a hypothesis for the "mechanism" of flame suppression and why Generation 6 was the most successful out of the tested formulations. The sPI and sPAAS/DMAE contributed differently to build a synergistic formula (**Figure A5**). sPI provided efficient drainage time and foam stability, while sPAAS/DMAE contributed more to expansion and foam fluidity. Combined, the polymers of Generation 6 afforded simultaneous knockdown and cooling effects stemming from the insulative and thermal properties of the sPI/sPAAS and the aqueous foam media.

As the foam was initially poured over the 1x1 ft. gasoline pan fire, initial knockdown, and cooling established control over the fire- flames confined to the edges or corners of the pan. Further spreading and separating allowed for further suppression of the gasoline fire- flamelets confined to a single corner of the pan. The applied foam smothered the remaining flamelets and extinguished the pan fire. The foam's lacking sealability allowed for the relatively rapid burn-back, however. This drawback leaves much room for improvement of the presented polyimide fire suppression system.

a)

sPI	Combined	sPAAS (with DMAE)
• Drainage Time • Foam Stability	• Knock-down and cooling effects • Thermal stability of polymers combined aqueous foam	• Expansion ratio • Foam Fluidity

b)

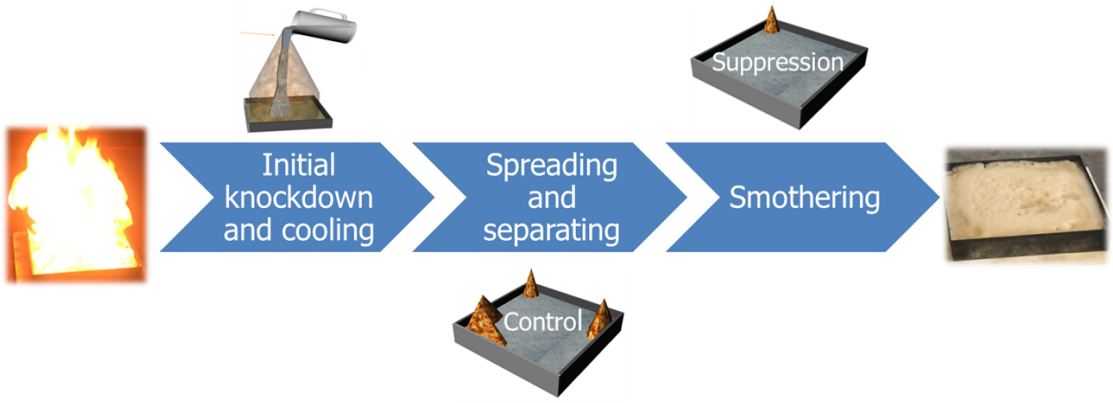

Figure A5. a). Table comparing the contributing characteristics of sPI and sPAAS with DMAE to fire suppression. b). Schematic depiction for the stages of fire suppression that shows Generation 6 passing through each stage.

2.7. References

1. Yang, J.; Xiao, B.; Tang, A.; Li, J.; Wang, X.; Zhou, E. *Adv. Mater.* **2019**, *31*, 1804699.

2. Puthiaraj, P.; Lee, Y.-R.; Ahn, W.-S. *Chem. Eng.* **2017**, *319*, 65-74.

3. Chen, T.; Qiu, J.; Zhu, K.; Li, J.; Wang, J.; Li, S.; Wang, X. *J. Phys. Chem. B* **2015**, *119*, 4521-4530.

4. Xu, H.; Bijleveld, J.; Hedge, M.; Dingemans, T. *Polym. Chem.* **2019**, *10*, 5052-5069.

5. Yen, H.-J.; Liou, G.-S. *Polym. J.* **2016**, *48*, 117-138.

6. Herzberger, J.; Meenakshisundaram, V.; Williams, C. B.; Long, T. E. *ACS Macro Lett.* **2018**, *7*, 493-497.

7. Hegde, M.; Meenakshisundaram, V.; Chartrain, N.; Sekhar, S.; Tafti, D.; Williams, C. B.; Long, T. E. *Adv. Mater.* **2017**, *29*, 1701240.

8. Cao, K.; Serrano, J. M.; Liu, T.; Stovall, B. J.; Xu, Z.; Arrington, C. B.; Long, T. E.; Odle, R. R.; Liu, G. *Polym. Chem.* **2020**, *11*, 393-400.

9. Rau, D. A.; Herzberger, J.; Long, T. E.; Williams, C. B. *ACS Appl. Mater. Interfaces* **2018**, *10*, 34828-34833.

10. Yang, J.; Lee, M.-H. *Macromol. Res.* **2004**, *12*, 263-268.

11. Facinelli, J. V.; Gardner, S. L.; Dong, L.; Sensenich, C. L.; Davis, R. M.; Riffle, J. S. *Macromolecules* **1996**, *29*, 7342-7350.

12. Gharavi, A.; Saadeh, H. Water-soluble polyimides and methods of making and using same. US6894174B1, May 15, 2003.

13. Erce, Ş.; Erdener, H.; Akay, R. G.; Yücel, H.; Baç, N.; Eroğlu, İ. *Int. J. Hydrog. Energy* **2009**, *34*, 4645-4652.

14. Anderson, L. J.; Yuan, X.; Fahs, G. B.; Moore, R. B. *Macromolecules* **2018**, *51*, 6226-6237.

15. Chang, Y.; Mohanty, A. D.; Smedley, S. B.; Abu-Hakmeh, K.; Lee, Y. H.; Morgan, J. E.; Hickner, M. A.; Jang, S. S.; Ryu, C. Y.; Bae, C. *Macromolecules* **2015**, *48*, 7117-7126.

16. Mohanty, A. D.; Lee, Y.-B.; Zhu, L.; Hickner, M. A.; Bae, C. *Macromolecules* **2014**, *47*, 1973-1980.

17. Fang, J.; Guo, X.; Harada, S.; Watari, T.; Tanaka, K.; Kita, H.; Okamoto, K.-i. *Macromolecules* **2002**, *35*, 9022-9028.

18. Genies, C.; Mercier, R.; Sillion, B.; Cornet, N.; Gebel, G.; Pineri, M. *Polymer* **2001**, *42*, 359-373.

19. Wang, Y.; Chen, Y.; Gao, J.; Yoon, H. G.; Jin, L.; Forsyth, M.; Dingemans, T. J.; Madsen, L. A. *Adv. Mater.* **2016**, *28*, 2571-2578.

20. Wang, Y.; He, Y.; Yu, Z.; Gao, J.; ten Brinck, S.; Slebodnick, C.; Fahs, G. B.; Zanelotti, C. J.; Hegde, M.; Moore, R. B.; Ensing, B.; Dingemans, T. J.; Qiao, R.; Madsen, L. A. *Nat. Comm.* **2019**, *10*, 801.

21. Reisch, M. S. *C&EN Glob. Entep.* **2019**, *97*, 16-19.

22. Ananth, R.; Snow, A. W.; Hinnant, K. M.; Giles, S. L.; Farley, J. P. *Colloids Surf. A* **2019**, *579*, 123686.

23. Sheng, Y.; Jiang, N.; Lu, S.; Wang, Q.; Zhao, Y.; Liu, X. *Fire Technol.* **2020**, *56*, 1059-1075.

24. Hetzer, R. H.; Kummerlen, F. *SUPDET* **2016**.

25. Cao, K.; Zhou, Z.; Liu, G. *Polym. Chem.* **2018**.

26. Cao, K.; Serrano, J. M.; Liu, T.; Stovall, B. J.; Xu, Z.; Arrington, C. B.; Long, T. E.; Odle, R. R.; Liu, G. *Polym. Chem.* **2019**.

27. Cao, K.; Stovall, B. J.; Arrington, C. B.; Xu, Z.; Long, T. E.; Odle, R. R.; Liu, G. *ACS Appl. Polym. Mater.* **2020**, *2*, 66-73.

28. Bryant, R. G. Polyimides. In *Ullmann's Encyclopedia of Industrial Chemistry*, 2014; pp 1-27.

29. Zhai, Y.; Yang, Q.; Zhu, R.; Gu, Y. *J. Mat. Sci.* **2008**, *43*, 338-344.

30. Pryde, C. A. *J. Polym Sci. A Polym. Chem.* **1989**, *27*, 711-724.

31. Seo, Y.; Lee, S. M.; Kim, D. Y.; Kim, K. U. *Macromolecules* **1997**, *30*, 3747-3753.

32. Martos, A. M.; Biasizzo, M.; Trotta, F.; del Río, C.; Várez, A.; Levenfeld, B. *Euro. Polym. J.* **2017**, *93*, 390-402.

33. Mattera Jr, V. D.; Risen Jr, W. M. *J. Polym Sci. B Polym. Phys.* **1986**, *24*, 753-760.

34. Moroi, Y.; Motomura, K.; Matuura, R. *J. Colloid Interface Sci.* **1974**, *46*, 111-117.

35. Khan, N.; Brettmann, B. *Polymers* **2019**, *11*, 51.

2.8. Supporting Information

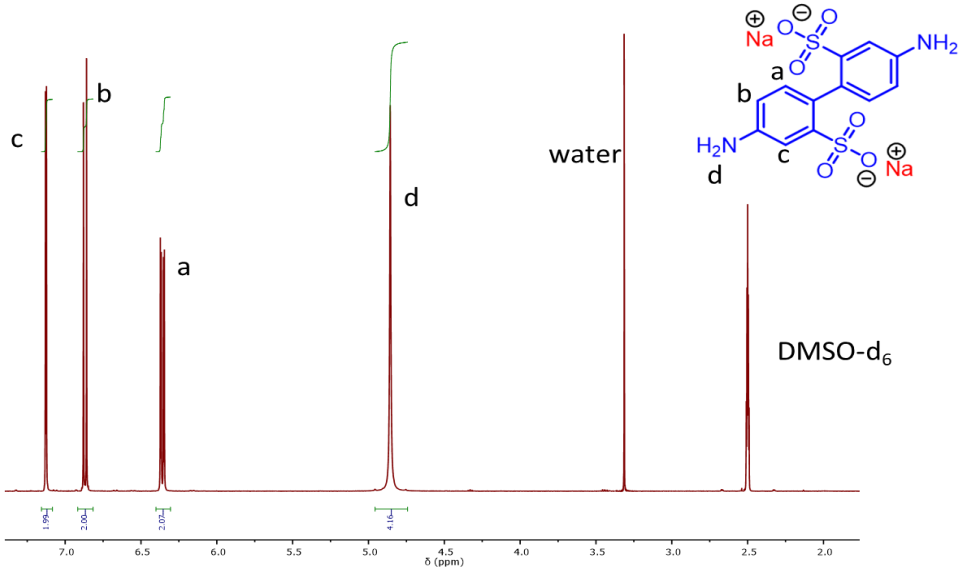

Figure S1. ^{1}H NMR of BDSA-Na (DMSO-d_6, 400 MHz)

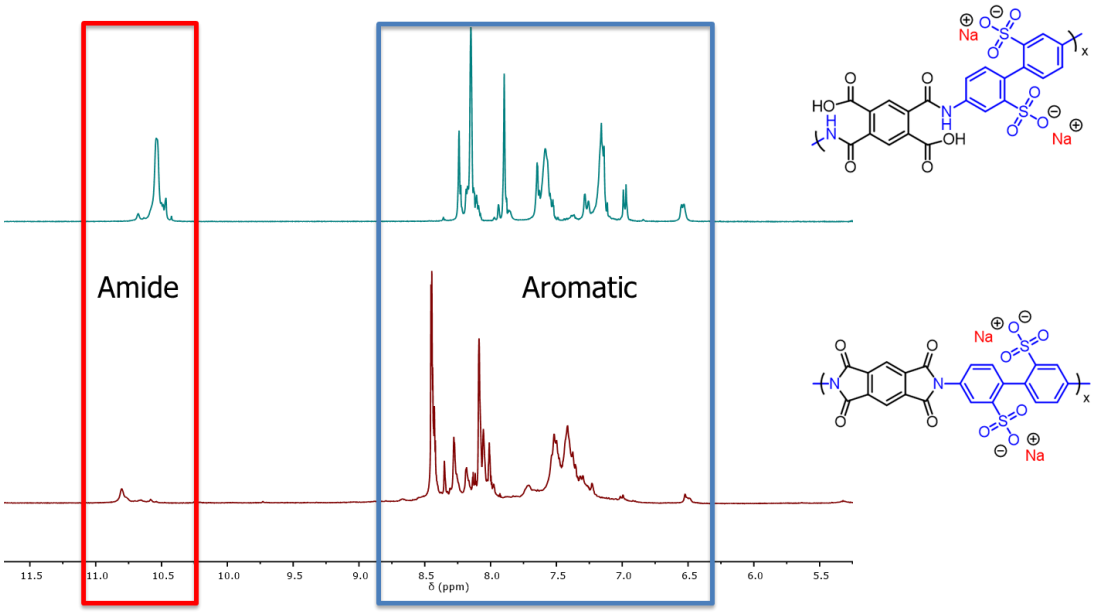

Figure S2. ^{1}H NMR of the sPAA and sPI imidized to 400 °C showing the residual amide signal (DMSO-d_6, 400 MHz)

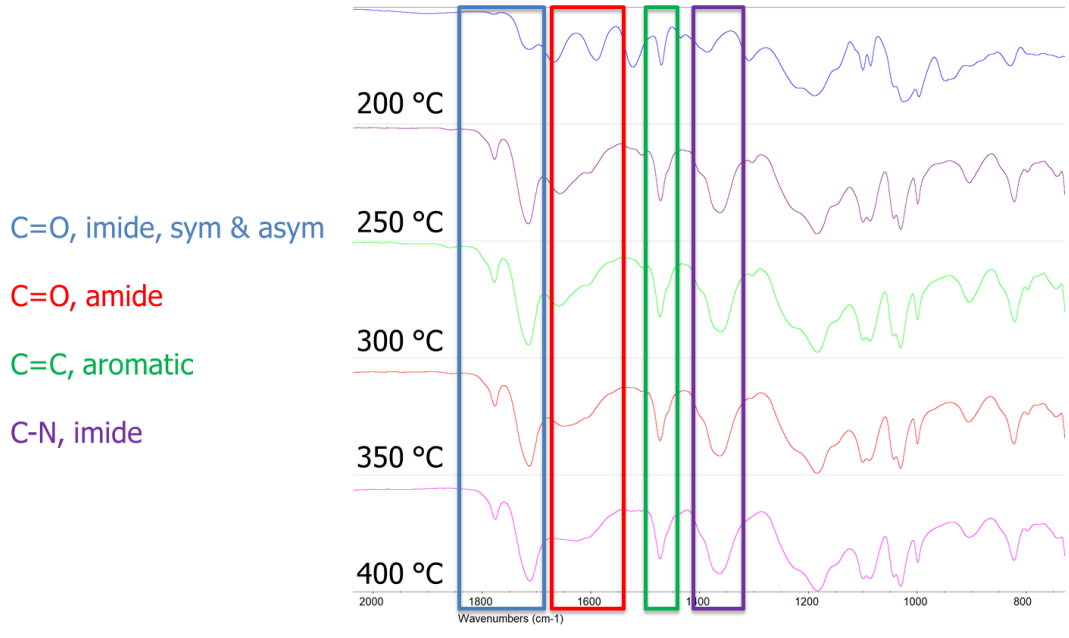

Figure S3. FT-IR spectra of a 100 mol% BDSA-Na containing sPI at different temperatures throughout the imidization process. Notice the reduction of the amide C=O stretch at 1660 cm^{-1} and the emergence of the imide C=O stretches at 1740 cm^{-1} and 1775 cm^{-1}.

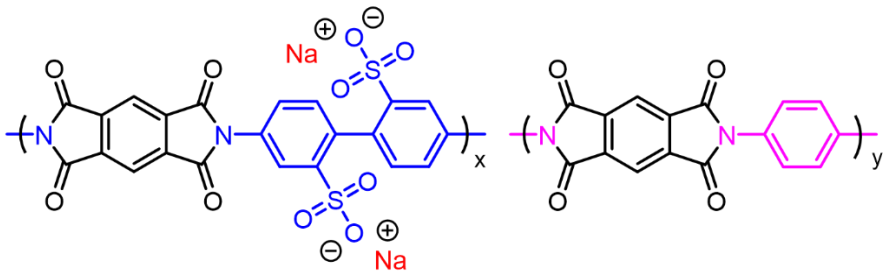

Figure S4. Structure of BDSA-Na/*p*PD-PMDA copolyimide. At 50 mol% *p*PD, this polymer is fully water-soluble as opposed to that with the same mol% of ODA.

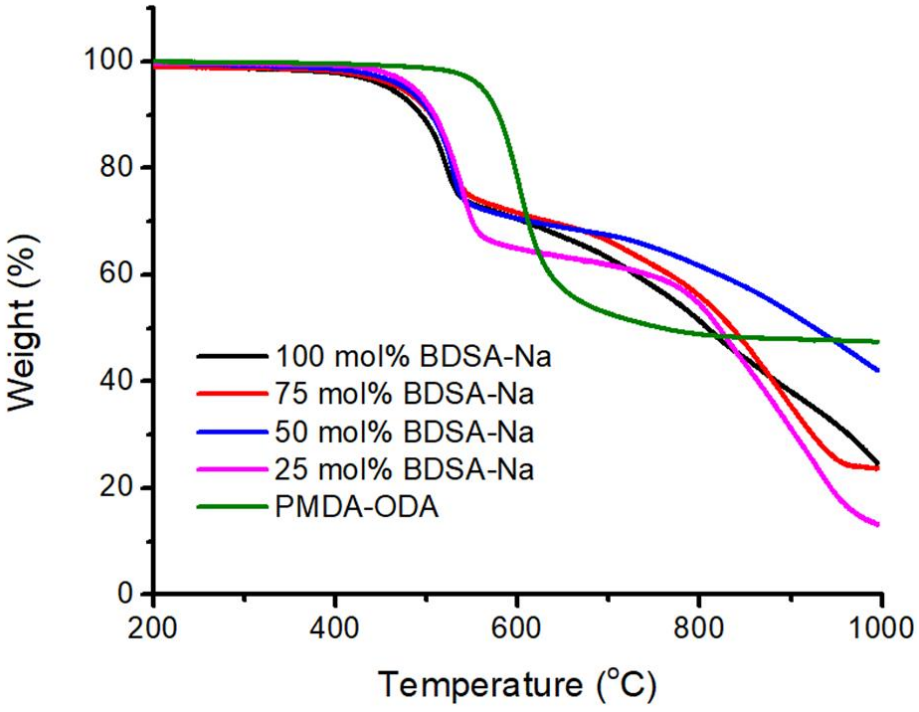

Figure S5. TGA thermograms of sPIs up to 1000 °C (10 °C/min ramp, N_2)

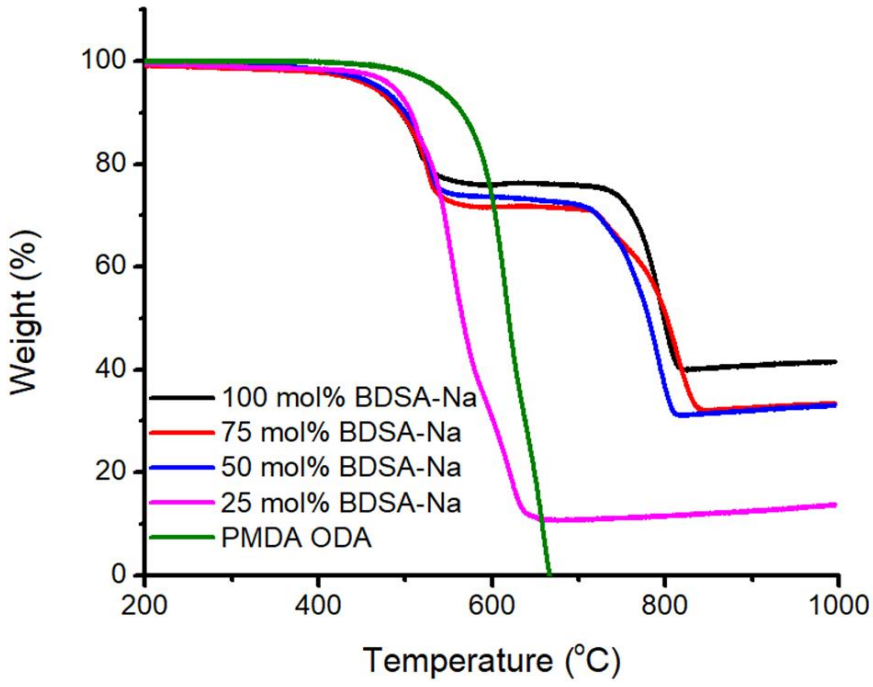

Figure S6. TGA thermograms of sPIs under air up to 1000 °C (10 °C/min ramp, air)

Table S1. Summary of $T_{d,5\%}$ and char yields of sPI under N_2 and Air

Polyimide (BDSA-Na mol%)	$T_{d,5\%}$ in N_2 (°C)	Char yield in N_2 at 600 °C (wt%)	$T_{d,5\%}$ in air (°C)	Char yield in air at 600 °C (wt%)
0 (PMDA-ODA)	561	78	536	74
25	486	65	486	32
50	477	71	470	74
75	472	72	463	72
100	460	71	463	76

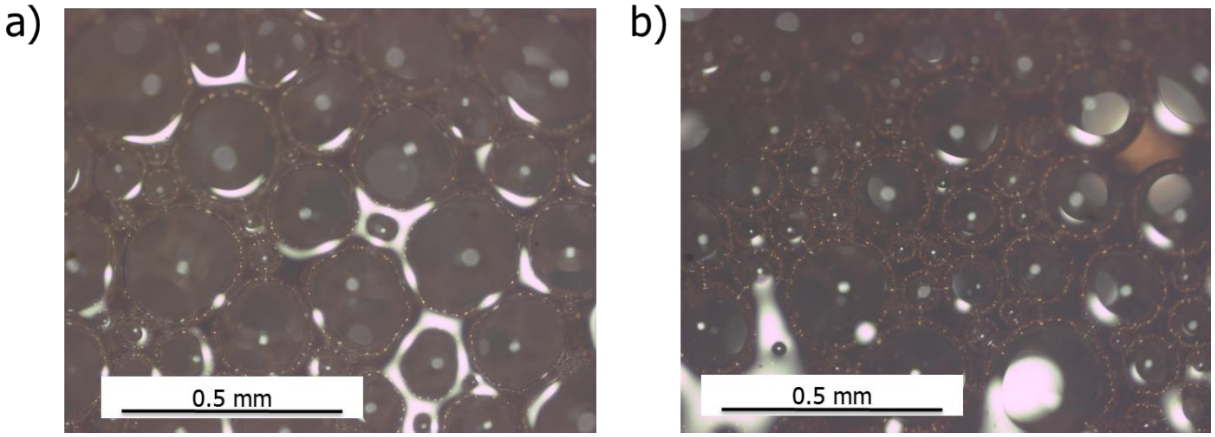

Figure S7. Optical microscope photographs of sPI foams at a) 3% polymer with 0.15% SDS and b) 6% polymer with 0.15% SDS. Foams were allowed to rest on a glass slide for 2 min, and images were taken within 3 min. Notice the denser foam and smaller bubbles of the 6% solution compared to the 3% solution.

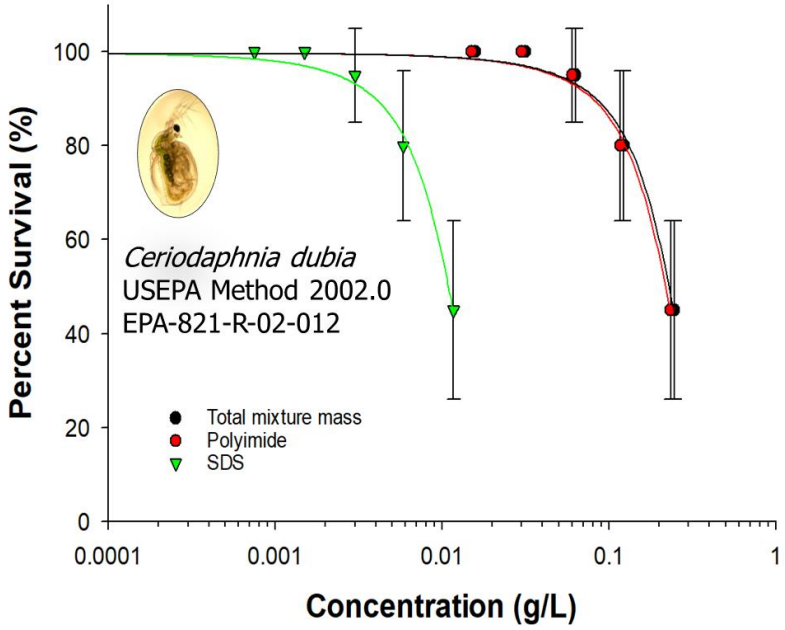

Figure S7. Ecotoxicology results of sPI foam formulation as reported by the Army EDRC. A 48 h Ceriodaphnia dubia acute toxicity test was conducted for the 3% formulation. As this was preliminarily tested as a mixture, the cause for toxicity remains uncertain, but tests of the individual components are planned and being conducted. All concentrations are nominal, and the average LC50 expressed in terms of the polyimide is 216 mg/L. This places the toxicity in the practically nontoxic regime.

Chapter 3. Solution behavior of wholly aromatic sulfonated polyimide in aqueous media

Benjamin Stovall and Timothy E. Long

Department of Chemistry, Macromolecules Innovation Institute (MII),
Virginia Tech, Blacksburg, VA, 24061

3.1. Abstract

This chapter aims to elucidate the solution behavior and viscosity scaling relationships of a wholly aromatic, water-soluble sulfonated polyimide (sPI) in salt-free and salt-present solutions. sPI exhibited larger scaling exponents than predicted theory across solution regimes. The addition of salt to the sPI solutions caused increases in viscosity and salting-out of the polyelectrolyte. The deviations from theory and expected behavior were attributed to molecular weight and intermolecular interaction considerations. As aqueous fire suppression foams are highly dependent on their components' solution behavior, the elucidation of sPI solution behavior is both fundamentally important and influential to the continual development of polyimide-based fire suppression foams.

3.2. Introduction

A polymer's behavior in solution has a profound effect on solution properties. The interactions amongst polymer chains, the solvent, and other polymer chains dictate the vast and variable rheological response, which thusly informs their practical use.[1] Polyelectrolytes are those polymers with a high degree of ionic groups (commonly pendant) on their backbone that ionize when in solution. Generally, this renders good solubility in solvents like water, permitting their use in many applications from paint thickeners, drug delivery, and fire suppression foams.[2-4]

As opposed to neutral polymers in a good solvent that take on a slightly expanded self-avoiding walk conformation, polyelectrolytes (in solutions without added salt) adopt a highly extended, rodlike conformation due to the domination of charge repulsion.[5] Polyelectrolyte solutions (as with neutral polymers) exist in three main regimes: dilute, semidilute (unentangled and entangled), and concentrated. Perhaps the most common way to investigate polyelectrolytes in solution is to relate specific viscosity (where η is the solution viscosity- taken as the zero shear viscosity, η_0, in this case- and η_{sp} is the viscosity of the solvent. **Equation 1**) to polymer concentration by recalling the scaling theories pioneered by de Gennes and Pfeuty and extensively expanded upon by Dobrynin, Colby, and Rubinstein, among others.[6-10]

$$\eta_{sp} = (\eta - \eta_s)/\eta_s \quad \textbf{(1)}$$

The following general scaling predictions have been described for flexible and semiflexible polyelectrolyte solutions. As polyelectrolytes exceed their overlap concentration, c*, solutions enter the semidilute unentangled regime where other chains and counterions screen electrostatic

interactions on length scales greater than the correlation length, ξ. Specific viscosity scales as η_{sp}~$c^{1/2}$ (Fuoss' Law) and can cover a broad concentration range due to a strong inverse concentration dependence of chain size.[6] The entanglement concentration, c_e, then initiates the semidilute entangled regime where specific viscosity scales as η_{sp}~$c^{1.5}$. Entanglement is considered when a set number of chains within a polyelectrolyte pervaded volume constrain its motion, after which ξ continues to decrease with concentration and reaches the value of the Kuhn length where chain size is independent of concentration. This initiates the concentrated regime, c** for the purposes of this discussion, where all electrostatic interactions are screened, and specific viscosity scales as η_{sp}~$c^{3.75}$, similar to that of neutral polymers. Below, these scaling predictions are summarized (**Equation 2**).[9, 11]

$$\eta_{sp} \sim \begin{cases} c^{0.5}, & c^* < c < c_e \\ c^{1.5}, & c_e < c < c^{**} \\ c^{3.75}, & c > c^{**} \end{cases} \quad \textbf{(2)}$$

Scaling theory is continually evolving, and there can be deviations from theory for various reasons; polyelectrolyte theory has been somewhat controversial and contentious. DNA and xanthan are examples that deviate from theory as they exhibit significant interchain interactions.[12-14] Polyelectrolytes like poly(2,2'-benzidine-4,4'-disulfonyl terephthalamide) (PBDT), which has gathered significant literature attention, show "true" rigid rod behavior as they assemble into double helix structures in solution. They exhibit liquid crystalline phases at low concentrations, deviating from polyelectrolyte theory and reflecting that of Doi-Edwards theory for neutral rigid rods.[15-18]

This study aims to elucidate the solution behavior of a sulfonated polyimide (sPI) from BDSA-Na and PMDA in the context of the polyelectrolyte scaling theory described above. To our knowledge, this is the first rheological study on water-soluble polyimide polyelectrolytes. Solution rheology preliminarily affords structural insights that are fundamentally important and may be advantageous when further developing water-soluble polyimide-based fire suppression foams.

3.3. Experimental

Materials: Sodium dodecyl sulfate (SDS) (Sigma Aldrich, 98%), hydrochloric acid (Fisher Chemical, certified ACS), sodium chloride (NaCl) (Fisher Chemical, certified ACS), water (Fisher Chemical, HPLC grade), acetone (Pharmco-AAPER) and ethanol (Deacon Laboratories, 200 proof) were used as received. Dimethyl sulfoxide anhydrous (Acros Organics, 99.5%) and N-methyl-2-pyrrolidone anhydrous (NMP) (Acros Organics, 99.5%) were stored over activated molecular sieves. Pyromellitic dianhydride (PMDA) (Acros Organics, > 98%), and 4, 4'-oxydianiline (ODA) (Acros Organics, 98%) were sublimed before use. 2,2'-Benzidinedisulfonic acid (BDSA) (TCI, > 70 %) was dried and titrated with NaOH and stored in a vacuum oven at 150 °C before use.

Synthesis of sulfonated polyimide (sPI): A 500 mL 3-neck round bottom flask equipped with a mechanical stirrer and nitrogen inlet was charged BDSA-Na (35.00 g, 0.0901 mol). The flask was purged and backfilled with N_2 three times before addition of 280 mL of anhydrous DMSO. Following dissolution of the amine, PMDA (19.66 g, 0.0901 mol) was added to the solution with an additional 5-7 mL of DMSO to wash any dianhydride of the walls of the flask. The resultant viscous solution was allowed to stir under nitrogen for 18 h. After 18 h, the PAA viscous solution

was diluted with NMP (2:1) and precipitated into an 80:20 mixture of acetone and ethanol and subsequently washed thoroughly with acetone. The dark yellow powder was placed inside a vacuum chamber and heated at a rate of approximately 2 °C/ min to 400 °C and held for 1 hr. sPI bulk polymer was stored under vacuum at 150 °C prior to use.

Dialysis of sPI: sPI powder was dissolved in HPLC-grade water at about 10-15%(w/v) and filtered through a 0.45 μm PTFE filter before being dispensed into a dialysis bag (1 kD cutoff). The solutions were dialyzed in a beaker with moderate stirring against 1000 times their volume in DI water. Water was changed 2-3 times over a 24-30 h period. Polymers were then isolated from dialysis solutions by evaporating the water and recovering the polymer powder. The dialyzed polymers were stored in an oven under vacuum at 150 °C before preparing rheology solutions.

Preparation of rheology solutions: Aqueous solutions were prepared in HPLC grade water and on a weight/ volume percent (%(w/v)) basis ranging from 1%(w/v) to 30%(w/v). Careful serial dilutions by weight were also performed in some instances to conserve materials and were confirmed for consistency. Solutions were kept in 6-dram vials sealed with parafilm to prevent evaporation and equilibrated at 80 °C for 24-48 h for complete dissolution and homogenization.

Analytical Methods: Polarized optical microscopy (POM) was conducted on a Meiji Technology MX9430 Japan optical microscope fitted with crossed polarizers. Solutions were dropped onto a glass slide and covered with a coverslip. Solution rheology was performed using TA Instruments DHR-3 and DHR-2 rheometers with a DIN cup (Peltier steel) and bob geometry in water at 23 °C.

Continuous flow sweeps were conducted from 1 to 100 s^{-1} with ten points per decade. Scaling relationships were calculated using a best power-law fit.

3.4. Results and Discussion

Synthesis of sPI and solution preparation

A classic two-step procedure for polyimides, as discussed in Chapter 2, afforded the 100% sulfonated sPI that was the basis for all rheological experiments (**Figure 1)**. This sPI also comprised the fire suppression foam formulations discussed in Chapter 2. Following imidization, a very black/dark brown powder was isolated and dissolved at various concentrations. Molecular weight was not attained via aqueous SEC due to potential ionic aggregation and non-size exclusion interactions. Monomers were charged in a 1:1 ratio to attain high relative molecular weight.[19-20] Testing solutions in HPLC water ranged from 1 wt% to 30 wt%, at which point it became too challenging to prepare solutions of higher concentration reliably. Solutions were brown in color, which intensified as concentration was increased.

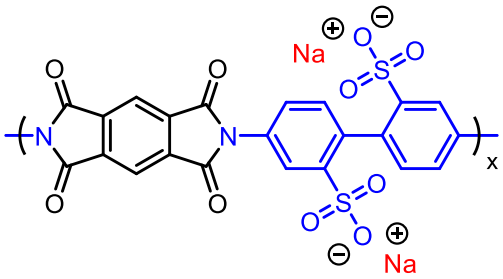

Figure 1. Structure of sPI used in this study.

The sPI, a polyimide, shares a very similar structure to PBDT, a polyamide; both use BDSA-Na as a sulfonated diamine amine monomer. PBDT exhibits very clear liquid crystalline behavior, and as such, POM enabled the study of sPI solutions at various concentrations. While sPI and PBDT maintain similar, "rigid" structures, POM revealed no birefringence in sPI solutions of 10, 15, and 30 wt%. Despite having a planar, rigid structure, sPI does not exhibit any liquid crystalline behavior and maintains a more semiflexible structure.[21-22] Polyimides, in general, actually make relatively poor mesogens.[23]

Solution Rheology and Scaling Relationships

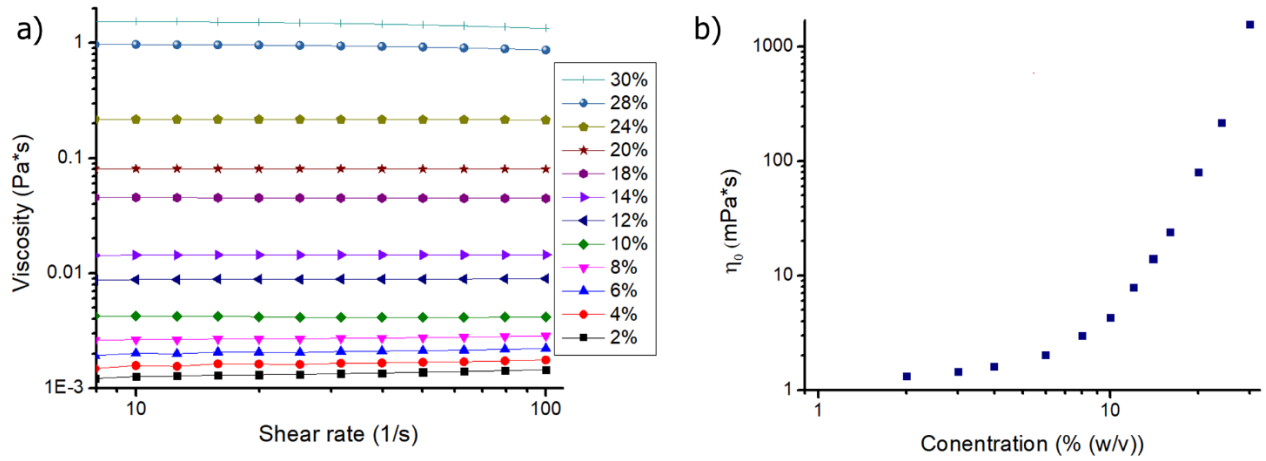

Figure 2. Plots of a) viscosity vs. shear rate and b) zero shear viscosity η_0 vs. concentration

Steady shear experiments over a broad concentration range gave a comprehensive viscosity profile of sPI solutions (**Figure 2)**. In the low concentration range, up to about 6 wt%, viscosity is low enough (close to solvent viscosity) where solutions displayed secondary flow effects at higher shear rates which disappear as concentration and viscosity increase.[24] At high concentrations above approximately 24 wt%, sPI solutions exhibited slight shear thinning at higher shear rates. Zero

shear viscosity, η_0 versus concentration (**Figure 2b**), showed typical logarithmic increases similar to man polyelectrolytes.

Figure 3a shows the dependence of specific viscosity, η_{sp}, on sPI concentration. The profile showed that the solutions span through the semidilute unentangled/ semidilute entangled regimes into the concentrated regime. The c_e crossover occurred at approximately 4 wt%, and c** occurred at approximately 11 wt%. There are noteworthy deviations from scaling theory, however. The breadth of the semidilute unentangled regime is relatively short, and all of the scaling relationships are above the theoretical predictions ($\eta_{sp} \sim c^{0.92}$, $\eta_{sp} \sim c^{1.76}$, and $\eta_{sp} \sim c^{4.85}$). **Figure 3b** plots the reduced viscosity vs. the sPI solution concentration and also shows deviations from theory. The red inset line represents theoretical polyelectrolyte behavior, which emphasizes Fuoss Law behavior ($\eta_{red} \sim c^{-1/2}$) in the low concentration regime, corresponding to the semidilute unentangled regime.[25] This behavior is suppressed as salts are introduced into the solution and begin to screen electrostatic interactions. At the high salt/ neutral limit, the negative slope is entirely suppressed. The sPI solutions in this regime exhibited no such Fuoss behavior, only a slight negative slope as concentration before the concentration increased into the entanglement regimes.

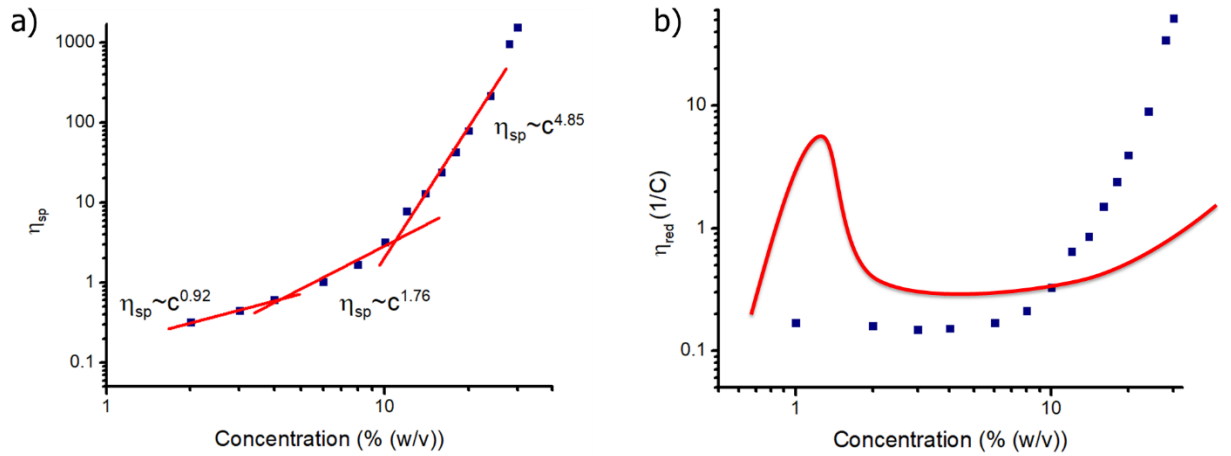

Figure 3. a) Plot of specific viscosity as a function of concentration and b) reduced viscosity vs. concentration with the predicted representation of polyelectrolyte behavior (in Fuoss regime)

The deviations from scaling theory and the partial suppression of the Fuoss regime in the plot of η_{red} suggested a residual salt concentration. This was possible as salts may be produced from the residual solvent due to the high-temperature imidization process. Dialysis of sPI solutions aimed to remove any residual salts, thereby enabling reevaluation of viscosity scaling relationships.

Viscosities of sPI solutions of the same concentration increased following dialysis (and polymer recovery), shifting the concentration crossovers to lower values of approximately 3% for c_e and 6% for c**. Viscosity increases suggest the dialysis of some material, but **Figure 4a** indicates that the scaling relationships remain largely similar to those before dialysis (above the prediction). What exactly was dialyzed is not known and may be the subject for future experiments. However, as the scaling relationships stayed the same after dialysis and were not reduced to near the predicted values, it can be concluded that the presence of salt is not responsible for deviations from theory. **Figure 4b** supplements this conclusion as the curves collapse onto each other as specific viscosity is plotted as a function of the reduced concentration (c/c_e).

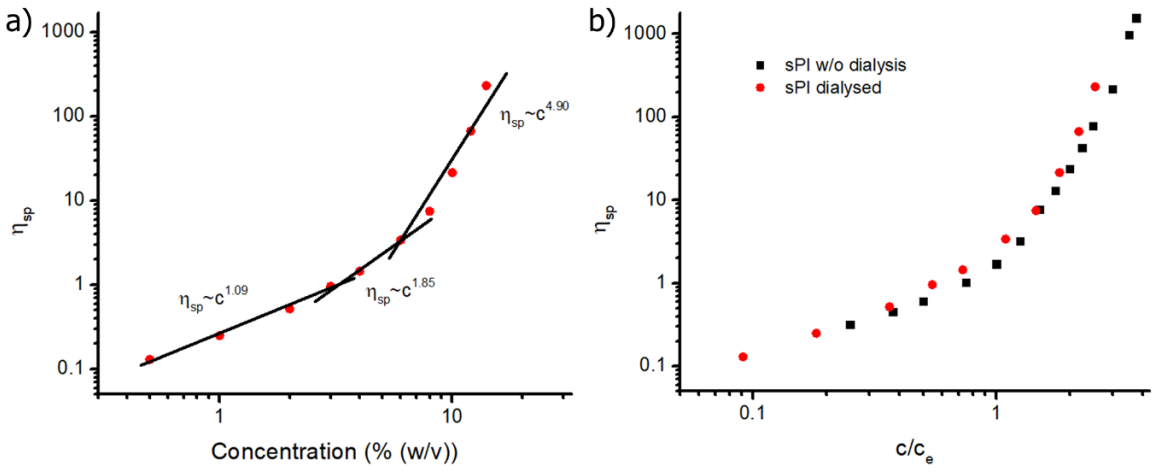

Figure 4. a) Plot of specific viscosity vs. concentration for dialyzed sPI solutions and b) specific viscosity as a function of the reduced concentration showing the collapse of the individual curves onto each other.

Effects of Added Salt

The addition of salt to polyelectrolyte solutions at high concentrations screens electrostatic interactions between chains, causing them to adopt more coil-like conformations. Viscosity scaling relationships thusly reflect neutral polymers in solution, and viscosity decreases in the semidilute regime.[11] NaCl was added to sPI solutions to evaluate its effects on solution behavior. As a starting point, the high salt concentrations were used to invoke the neutral limit. Interestingly, 25 wt% salt in a 20 wt% sPI solution and 50 wt% salt in a 10 wt% sPI solution caused the polymers to precipitate, or "salt out" (**Figure 5a**). Salting-out occurs due to anion-water hydration complex formation, which decreases hydration and thusly the solubility of the polymer.[26] In this case, it appears to be dependent on both salt concentration and sPI concentration. 25 wt% NaCl in 10 wt% sPI solution afforded homogenous solutions of high salt concentration for solution rheology. **Figure 5b** shows that viscosity certainly increased with high salt concentration. The reduced viscosity, η_{red}, of the measurable solutions did not show any negative slope in the Fuoss regime, indicating salt screening in that region (**Figure S3**).

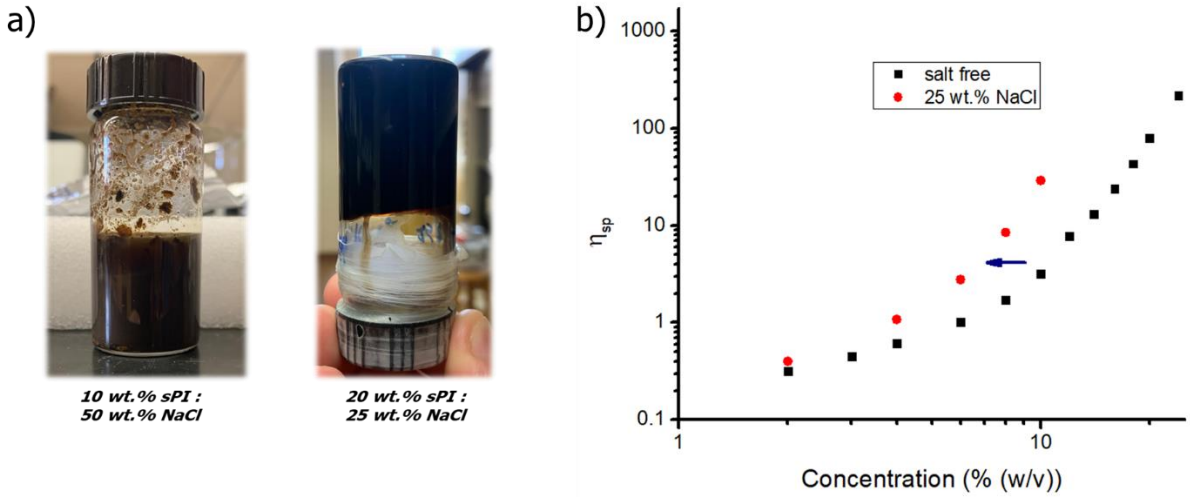

Figure 5. a) Solutions of sPI with high salt concentration exhibiting the salting-out effect and b) specific viscosity vs. concentration for salt-free sPI solutions and solutions with 25% NaCl by weight

Rheology of low salt concentration solutions attempted to exploit any salt screening effects as even at low concentrations; it is still detectable.[11] However, sPI solutions with 1 wt% added NaCl fell almost perfectly onto the η_{sp} vs. polymer concentration curve, showing that even low salt concentrations do not decrease viscosity, thereby not shifting scaling relationships to values more akin to neutral polymers (**Figure 7a**). **Figure 7b** confirmed the perceived salt effects on sPI solutions by comparing the zero shear viscosities of representative 3 wt% and 6 wt% sPI solutions against salt concentration (in M). The addition of salt seems to increase viscosity, which is more pronounced as polyelectrolyte concentration increases.

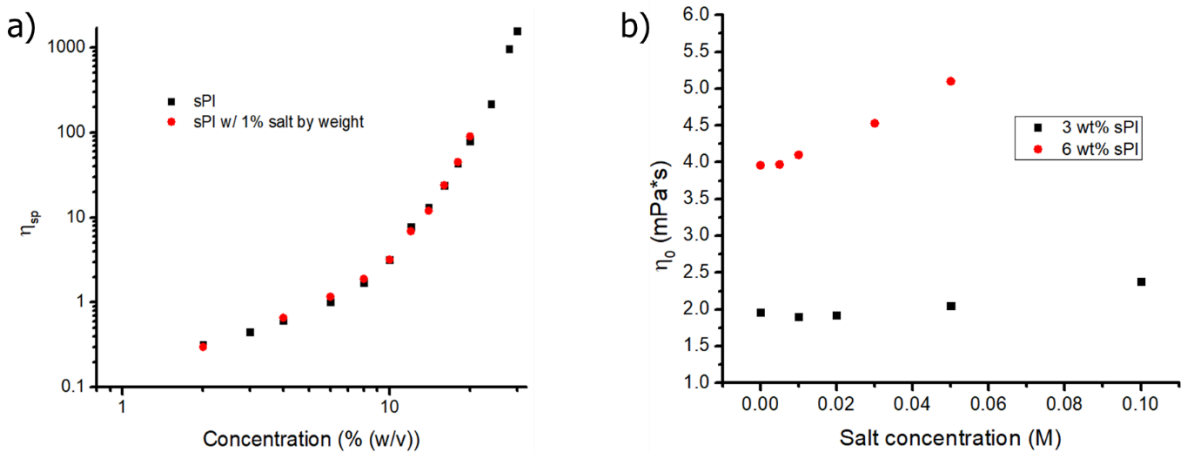

Figure 7. a) Plot of specific viscosity vs. concentration for sPI solutions with and without 1 wt% NaCl and b) plot of zero shear viscosity vs. salt concentration for 3 and 6 wt% (dialyzed) sPI solutions.

Hypotheses for Deviant Solution Behavior

Considering the whole picture of measured sPI solution behavior presented here, it is reasonable to ascribe two main factors responsible for deviations from predicted scaling theory: molecular weight and intermolecular (interchain) interactions. However, the polyelectrolyte

literature is still continuously evolving, and more precise models may be developed in the future to help describe various phenomena. It is interesting to note that current reports are still adjusting our understanding of polyelectrolyte entanglement.[27]

Molecular Weight Considerations:

Polyelectrolytes that have exhibited the predicted scaling relationships are generally of molecular weights greater than 100 kD. In contrast, the polyimides of this study are predicted to be of lower relative molecular weight, presumably lower than 25 kD.[28] Few studies have explicitly studied a molecular weight dependence as a function of specific viscosity and concentration, but many do describe similar observations related to low molecular weight deviations.[25, 29-31] Studies by Lopez et al.[30-31] have shown that for low MW polyelectrolytes (NaPSS) (~30 kD), scaling relationships for the different regimes are higher than predicted, comparable to sPI of this study. Reduced viscosity vs. concentration curve for low MW NaPSS also showed a slight negative slope in the Fuoss regime followed a starker increase in η_{red} with polymer concentration, unlike higher MW samples. Uzum et al.[29] reported for low molecular weight NaPSS the scaling relationship for the semidilute unentangled regime was $\eta_{sp} \sim c^{0.85}$. They reasoned that a broader transition between the unentangled and entangled semidilute regimes and thus a less precise scaling transition could be responsible for this behavior in low MW polyelectrolyte solutions. It is also noteworthy to mention that since these transitions are less well defined and are continuously being redefined in the literature, it is possible to interpret an overlap concentration (c*) in the lower concentration range with an estimation "around" $\eta_{sp}(c^*)= 1$.[11, 27] However, this is again subject to data fit and the fact lower MW systems deviate from predicted behavior, that is not explained by theory.[29, 32]

Intermolecular/ Interchain Interactions

In Chapter 2, it was shown that sPIs contain a small amount of amide functionality due to incomplete imidization. The amide groups can induce hydrogen bonding between chains. Combined with intermolecular forces such as dipole-dipole, pi-pi stacking, and other electrostatic interactions, they begin to influence scaling (positively) on some level that grows stronger with increasing concentration.[18, 33] Though not nearly as drastic as PBDT, this can be perceived as an increase in "chain stiffness," which results in a weaker variation of chain length with concentration and thusly a higher scaling power-law exponent.[34] The salt solution behavior of sPI supports this hypothesis; as salts screen the electrostatic interactions, intermolecular interactions can begin to take over more strongly, causing chain aggregation, increasing viscosity, and salting-out at high enough salt concentrations.[13, 35]

3.5. Conclusions

Polyelectrolyte solution behavior remains a very complex issue. Many factors can influence scaling relationships across the semidilute unentangled, semidilute entangled, and concentrated regimes. sPI solutions deviated from scaling theory, with power-law exponents consistently higher than the predictions. The addition of salt (NaCl) to sPI solutions did not exhibit any electrostatic screening effects and, at high salt concentration, even precipitated the polymers from the solution (salting-out). The deviations from scaling theory are hypothesized to arise from a combination of two main factors: molecular weight and intermolecular interactions. This study provides preliminary insight into these polyelectrolyte solutions, which may enhance the development of polyimide-based fire suppression foams.

3.6. References

1. Polymer Solution Behavior: Polymer in Pure Solvent and in Mixed Solvent. In *Physicochemical Behavior and Supramolecular Organization of Polymers*, Ligia, G.; Deodato, R., Eds. Springer Netherlands: Dordrecht, 2009; pp 1-42.

2. Séon, L.; Lavalle, P.; Schaaf, P.; Boulmedais, F. *Langmuir* **2015**, *31*, 12856-12872.

3. Catarata, R.; Azim, N.; Bhattacharya, S.; Zhai, L. *J. Mat. Chem. B* **2020**, *8*, 2887-2894.

4. Xu, C.; Wang, H.; Wang, D.; Zhu, X.; Zhu, Y.; Bai, X.; Yang, Q. *Polymers* **2020**, *12*, 571.

5. Colby, R. H. *Rheologica Acta* **2010**, *49*, 425-442.

6. Dobrynin, A. V.; Colby, R. H.; Rubinstein, M. *Macromolecules* **1995**, *28*, 1859-1871.

7. Krause, W. E.; Tan, J. S.; Colby, R. H. *J. Polym. Sci. B Polym. Phys.* **1999**, *37*, 3429-3437.

8. Lopez, C. G.; Richtering, W. *j. Chem. Phys.* **2018**, *148*, 244902.

9. Dobrynin, A. V. *Polymer* **2020**, *202*, 122714.

10. Dobrynin, A. V.; Rubinstein, M. *Prog. Polym. Sci.* **2005**, *30*, 1049-1118.

11. Lopez, C. G.; Colby, R. H.; Graham, P.; Cabral, J. T. *Macromolecules* **2017**, *50*, 332-338.

12. Milas, M.; Rinaudo, M.; Knipper, M.; Schuppiser, J. L. *Macromolecules* **1990**, *23*, 2506-2511.

13. Wyatt, N. B.; Gunther, C. M.; Liberatore, M. W. *Polymer* **2011**, *52*, 2437-2444.

14. Bravo-Anaya, L. M.; Rinaudo, M.; Martínez, F. A. *Polymers* **2016**, *8*.

15. Fox, R. J.; Chen, W.-R.; Do, C.; Picken, S. J.; Forest, M. G.; Dingemans, T. J. *Rheo. Act.* **2020**, *59*, 727-743.

16. Fox, R. J.; Hegde, M.; Zanelotti, C. J.; Kumbhar, A. S.; Samulski, E. T.; Madsen, L. A.; Picken, S. J.; Dingemans, T. J. *ACS Macro Lett.* **2020**, *9*, 957-963.

17. Wang, Y.; Gao, J.; Dingemans, T. J.; Madsen, L. A. *Macromolecules* **2014**, *47*, 2984-2992.

18. Wang, Y.; He, Y.; Yu, Z.; Gao, J.; ten Brinck, S.; Slebodnick, C.; Fahs, G. B.; Zanelotti, C. J.; Hegde, M.; Moore, R. B.; Ensing, B.; Dingemans, T. J.; Qiao, R.; Madsen, L. A. *Nat. Comm.* **2019**, *10*, 801.

19. Dine-Hart, R. A.; Wright, W. W. *J. Appl. Polym. Sci.* **1967**, *11*, 609-627.

20. Harris, F. W.; Wilson, D.; Stenzenberger, H. D.; Hergenrother, P. M., Chapter 1. In *Polyimides*, Chapman and Hall: New York, 1990.

21. Schmitz, L.; Ballauff, M. *Polymer* **1995**, *36*, 879-882.

22. Brodowski, G.; Horvath, A.; Ballauff, M.; Rehahn, M. *Macromolecules* **1996**, *29*, 6962-6965.

23. Kricheldorf, H. R. Liquid-Crystalline Polyimides. In *Progress in Polyimide Chemistry II*, Kricheldorf, H. R., Ed. Springer Berlin Heidelberg: Berlin, Heidelberg, 1999; pp 83-188.

24. Ewoldt, R. H.; Johnston, M. T.; Caretta, L. M. Experimental Challenges of Shear Rheology: How to Avoid Bad Data. In *Complex Fluids in Biological Systems: Experiment, Theory, and Computation*, Spagnolie, S. E., Ed. Springer New York: New York, NY, 2015; pp 207-241.

25. Izzo, D.; Cloitre, M.; Leibler, L. *Soft Matter* **2014**, *10*, 1714-1722.

26. Sadeghi, R.; Jahani, F. *J. Phys. Chem. B* **2012**, *116*, 5234-5241.

27. Dobrynin, A. V.; Jacobs, M. *Macromolecules* **2021**, *54*, 1859-1869.

28. Fang, J.; Guo, X.; Harada, S.; Watari, T.; Tanaka, K.; Kita, H.; Okamoto, K.-i. *Macromolecules* **2002**, *35*, 9022-9028.

29. Üzüm, C.; Christau, S.; von Klitzing, R. *Macromolecules* **2011**, *44*, 7782-7791.

30. Lopez, C. G.; Richtering, W. *J. Phys. Chem. B* **2019**, *123*, 5626-5634.

31. López, C. G.; Linders, J.; Mayer, C.; Richtering, W. J. a. S. C. M. *Soft Cond. Mater.* **2020**.

32. Lopez, C.; Linders, J.; Mayer, C.; Richtering, W. *Diffusion and viscosity of unentangled polyelectrolytes*. 2020.

33. Zhang, E.; Dai, X.; Dong, Z.; Qiu, X.; Ji, X. *Polymer* **2016**, *84*, 275-285.

34. Lopez, C. G.; Rogers, S. E.; Colby, R. H.; Graham, P.; Cabral, J. T. *J. Polym. Sci. B Polym. Phys.* **2015**, *53*, 492-501.

35. Sarkar, N.; Kershner, L. D. *J. Appl. Polym. Sci.* **1996**, *62*, 393-408.

3.7. Supporting Information

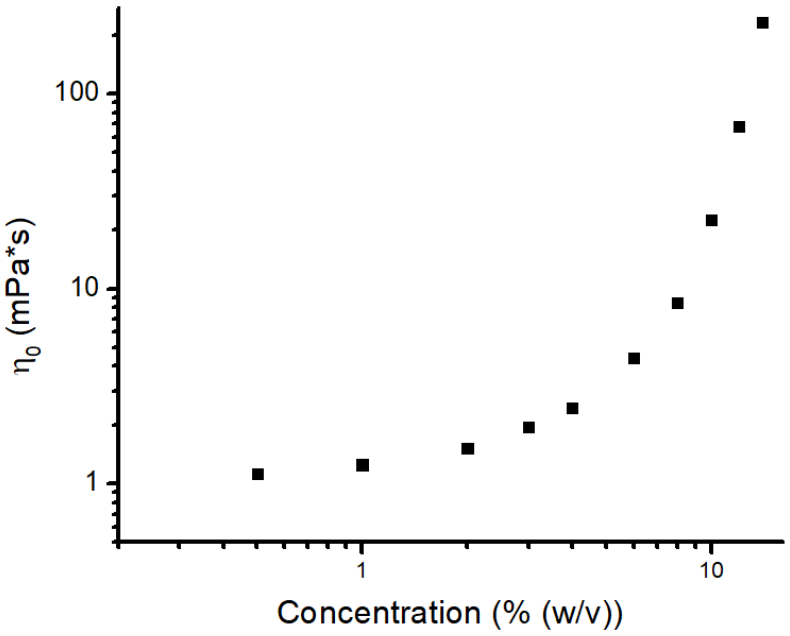

Figure S1. Zero shear viscosity dependence on concentration for dialyzed sPI solutions

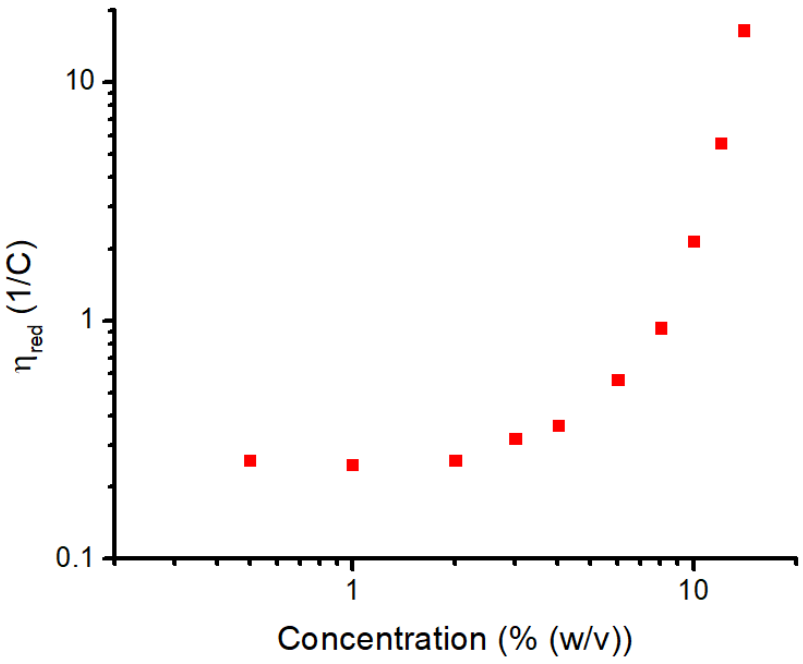

Figure S2. Reduced viscosity dependence on concentration for dialyzed sPI solutions

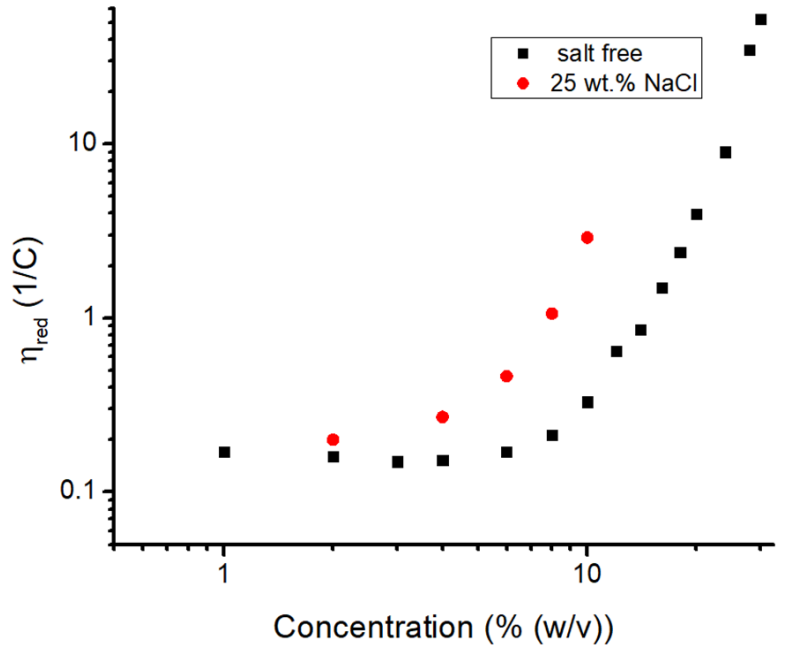

Figure S3. Reduced viscosity dependence on concentration for salt-free sPI solutions and sPI solutions with 25 wt% salt

Chapter 4. Synthesis and characterization of water-soluble phosphonium-containing polyimides

Benjamin Stovall and Timothy E. Long

Department of Chemistry, Macromolecules Innovation Institute (MII),
Virginia Tech, Blacksburg, VA, 24061

4.1. Abstract

Ionic polyimides are a decades-old research interest, and research in this area remains strong. From additive manufacturing to flame retardant materials, the chemical space of polyimides utilizing ionic functionality is broadening. This study presents the facile synthesis of a novel phosphonium-containing diamine, methyltriphenylphosphonium 2,2'-benzidinedisulfonate (BDSA-MTPP). Two sets of sulfonated polyimides (sPI) were subsequently synthesized using the monomer with pyromellitic dianhydride (PMDA) and either 4,4'-oxydianiline or sodium salt of 4,4'-diamino diphenyl 2,2'-disulfonic acid (BDSA-Na). Overall, the polymers maintained competitive thermal stability (>375 °C) while it was also shown that the bulky MTPP cation acted as a plasticizer that reduced the glass transition temperature (T_g). Only sPIs containing ≥75 mol% BDSA-Na: BDSA-MTPP due to the electrostatic nature of the bulky cation. Upon neutralization of a 100 mol% BDSA-MTPP containing poly(amic acid), however, the formed sulfonated poly(amic acid) salt (sPAAS) became fully soluble in water, which allows for more modular exploration of these polymers in applications like fire suppression.

4.2. Introduction

Polyimides epitomize one of the most valuable classes of polymers- high-performance polymers. Within their class, polyimides are some of the most versatile polymers. Due to their excellent chemical and radiation resistance, thermal stability, and mechanical properties,

polyimides function in many areas, from aerospace and transportation to the medical and electronics industries. Historically, polyimides incorporate various functional groups (i.e., phosphorous-containing groups, siloxanes, crosslinking moieties) directly into the polymer backbone via the diamine or the dianhydride. While these synthetic methods are generally well optimized, they still are susceptible to limitations regarding solubility, harsh solvents, or monomers.[1-2] Many functional monomers are not readily commercially available and require multi-step syntheses and metal catalysts as well as harsh solvents, while often resulting in low yields.[3-4]

The incorporation of ionic groups into the polymer structure is an effective way to impart functionality in polymers. Utilization of polymer-bound cations or anions, such as sulfonates and ammoniums, enables the tethering of other organic or inorganic ions to the polymer backbone.[5-6] In recent literature, these techniques have pioneered the design of macromolecular ionic liquids, which are used in electrochemical materials, nanocomposites, stimuli-responsive materials, etc.[7-11] In the area of polyimides, the employment of ionic groups to tether molecular ions has been very limited, however. Many polyimide ionomers use sulfonate or carboxylate groups with metal cations to improve mechanical properties or processing.[12-13] Sulfonic acid groups are most commonly used for proton exchange fuel cell membranes.[1, 3] A handful of recent studies and the bulk of the research in this field have integrated polymeric ionic liquid concepts with polyimides for applications such as non-humidified fuel cells[14] and selective CO_2 gas separation composite membranes.[15-17] In 2016, Vygodskii et al.[15] used a multi-step post-polymerization modification of benzimidazole and quinuclidine moieties in the polyimide backbone via an N-alkylation step followed by quaternization, with subsequent ion exchange with bis(trifluoromethylsulfonyl)imide anions. Studies by Watanabe et al.[14, 16-17] focus on post-polymerization neutralization of the

sulfonic acid groups of 4,4'-diaminodiphenyl-2,2'-disulfonic acid (BDSA) moiety with various imidazolium or ammonium cations; these polyimides are also composited with various loadings of the corresponding ionic liquids.

Phosphorous-containing polymers and ionomers are useful in many capacities from engineering, biomaterials, and flame retardants.[9, 18-19] Jiang et al.[20] successfully prepared phosphonium sulfonate/ polycarbonate composites with improved flame retardant performance, highlighting phosphorous and sulfur functionality. Furthermore, in research conducted between the Liu and Long groups at Virginia Tech, telechelically terminated poly(ether imide)s (PEI) with phosphonium and sulfonate end groups were synthesized and "neutralized" with each other, effectively removing halogen counterions.[21] In addition to improving char yields and competitive performance to commercial PEIs, the study further demonstrated the ability to utilize sulfonate groups in polyimides.

This study presents the facile, high-yielding synthesis of a sulfonated aromatic diamine, phosphonium-neutralized monomer, methyltriphenylphosphonium 2,2'-benzidinedisulfonate (BDSA-MTPP). This monomer was then polymerized with pyromellitic dianhydride and copolymerized with 4,4'-oxydianiline (ODA) and the sodium salt of 4,4'-diaminodiphenyl-2,2'-disulfonic acid (BDSA). The resulting polyelectrolytes maintained competitive thermal stability and were characterized regarding their water solubility. These polymers represent a platform for future development; this method further broadens the modularity of this family of polyimides and opens up a broader chemical space for the use of these polymers in adhesion, coatings, and flame retardant materials, including fluorine-free fire-fighting foams.

4.3. Experimental

Materials: Methytriphenylphosphonium bromide (MTPP-Br) (Acros Organics, 98%), (1-dodecyl)triphenylphosphonium bromide (DDMTPP-Br) (Alfa Aesar, 98+%), Amberlite IRN 78 strong anionic exchange resin (Acros Organics, OH-form), dimethylaminoethanol (Acros Organics, 99%), hydrochloric acid (Fisher Chemical, certified ACS), deuterated chloroform (CIL, 99.8%), deuterated dimethyl sulfoxide (DMSO- d_6) (CIL, 99. %), methanol (Fisher, HPLC grade) were used as received. Dimethyl sulfoxide anhydrous (Acros Organics, 99.5%) and N-methyl-2-pyrrolidone anhydrous (NMP) (Acros Organics, 99.5%) were stored over activated molecular sieves. Pyromellitic dianhydride (PMDA) (Acros Organics, > 98%) was sublimed before use. 2,2'-benzidinedisulfonic acid (BDSA) (TCI, > 70 %) was dried and titrated with NaOH and stored in a vacuum oven at 150 °C before use.

Analytical Methods: ^{1}H and ^{31}P nuclear magnetic resonance (NMR) spectroscopy were performed using a Varian Unity U4-DD2 400 at 25 °C. $CDCl_3$ or DMSO-d_6 was used as the solvent for NMR analysis. Thermogravimetric analysis (TGA) was performed on a T.A. Instruments Q500 with a 10 °C/min heating rate from 25 °C to 600 °C/1000 °C under N_2 or air. Differential scanning calorimetry (DSC) was conducted using a T.A. Instruments Q2000 DSC coupled with an RCS90 cooling system, utilizing a heat/cool/heat cycle with a 30 °C/min rate and N_2 cell purge. Glass transition (T_g) values (if present) were determined from the midpoint of the thermal transition in the second heat cycle using T.A. Universal Analysis software. Dynamic mechanical analysis (DMA) was performed on a T.A. Instruments Q800 in tension mode at a frequency of 1Hz with an oscillatory amplitude of 5 μm, a static force of 0.01 N, and a force track of 125%. Samples were heated at 3 °C/min to 380 °C. FTIR analysis was performed using a Nicolet iS5 equipped with an iD7 ATR stage at room temperature.

Synthesis of phosphonium-containing diamine monomer, methyltriphenylphosphonium 2,2'-benzidinedisulfonate (BDSA-MTPP): This process was partly based on a technique used in a study by Brennecke et al.[22] Amberlite IRN 78 ion-exchange resin (15 g) was added to a 100 mL round bottom flask containing 50 mL of methanol. MTPP-Br (6.223 g, 0.017 mol) was added, and the mixture was stirred at room temperature until completely dissolved. Upon complete dissolution, BDSA (3 g, 0.008 mol, in slight excess) was added and stirred at room temperature until the solution turned a light yellow and the approximate stoichiometric amount of BDSA was dissolved (approx. 15 min). The solution was vacuum filtered to remove the resin and excess BDSA, and the filtrate was rotary-evaporated to afford an off-white/ light yellow powder (BDSA-MTPP). The product was dried in a vacuum oven at 150 °C before use. Yield: 92.5%. ^{1}H NMR (400 MHz, DMSO-d_6, Figure 1) δ 8.03 – 7.63 (m, 30H), 7.22 (d, J = 8.2 Hz, 2H), 7.12 (d, J = 2.5 Hz, 2H), 6.27 (dd, J = 8.2, 2.6 Hz, 2H), 4.71 (s, 4H), 3.14 (d, J = 14.6 Hz, 6H).

Representative poly(amic acid) synthesis (50 mol% BDSA-Na). A two-neck round bottom flask equipped with a magnetic stir bar and nitrogen inlet was charged with BDSA-Na (0.4451 g, 1.146 mmol) and BDSA-MTPP (1.028 g, 1.146 mmol). The flask was purged and backfilled with N_2 three times before adding 8-10 mL of anhydrous DMSO. Following complete dissolution of the amines, PMDA (0.5 g, 2.292 mmol) was added to the solution with an additional 2-3 mL of DMSO. The resultant viscous solution was allowed to stir under nitrogen for 12 h before being stored in a refrigerator at 8 °C until ready to use.

Representative sulfonated poly(amic acid) salt (sPAAS) formation: Addition of an equal molar equivalent of DMAE to the carboxylic acid functionalities of a poly(amic acid) polymerization solution permitted formation of carboxylate-ammonium interactions. Following 6 h of stirring at

room temperature under air, the sPAAS solutions were diluted by half with DMSO before being precipitated into 80/20 (v:v) acetone/ethanol. After 4 h of stirring in the precipitation media, the solid powder was collected and subsequently washed with another 10x (by approximate filtrate mass) of acetone. Filtering and drying under vacuum at room temperature enabled final isolation of the slightly yellow sPAAS powder.

Film fabrication. Poly(amic acid) solution was allowed to warm to room temperature and was bladed on a glass slide on a level surface (additional DMSO added if necessary). The slide was then placed into a vacuum oven and kept at room temperature for 1 hour before being slowly ramped to 200 °C. The film was then held at 200 °C for 0.5 h and then transferred to a vacuum chamber residing in a metal bath. The chamber was then heated slowly (approximately 2 °C/min) to 350 °C and held at that temperature for 1 h. Films were then cooled slowly to room temperature, delaminated using acetone, dried at 60 °C overnight, and stored in a desiccator before analysis.

4.4. Results and Discussion

Synthesis methyltriphenylphosphonium 2,2'-benzidinedisulfonate (BDSA-MTPP)

BDSA is readily neutralized with organic bases, such as various amines (discussed in Addendum). For BDSA to be neutralized by a phosphonium compound, it was helpful to convert methyltriphenylphosphonium bromide to methytriphenylphosphonium hydroxide. Hydroxide ions are harder bases (HSAB theory) than bromide ions, and as counter ions react with acids more readily in exchange reactions. Therefore, MTPP-Br was conveniently treated with a strongly basic ionic exchange resin, Amberlite IRN-78, in methanol to give the hydroxide form. The hydroxide counterions of MTPP-OH were subsequently exchanged with the sulfonic acids of BDSA to give a novel phosphonium-containing aromatic diamine monomer. Throughout the reaction

(approximately 15 min), the solution began to turn a light yellow as the stoichiometric amount of BDSA dissolved. After filtration of the anion exchange resin and excess BDSA, the homogenous light yellow solution was placed on a rotary evaporator to remove solvent. BDSA-MTPP (**Scheme 1**). The reaction gave a slight-yellow powder in a yield greater than 90%.

Scheme 1. Synthesis of BDSA-MTPP

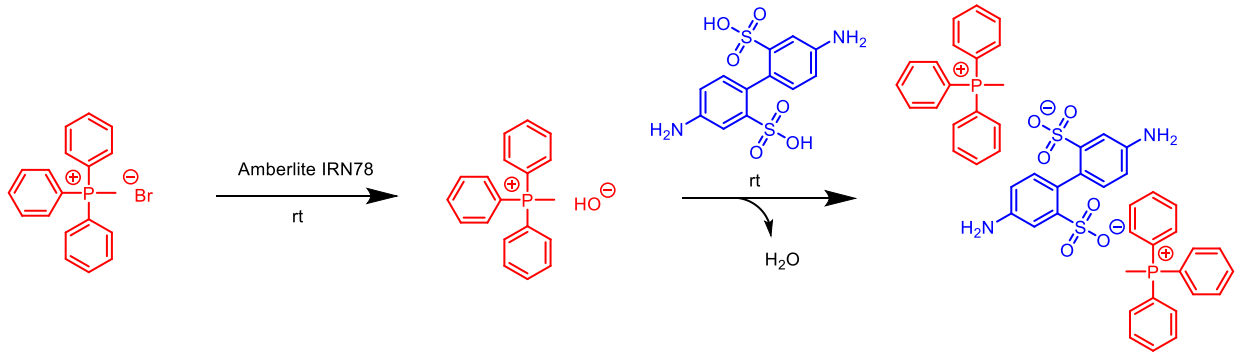

^{1}H NMR spectroscopy in DMSO-d_6 (**Figure 1)** enabled structural analysis of BDSA-MTPP. Interestingly, incorporating a bulkier cation caused an upfield shift in the BDSA amine and aromatic proton resonances.[23] The signal of the methyl group protons of the MTPP remained a distinctive doublet due to the two-bond coupling with phosphorus ($^{2}J_{PH}$=14.6 Hz) and also shifted slightly upfield. ^{31}P-NMR (**Figure S2**) did not show any changes from MTPP-Br to BDSA-MTPP. The chemical environment did not change significantly enough for the phosphorus signal to change, and a single resonance around 30 ppm remained the same in the spectrum of the product. The proton signals of BDSA and MTPP integrated quantitatively in a 1:2 molar ratio corresponding to 2 phosphonium cations per one benzidine sulfonate (2 sulfonate groups). Integration confirmed quantitative conversion and purity of novel BDSA-MTPP monomer. The

monomer, being fairly hygroscopic similarly to BDSA-Na, displayed a significant water signal in the ^{1}H-NMR despite being dried in a vacuum oven before use.

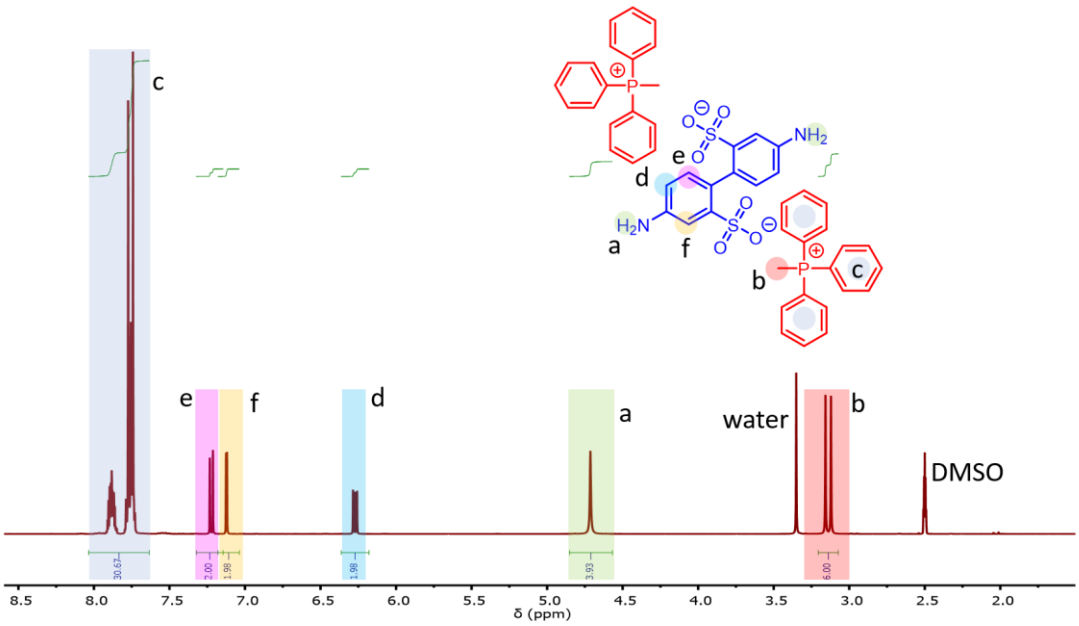

Figure 1. ^{1}H NMR spectrum of BDSA-MTPP (DMSO-d_6, 400 MHz)

Monomer Thermal Analysis

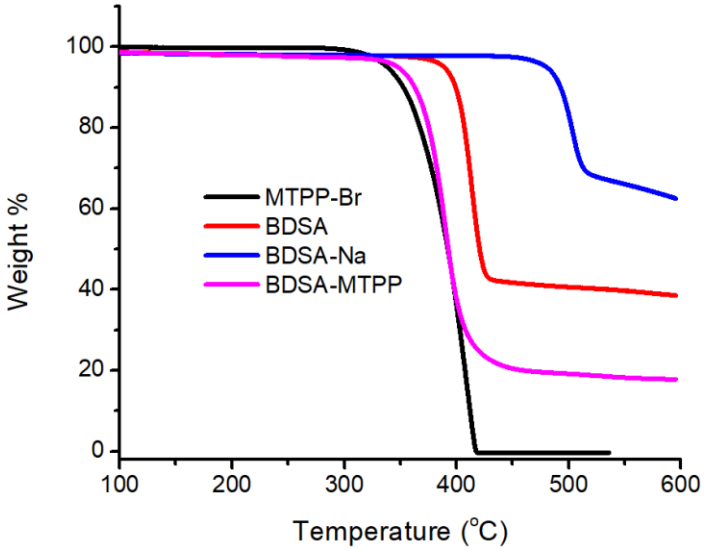

Figure 2. TGA comparison of BDSA monomers. BDSA-MTPP shows a $T_{d,5\%}$ of 365 °C compared to BDSA-Na, which is over 500 °C (10 °C/min ramp, N_2)

Thermogravimetric analysis (TGA) assessed the weight-loss behavior of BDSA-MTPP (**Figure 2**). BDSA-MTPP shows a single-step weight loss at approximately 365 °C, whereas BDSA-Na has an onset weight-loss over 500 °C. The size of the sulfonate counterion, as well as intrinsic thermal stability, contributed to the differences seen in the degradation temperature. Sulfonate counterion size can dictate the thermal stability of a monomer or polymer as decomposition is strongly influenced by ionic interaction, ionic strength, and sulfonate-counterion interaction.[24] MTPP is a much larger, bulkier cation than Na and thusly formed a weaker ionic pair with the sulfonate groups of BDSA. Additionally, MTPP as an organic cation is naturally less thermally stable, contributing to the reduction in the onset weight loss. As this was the case, we only conducted imidization reactions up to 350 °C, slightly under the weight-loss onset of BDSA-MTPP, to avoid any potential degradation. The BDSA-MTPP based polyimides also exhibited reductions in weight-loss temperatures compared to the BDSA-Na polyimides, discussed in more detail later in this report.

Polymer Synthesis of BDSA-MTPP Copolymers

Similar to our BDSA-Na study, we first investigated copolymers of BDSA-MTPP and ODA with PMDA. **Scheme 2** shows the synthesis and copolymerization with ODA of fully aromatic sulfonated polyimides containing the phosphonium counterion via the classic two-step route to polyimide formation. BDSA-MTPP also maintained limited solubility in typical organic solvents that facilitate poly(amic acid) (PAA) reactions, and although it was slightly soluble in NMP, unlike BDSA-Na, DMSO was still used as the reaction solvent. Upon full dissolution of the diamines in the reaction solvent, PMDA was added under a nitrogen cushion (as discussed in Chapter 2), and the perceivable viscosity of the reaction solution increased as the ratio of BDSA-MTPP/ODA was

decreased. In the second step, solutions cast onto glass slides enabled film formation via an imidization schedule up to 350 °C, as limited by the thermal characteristics of BDSA-MTPP. As seen in **Figures S3** and **S4** and as evidenced by the imidization kinetic study presented in Chapter 2, these polymers do not reach full degrees of imidization due to their backbone rigidity. However, a 350 °C temperature ceiling still achieves high degrees of "attainable" imidization. Copolyimide compositions of 100%, 75%, 50%, 25%, and 0% BDSA-MTPP/ODA were synthesized.

Scheme 2. Synthesis of PMDA/BDSA-MTPP sulfonated polyimide (sPI) and copolymers with ODA

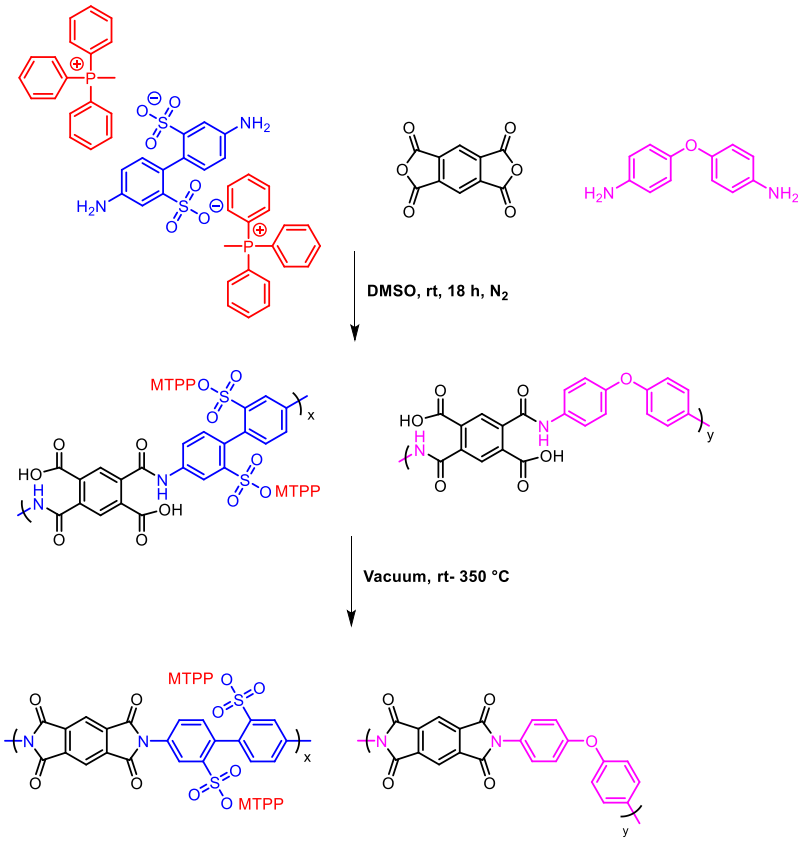

We also synthesized copolymers of BDSA-MTPP and BDSA-Na with PMDA (**Scheme 3**). These PAA reactions did not have the same visual increases in viscosity as those with ODA due to the lower polyaddition reactivity of both sulfonated monomers.[25-26] Copolyimide compositions

of 100%, 75%, 50%, 25%, and 0% BDSA-MTPP: BDSA-MTPP were synthesized. The same imidization procedure afforded this set of copolymers.

Scheme 3. Synthesis of PMDA/BDSA-MTPP/BDSA-NA copolymers

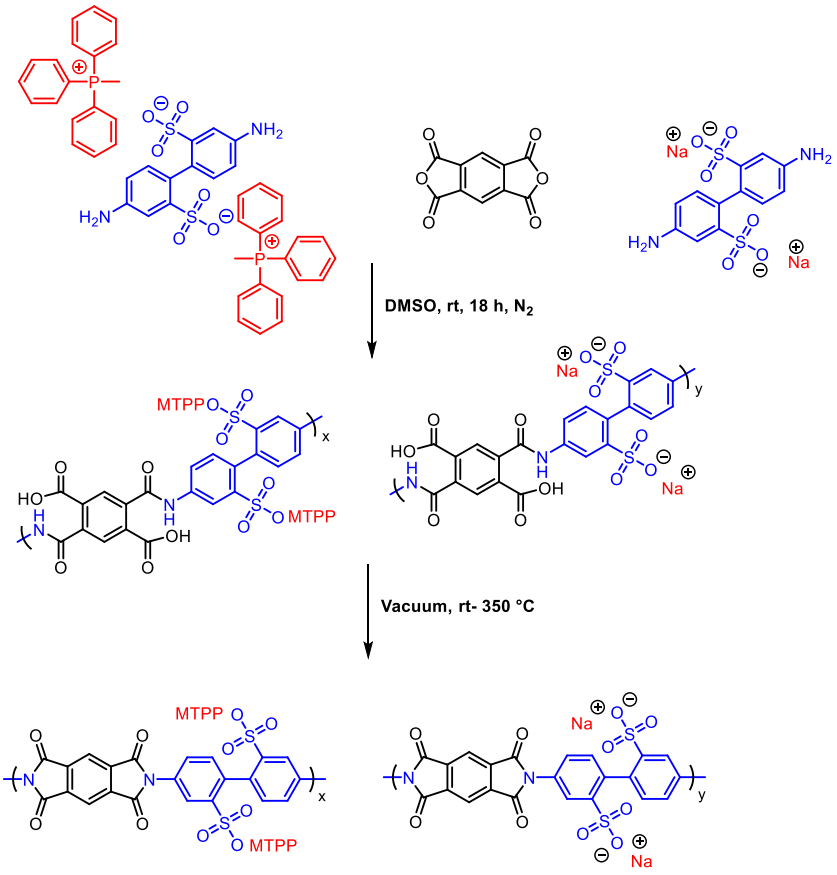

Film Formation and Thermal Properties

All compositions of the sPIs produced free-standing films of varying mechanical robustness, though copolymers containing BDSA-Na/ODA behaved much differently than those of BDSA-MTPP/BDSA-Na copolymers. All compositions of BDSA-MTPP/BDSA-Na copolymers were very brittle and increasable due to their fully sulfonated nature and possibly the incorporation of the bulky phosphonium cations (ref). The films of BDSA-MTPP/ODA copolymers were naturally more similar to those of BDSA-Na/ODA polymers. Copolyimides containing 100

mol% and 75 mol% BDSA-MTPP gave very brittle and non-creasable films while increasing the content of ODA subsequently increased the robustness of the resulting films, strongly correlating film toughness to diamine monomer content.

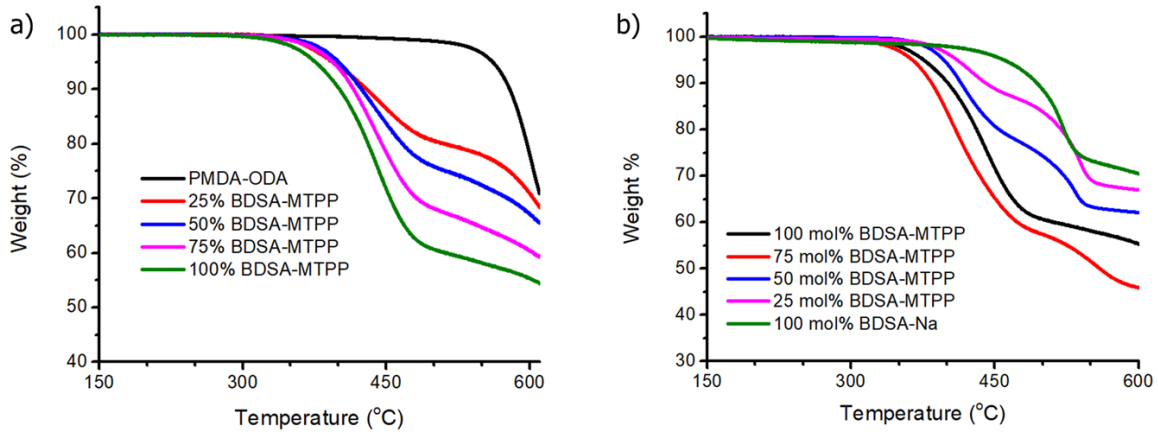

Figure 3. TGA thermograms of a) BDSA-MTPP/ODA co-sPI series and b) of the BDSA-MTPP/BDSA-Na co-sPI series (10 °C/min ramp, N_2)

TGA elucidated the weight-loss profiles of both sets of copolyimides (**Figure 3**). The homopolymer of PMDA-ODA naturally has the highest $T_{d,5\%}$ of all the presented polyimides, at 560 °C, and proceeds through a one-step weight-loss akin to the decomposition of the backbone. The copolymers of BDSA-MTTPP/ODA all had $T_{d,5\%}$ of approximately 395 °C with a two-step weight-loss profile. In these copolymers, the first step neatly accounted for the decomposition of the methyltriphenylphosphonium cation at the various percent of incorporation into the onset of desulfonation, while the second step corresponded to the remaining backbone. As the percent of BDSA-MTPP monomer (sulfonation content) increased in the copolymer composition, the second weight-loss step broadened and became less defined. Interestingly, the homopolymer of BDSA-MTPP/ODA exhibited a $T_{d,5\%}$ lower than that of the copolyimides, at approximately 375 °C, perhaps highlighting the differences between a fully ionic backbone and a copolymer with a

nonionic comonomer. It is worth noting that the residual weight for the copolyimides at 1000 °C was higher than the residual weight of PMDA-ODA (**Figure S6**).

This difference is also noticed in the weight-loss profiles of the BDSA-MTPP: BDSA-Na copolyimides. As the mol% of BDSA-MTPP deceased, the $T_{d,5\%}$ of the copolymers steadily increased. The trend is in contrast to the last set of copolymers that shared approximately the same $T_{d,5\%}$. This may be due to combinations of different ionic interactions between the phosphonium sulfonate groups and the sodium sulfonate groups, which delayed the decomposition of the MTPP moiety. Additionally, the $T_{d,5\%}$ of the 75 mol% BDSA-MTPP copolymer was 366 °C and repeatedly fell below that of the homopolymer, also possibly due to various ionic interactions. However, this phenomenon is difficult to elucidate and will require further analysis to determine the origin of this behavior. Nevertheless, all copolymers exhibited a similar two-step weight-loss profile. The first step corresponds to the decomposition of the MTPP, and the second step to backbone decomposition at approximately 480 °C.

DSC did not discern any transitions for these sPIs in appropriate temperature ranges concerning their weight-loss temperatures. DMA, however, was able to provide insight into thermomechanical behavior (**Figure 4**). All films of the BDSA-MTPP/BDSA-Na copolymer series were too brittle and could not be loaded into the DMA. Similarly, co-sPIs of BDSA-MTPP/ODA above 50 mol% incorporation were too fragile to prepare DMA specimens, and only 25 and 50 mol% BDSA-MTPP/ODA were tested. DMA runs were limited to temperatures below 2% weight loss of the co-sPIs.

As seen and discussed in Chapter 2, the addition of the sulfonated diamine monomer increased the storage modulus T_g compared to PMDA-ODA. PMDA-ODA exhibits the onset of a glass transition around 365 °C. While the 50 mol% BDSA-Na/ODA co-sPI did show some relaxations

in modulus, it did not pass through any transitions. However, when the Na counter ion was substituted for MTPP at the same mol%, a broad glass transition became evident, with tan δ appearing to peak at 375 °C just before the end of the run. While the structural nature of these polyimides and a large dispersity can give rise to broad, shallow transitions, the presence of a large, bulky counterion reduces T_g. Large counterions associate less and form weaker ionic interactions.[27] In this case, the counterion plasticization effect seems strong enough to disrupt intermolecular chain interactions and chain transfer complexes present in neutral polyimides, effectively lowing the T_g below that of PMDA-ODA. As the mol% of BDSA-MTPP decreased to 25% and thusly the amount of the large phosphonium cation, the effect became less drastic, shifting the T_g to higher temperatures, albeit still below PMDA-ODA. The storage modulus at 100 °C also decreased as the ionic/ rigid monomer content decreased.

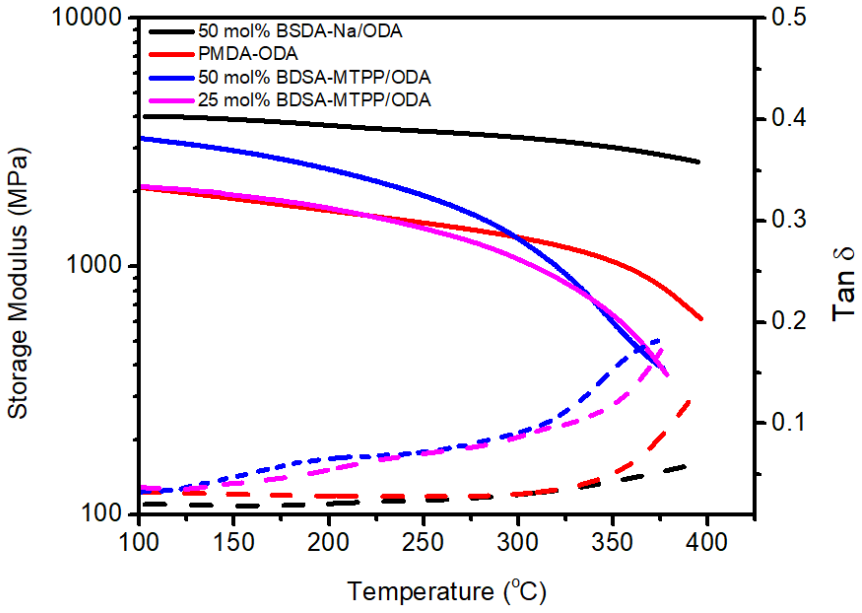

Figure 4. Dynamic mechanical comparison of storage modulus and tan δ of two BDSA-MTPP/ODA copolymers of differing composition, PMDA-ODA, and a copolymer of BDSA-Na/ODA (0.1% strain, 3 °C/min)

Water Solubility

To advance our SERDP directives of utilizing sulfonated polyimides to replace conventional AFFF agents, we explored the water solubility of both sets of co-sPIs. Unsurprisingly, the BDSA-MTPP/ODA poly(amic acid)s and corresponding polyimides, as well as the BDSA-MTPP homopolymer, are not water-soluble. Despite high ionic content, hydrophobic interactions of the backbone overwhelm electrostatic interactions, like hydration, of MTPP and the pendant sulfonate groups with water.[28] Upon copolymerization of BDSA-MTPP with BDSA-Na at mol% above 50, the PAA became readily water-soluble. **Figure 5** illustrates a progression in water solubility of the BDSA-MTPP/BDSA-Na co-poly(amic acid)s. However, for the corresponding polyimides to be water-soluble, BDSA-Na incorporation needed to be 75 mol% or greater, limiting sPIs to low phosphonium content. **Table 1** summarizes the solubility behaviors as well as their thermal characteristics.

Figure 5. Comparison of water solubility of BSDA-MTPP/BDSA-Na/ODA poly(amic acid)s. As the indicated mol % of BDSA-MTPP decreases, the solubility of the PAA increases. At 25 mol% BDSA-MTPP, the PAA is fully soluble.

Table 1. Summary of water solubility and thermal properties of BDSA-MTPP copolymers

BDSA-Na mol%	Polyamic acid solubility	Polyimide solubility	$T_{d,5\%}$ (°C)	T_g (°C)*
100	++	++	**460**	-
75	++	+	**411**	-
50	+-	-	**396**	-
25	-	-	**364**	-
0†	-	-	**376**	-
ODA mol%				
25	-	-	**394**	-
50	-	-	**400**	**325**
75	-	-	**395**	**345**
100	-	-	**561**	**365**

† 100 mol % BDSA-MTPP
* measured from onset T_g, DMA

In light of the low solubility of the MTPP containing polymers, dimethylaminoethanol (DMAE) was employed to improve the solubility of high MTPP content PAAs. The addition of a non-nucleophilic base like DMAE neutralized the carboxylic acids of the poly(amic acid)s, forming a poly(amic acid) salt, which is very stable in aqueous conditions (**Scheme 3**). This method facilitated the use of sulfonated poly(amic acid) salts (sPAAS) in Chapter 2. Upon addition of DMAE (1:1 to carboxylic acids) to the DMSO reaction solution, the reaction visibly increased in viscosity as it was mixed. When using a mechanical stirrer, addition of the DMAE causes the reaction mixture to wrap and climb the stir bar. The resulting sPAAS were fully soluble in water with 100 mol% phosphonium content (**Figure 6**), which allows for an investigation of these polymers in aqueous fire suppression formulations to study any enhanced behavior due to the incorporation of the phosphonium moiety.

Scheme 3. Synthesis of DMAE neutralized sPAAS

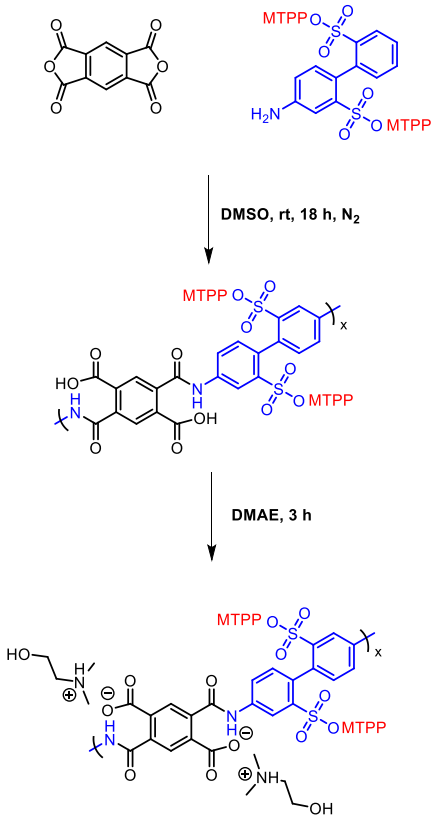

Figure 6. This image shows the distinct difference in the solubility of a sPAAS with 100 mol% BDSA-MTPP neutralized with DMAE vs. the unneutralized PAA.

4.4. Conclusions

This study presents the facile synthesis of a novel phosphonium-containing sulfonated diamine, BDSA-MTPP. The traditional 2 step polymerization for polyimides enabled the synthesis of two sets of copolyimides with BDSA-Na and ODA at various mol% from 0-100%. While all polymers produced free-standing films, those copolymers of BDSA-MTPP/ODA were much more robust and flexible overall. From DMA analysis of the films tested, MTPP was shown to have a plasticizing effect on the polymer matrix, lowering the T_g even below that of the neutral homopolymer. TGA revealed that all BDSA-MTPP copolyimides maintained competitive thermal stability and had higher char yields than the corresponding homopolymers at 1000 °C. Only those copolyimides with greater than 70 mol% BDSA-Na content were soluble in water. However, the addition of DMAE created an sPAAS which allowed for a polymer with 100 mol% BDSA-MTPP to be fully water-soluble. This enabled the continued development of aqueous polyimide fire suppression foams. Overall, the counterion exchange and ease of synthetic variability showcased the modularity that can be integrated into polyimide systems. Future work needs to be done to characterize the flame retardant properties of the BDSA-MTPP polymers as films and in aqueous solution, but these polymers and their method of preparation show great promise as a means to expand both the ionic polymer and polyimide vernacular.

4.5. References

1. Fang, J.; Guo, X.; Harada, S.; Watari, T.; Tanaka, K.; Kita, H.; Okamoto, K.-i. *Macromolecules* **2002**, *35*, 9022-9028.

2. Arnold, C. A.; Summers, J. D.; Chen, Y. P.; Bott, R. H.; Chen, D.; McGrath, J. E. *Polymer* **1989**, *30*, 986-995.

3. Genies, C.; Mercier, R.; Sillion, B.; Cornet, N.; Gebel, G.; Pineri, M. *Polymer* **2001**, *42*, 359-373.

4. Wozniak, A. I.; Yegorov, A. S.; Ivanov, V. S.; Igumnov, S. M.; Tcarkova, K. V. *J. Fluor. Chem.* **2015**, *180*, 45-54.

5. Kim, O.; Kim, K.; Choi, U. H.; Park, M. J. *Nat. Commun.* **2018**, *9*, 5029.

6. Lee, H.-J.; Jo, Y.-R.; Kumar, S.; Yoo, S. J.; Kim, J.-G.; Kim, Y.-J.; Kim, B.-J.; Lee, J.-S. *Nat. Commun.* **2016**, *7*, 12803.

7. Kaestner, P.; Strehmel, V. *J. Polym. Sci.* **2020**, *58*, 977-987.

8. Hemp, S. T.; Zhang, M.; Allen Jr, M. H.; Cheng, S.; Moore, R. B.; Long, T. E. *Macromol. Chem. Phys.* **2013**, *214*, 2099-2107.

9. Jangu, C.; Long, T. E. *Polymer* **2014**, *55*, 3298-3304.

10. Shaplov, A. S.; Vlasov, P. S.; Armand, M.; Lozinskaya, E. I.; Ponkratov, D. O.; Malyshkina, I. A.; Vidal, F.; Okatova, O. V.; Pavlov, G. M.; Wandrey, C.; Godovikov, I. A.; Vygodskii, Y. S. *Polym. Chem.* **2011**, *2*, 2609-2618.

11. Mecerreyes, D. *Prog. Polym. Sci.* **2011**, *36*, 1629-1648.

12. Cao, K.; Serrano, J. M.; Liu, T.; Stovall, B. J.; Xu, Z.; Arrington, C. B.; Long, T. E.; Odle, R. R.; Liu, G. *Polym. Chem.* **2020**, *11*, 393-400.

13. Cao, K.; Zhou, Z.; Liu, G. *Polym. Chem.* **2018**, *9*, 5660-5670.

14. Yasuda, T.; Nakamura, S.-i.; Honda, Y.; Kinugawa, K.; Lee, S.-Y.; Watanabe, M. *ACS Appl. Mater. Interfaces* **2012**, *4*, 1783-1790.

15. Shaplov, A. S.; Morozova, S. M.; Lozinskaya, E. I.; Vlasov, P. S.; Gouveia, A. S. L.; Tomé, L. C.; Marrucho, I. M.; Vygodskii, Y. S. *Polym. Chem.* **2016**, *7*, 580-591.

16. Hayashi, E.; Thomas, M. L.; Hashimoto, K.; Tsuzuki, S.; Ito, A.; Watanabe, M. *ACS Appl. Polym. Mater*. **2019**, *1*, 1579-1589.

17. Ito, A.; Yasuda, T.; Ma, X.; Watanabe, M. *Polym. J.* **2017**, *49*, 671-676.

18. Zhang, Y.; Chen, L.; Zhao, J.-J.; Chen, H.-B.; He, M.-X.; Ni, Y.-P.; Zhai, J.-Q.; Wang, X.-L.; Wang, Y.-Z. *Polym. Chem.* **2014**, *5*, 1982-1991.

19. Cao, K.; Guo, Y.; Zhang, M.; Arrington, C. B.; Long, T. E.; Odle, R. R.; Liu, G. *Macromolecules* **2019**, *52*, 7361-7368.

20. Hou, S.; Zhang, Y. J.; Jiang, P. *Polym. Degrad. Stab.* **2016**, *130*, 165-172.

21. Cao, K.; Stovall, B. J.; Arrington, C. B.; Xu, Z.; Long, T. E.; Odle, R. R.; Liu, G. *ACS Appl. Polym. Mater*. **2020**, *2*, 66-73.

22. Avelar Bonilla, G. M.; Morales-Collazo, O.; Brennecke, J. F. *J. Chem. Eng. Data* **2019**, *64*, 4875-4881.

23. Abdulahad, A. I.; Jangu, C.; Hemp, S. T.; Long, T. E. *Macromol. Symp*. **2014**, *342*, 56-66.

24. Feldheim, D. L.; Lawson, D. R.; Martin, C. R. *J. Polym. Sci. B Polym. Phys.* **1993**, *31*, 953-957.

25. Hodgkin, J. H. *J. Polym. Sci. Polym. Chem. Ed.* **1976**, *14*, 409-431.

26. Ratta, V. Crystallization, Morphology, Thermal Stability and Adhesive Properties of Novel High Performance Semicrystalline Polyimides. Virginia Tech, 1999.

27. Tudryn, G. J.; Liu, W.; Wang, S.-W.; Colby, R. H. *Macromolecules* **2011**, *44*, 3572-3582.

28. Ranke, J.; Othman, A.; Fan, P.; Müller, A. *Int. J. Mol. Sci.* **2009**, *10*, 1271-1289.

4.6. Supporting Information

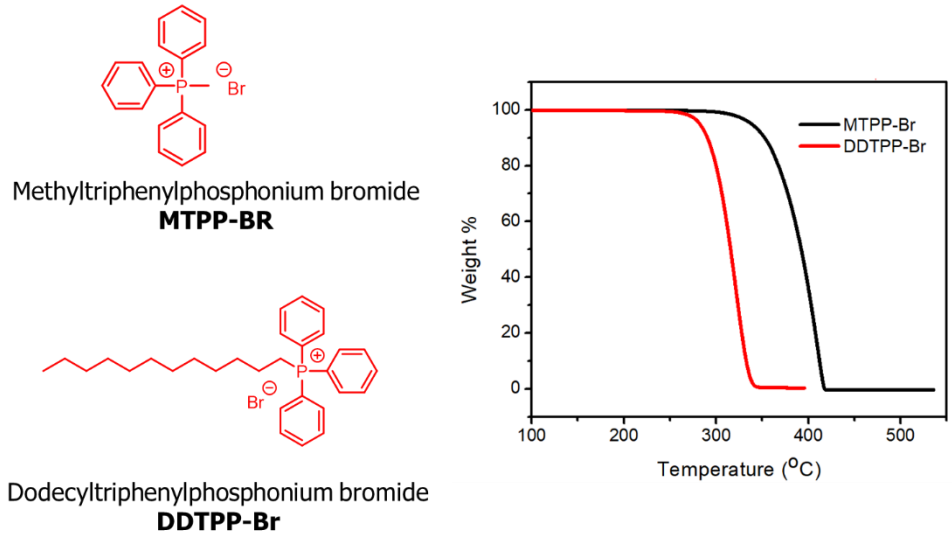

Figure S1. TGA highlighting the differences in thermal stability between MTPP-Br and DDTPP-Br (10 °C/min ramp, N_2)

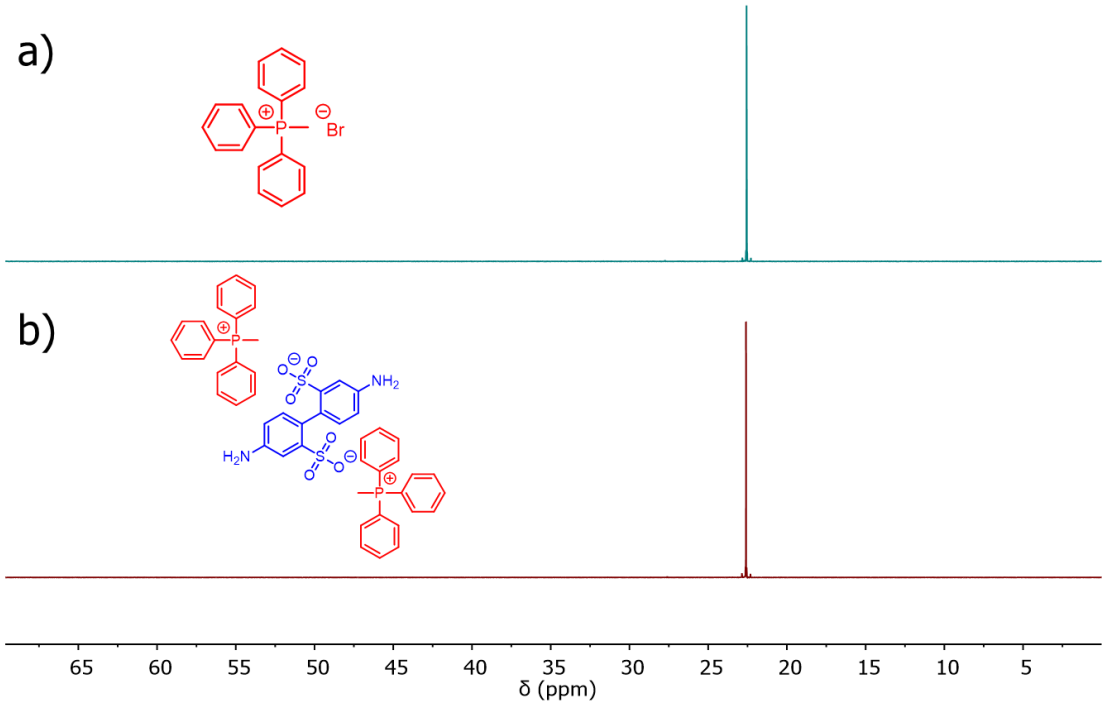

Figure S2. ^{31}P NMR spectrum of a) MTPP-Br and b) BDSA-MTPP

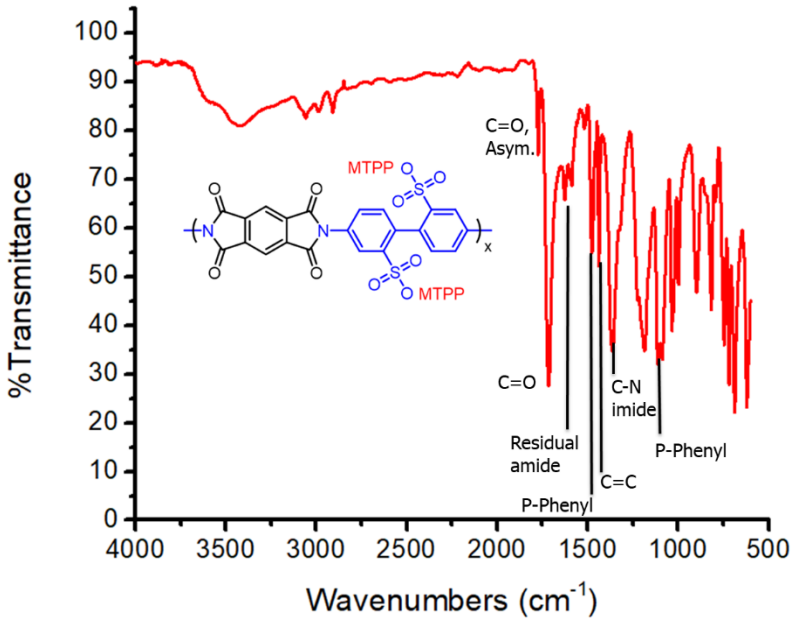

Figure S3. IR spectrum of BDSA-MTPP/PMDA homopolyimide.

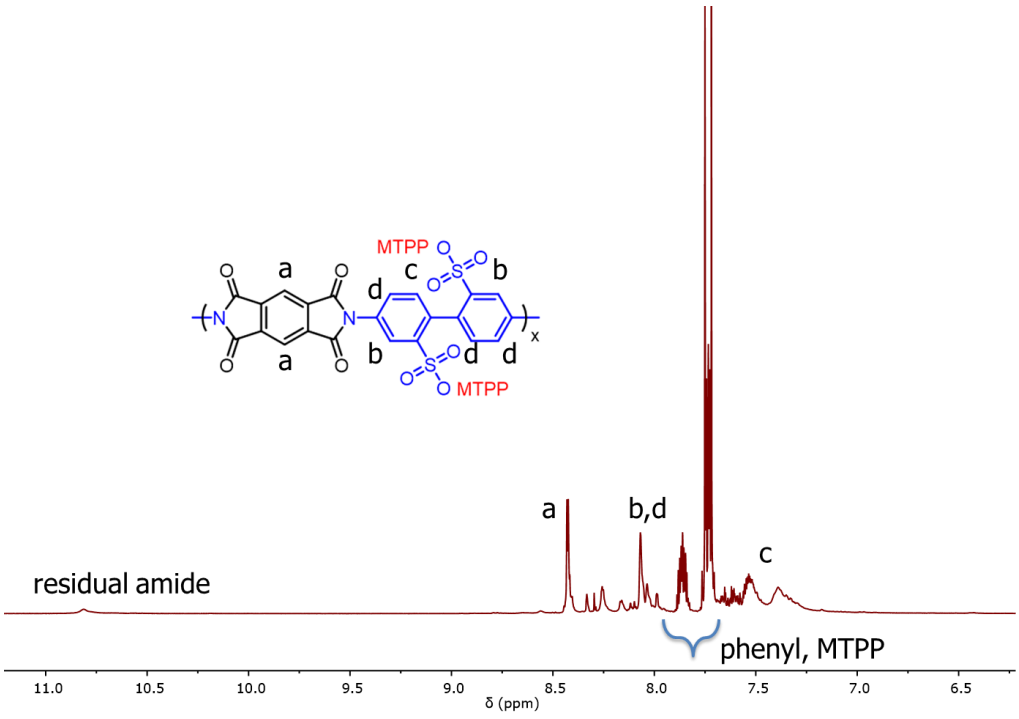

Figure S4. ^{1}H NMR spectrum of 25 mol% BDSA-MTPP: BDSA-Na polyimide (DMSO-d_6, 400 MHz)

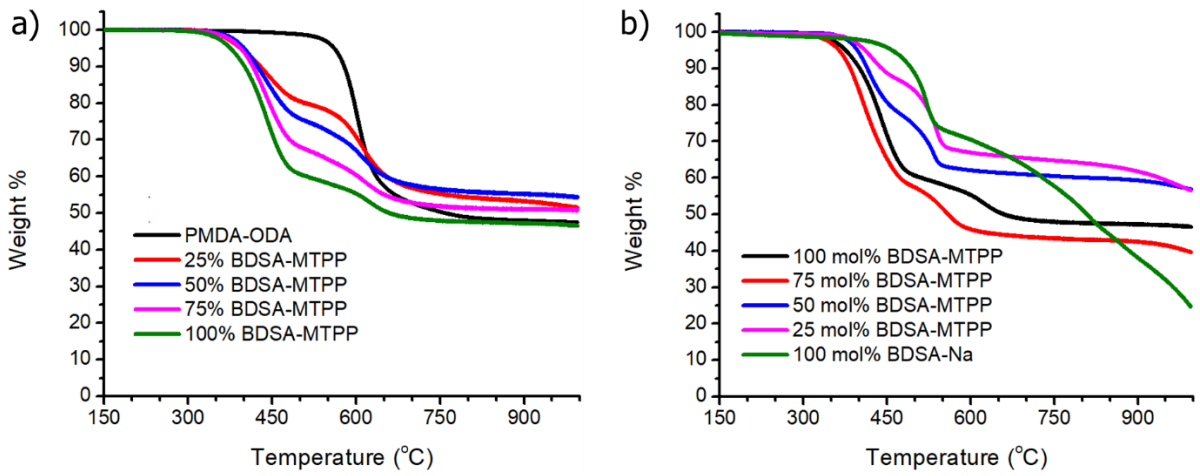

Figure S5. TGA thermograms of a) BDSA-MTPP/ODA co-sPIs and b) BDSA-MTPP/BDSA-Na co-sPIs under N_2 to 1000 °C (10 °C/min ramp)

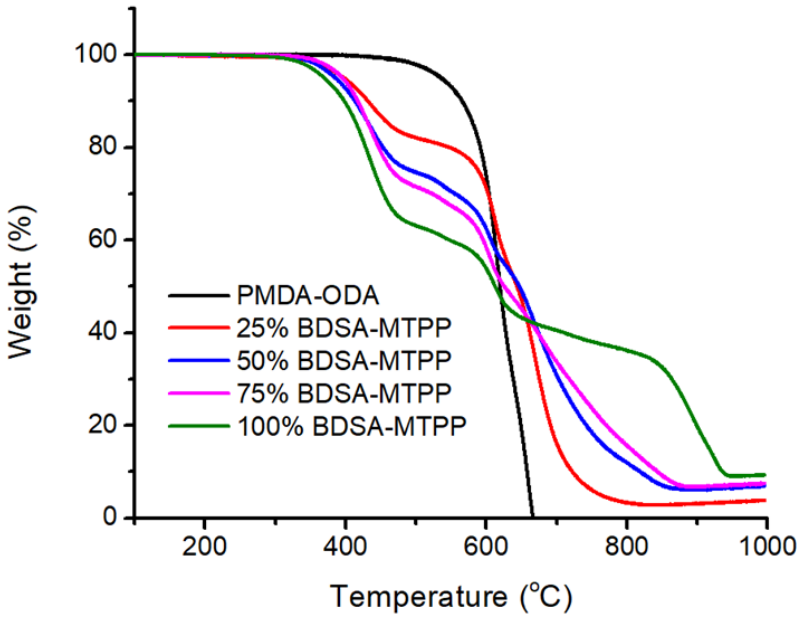

Figure S6. TGA thermogram of BDSA-MTPP/ODA co-sPIs under air to 1000 °C (10 °C/min ramp)

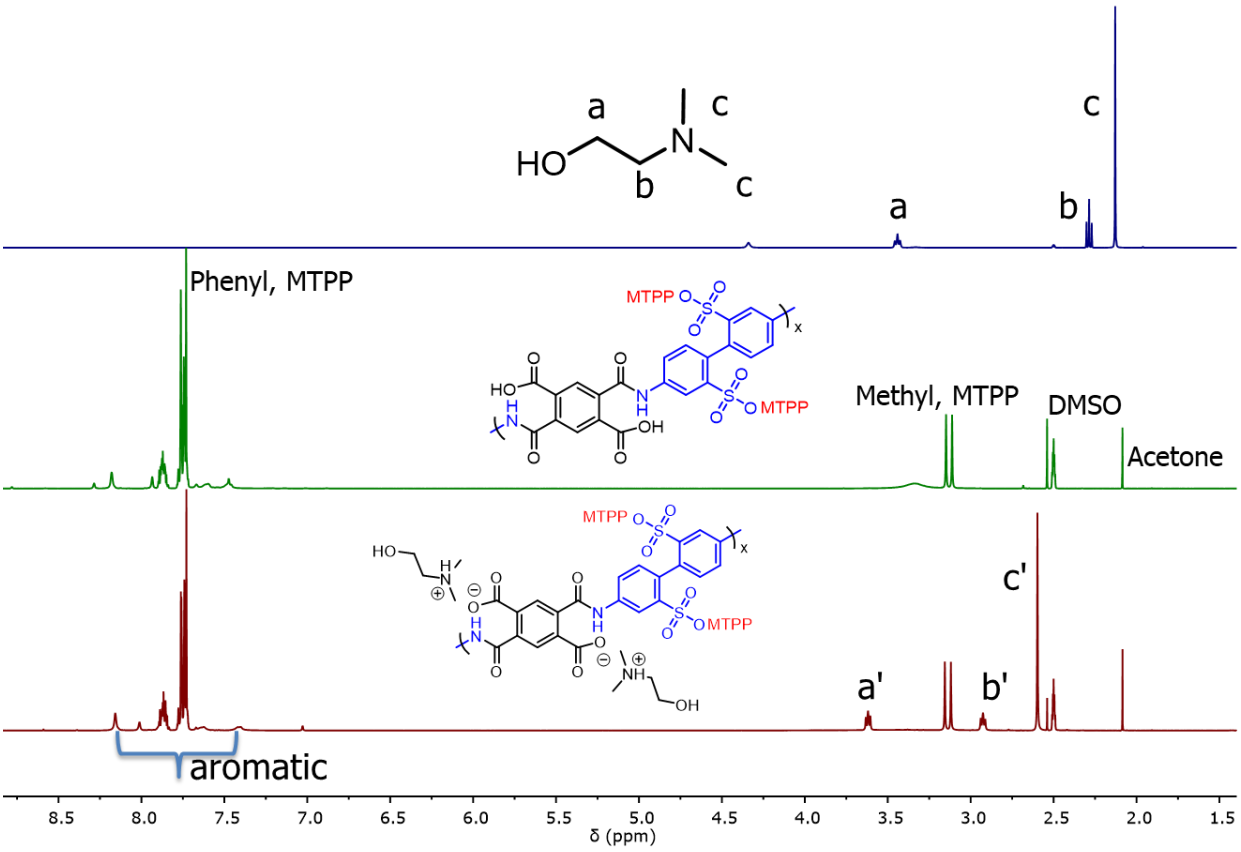

Figure S7. ^{1}H NMR spectra showing the sPAAS with DMAE and comparison to the components before neutralization (DMSO-d_6, 400 MHz)

Chapter 5. Efforts towards the synthesis of PDMS-containing, water-soluble sulfonated polyimides and poly(amic acids) for fire suppression foams

Benjamin J. Stovall, Clay B. Arrington, and Timothy E. Long

Department of Chemistry, Macromolecules Innovation Institute (MII)
Virginia Tech, Blacksburg, VA 24061

5.1. Abstract

Siloxanes show promise as components in fluorine-free fire suppression foams due to their surface properties and low flammability. With the inspiration to explore fire suppression foams based on water-soluble sulfonated polyimides, this chapter investigates the incorporation of PDMS moieties into sulfonated polyimides (sPI) and sulfonated poly(amic acid)s through copolymerization. Two pathways were promising; segmented copolymers using BDSA-MTPP/ atPDMS and copolymers using a novel sulfonated diamine with an ionically-linked matPDMS cation. Though calculated PDMS incorporation for both systems was about half of what was expected, these copolymers may enhance the platform of polyimide-based fire suppression foams with further development and optimization.

5.2. Introduction

The Aqueous Film Forming Foams (AFFFs) employed for Class B (liquid fuel) fire suppression by the military contain fluorinated surfactants, i.e., perfluorinated compounds (PFCs), that impose several serious environmental impacts. The persistence, bioaccumulation, and toxicity (PBT) of these compounds results in the appearance of fluorosurfactant chemicals in populations not directly exposed to AFFFs, but rather through chemical migration within the ecosystem.[1] Halogenated, specifically fluorinated surfactants provide desirable thermal stability and

flammability resistance; however, their environmental impact suggests a necessary paradigm shift that completely removes halogenated sequences in conventional formulations. Currently, a limited number of fluorine-free foams exist on the market, but none meet the performance requirements for military applications (i.e., pass the fire performance set by MIL-F-24385F). Several efforts explored the replacement of fluoro-chemical surfactants with other organic and inorganic molecules. The early work in this area was performed with replacing the fluoro-chemical surfactant with xanthan gum, leading to the creation of the commercial fluorine-free foam RF6.[2-3] Though the exact formulation of RF6 is proprietary, it displays equivalent if not superior behavior to AFFF in several studies.[4-5] Siloxane-based foam formulations, however, have been gaining recent traction towards fluorine-free foams and AFFF replacement.

Siloxanes display many advantageous properties that make them attractive for fire suppression and flame retardant materials. Siloxanes have excellent heat resistance and thermal stability while maintaining low flammability and toxicity (environmentally friendly) which sees them employed in many copolymer systems and as additives.[6-10] Additionally, siloxanes demonstrate enhanced surface activity and the ability to lower surface tension.[11] Because of this advantage, siloxane surfactants are often propitious over hydrocarbon surfactants and can take on various forms, such as even in block or segmented copolymers.[11-14] Thusly, the examination of siloxane surfactants with and without conventional surfactants enabled further development of fluorine-free AFFF replacements. In small scale fire testing, siloxane-based foams displayed enhanced performance compared to other commercially available fluorine-free foams and synergistic properties in combination with other surfactants but still fell short of sating MIL-F-24385F.[15-17]

In this study, we continued our investigations in utilizing water-soluble sulfonated polyimides (sPI) and sulfonated poly(amic acid)s (sPAAS) as next-generation fire suppression foams through the incorporation of PDMS. Researchers have studied polyimide-PDMS copolymers for decades in a multitude of capacities like ion exchange membranes for fuel cells as well as flame retardant materials.[18-22] We attempted to synthesize sPI-PDMS segmented copolymers using aminopropyl-terminated PDMS (atPDMS) using both sodium 2,2'-benzidinedisulfonate (BDSA-Na) and methyltriphenylphosphonium 2,2'-benzidinedisulfonate (BDSA-MTPP). Additionally, a new ionic PDMS-containing sulfonated diamine monomer was synthesized from BDSA and a monoamino-terminated PDMS (matPDMS) that was subsequently polymerized. While there were some synthetic successes, further experimentation is required. However, the prospects of these sPI-PDMS copolymers remain an interesting avenue to pursue both fundamentally and in the context of fire suppression foams.

5.3. Experimental

Materials: Methyltriphenylphosphonium 2,2'-benzidinedisulfonate (BDSA-MTPP) was synthesized as described in Chapter 4. Aminopropyl-terminated terminated polydimethylsiloxane (atPDMS) (Gelest DMA-A12), monoaminopropyl-terminated polydimethylsiloxane (matPDMS) (Gelest MCR-A11), dimethylaminoethanol (Acros Organics, 99%), hydrochloric acid (Fisher Chemical, certified ACS), deuterated chloroform (CIL, 99.8%), deuterated dimethyl sulfoxide (DMSO- d_6) (CIL, 99. %), methanol (Fisher, HPLC grade), *m*-cresol (Acros Organics 99%) were used as received. Dimethyl sulfoxide anhydrous (Acros Organics, 99.5%) and N-methyl-2-pyrrolidone anhydrous (NMP) (Acros Organics, 99.5%) and tetrahydrofuran (THF) (Acros Organics, 99.5%) were stored over activated molecular sieves. Pyromellitic dianhydride (PMDA)

(Acros Organics, > 98%) was sublimed before use. 2,2'-benzidinedisulfonic acid (BDSA) (TCI, > 70 %) was dried and titrated with NaOH and stored in a vacuum oven at 150 °C before use.

Analytical Methods: ^{1}H nuclear magnetic resonance (NMR) spectroscopy was performed using a Varian Unity U4-DD2 400 (400 MHz) at 25 °C. $CDCl_3$ or DMSO-d_6 was used as the solvent for NMR analysis.

Synthesis of sPI-PDMS segmented copolymer with BDSA-Na (20 wt% PDMS): To a two neck round bottom flask equipped with a magnetic stir bar and nitrogen inlet, PMDA (0.500 g, 2.29 mmol) and atPDMS (0.314 g, 0.019 mmol) were added with an anhydrous THF/NMP solvent mixture (2:2 mL). The flask was evacuated and refilled with N_2 three times and was left to stir for 3 h to facilitate the "capping" of the siloxane oligomers. Following this reaction, BDSA-Na (0.818 g, 2.11 mmol) was dissolved in the minimum amount of anhydrous DMSO and added to the reaction solution by syringe from a nitrogen purged flask. The solubility of the reagents in the solvent system made it too difficult to proceed.

Synthesis of sPI-PDMS segmented copolymers with BDSA-MTPP (20 wt% PDMS): To a two-neck round bottom flask equipped with a magnetic stir bar and nitrogen inlet, atPDMS (0.561 g, 0.332 mmol) was added with an anhydrous THF/NMP solvent mixture (2:3 mL). The flask was evacuated and refilled with N_2 three times before BDSA-MTPP (1.758 g, 1.960 mmol) (dissolved in a minimum amount of NMP was added via syringe. Once homogenization was insured, PMDA (0.5 g, 2.292 mmol) was added. Homogeneity was maintained by adding THF and NMP as needed. The reaction was allowed to stir for 12 h under nitrogen before being precipitated into an 80:20 acetone: ethanol mixture. The remaining solution was stored in a refrigerator at 8 °C until ready to use.

Synthesis of monoammonium-terminated PDMS 2,2'-benzidinedisulfonate (BDSA-matPDMS): BDSA (1 g in slight excess) was added to a flask with approximately 50 ml of methanol at 50 °C. BDSA was titrated with a stoichiometric amount of matPDMS. Excess BDSA was filtered off, and the solution was put on a rotary evaporator. A waxy off-white solid was isolated. Yield: 96.8%. ^{1}H NMR (400 MHz, chloroform-*d*, **Figure 2**) δ 7.48 – 7.30 (m, 2H), 7.19 – 6.97 (m, 2H), 6.65 (s, 2H), 2.73 (s, 4H), 1.47 (s, 4H), 1.43 – 1.24 (m, 8H), 0.95 – 0.80 (m, 6H), 0.69 – 0.36 (m, 7H).

Synthesis of sPI with BDSA-matPDMS/ODA (10 wt% PDMS): To a two neck round bottom flask equipped with a magnetic stir bar and nitrogen inlet, BDSA-matPDMS (0.105 g, 0.041 mmol) and ODA (0.451 g, 2.251 mmol) were added with an anhydrous THF/NMP solvent mixture (2:3 ml). The flask was evacuated and refilled with N_2 three times before adding 8-10 mL of anhydrous NMP. Following complete dissolution of the amines, PMDA (0.500 g, 2.292 mmol) was added to the solution with an additional 2-3 mL of NMP. The resultant viscous solution was allowed to stir under nitrogen for 12 h before being stored in a refrigerator at 8 °C until ready to use.

5.4. Results and Discussion

Attempts towards sPI-PDMS segmented copolymers with BDSA-Na

While polyimide-siloxane polymers have been studied for many years, a significant factor that inhibits successful reactions is solubility. The solubility behavior of siloxane oligomers is considerably different than aromatic monomers and generally requires co-solvent systems.[18, 23] Insuring homogeneity throughout a reaction is vital to reaction completion and predictable composition. **Scheme 1** depicts the synthetic route taken as a first attempt to incorporate PDMS

into the sPI. Straying from traditional monomer addition, atPDMS (charged for 20 wt% incorporation as a starting point) was first treated with PDMA in an NMP/THF mixture to "cap" the siloxane oligomers via a reaction with the amine end-groups. The anhydride-capped siloxanes display enhanced solubility in the co-solvent system.

Scheme 1. Synthetic scheme towards sPI-PDMS segmented copolymer with BDSA-Na

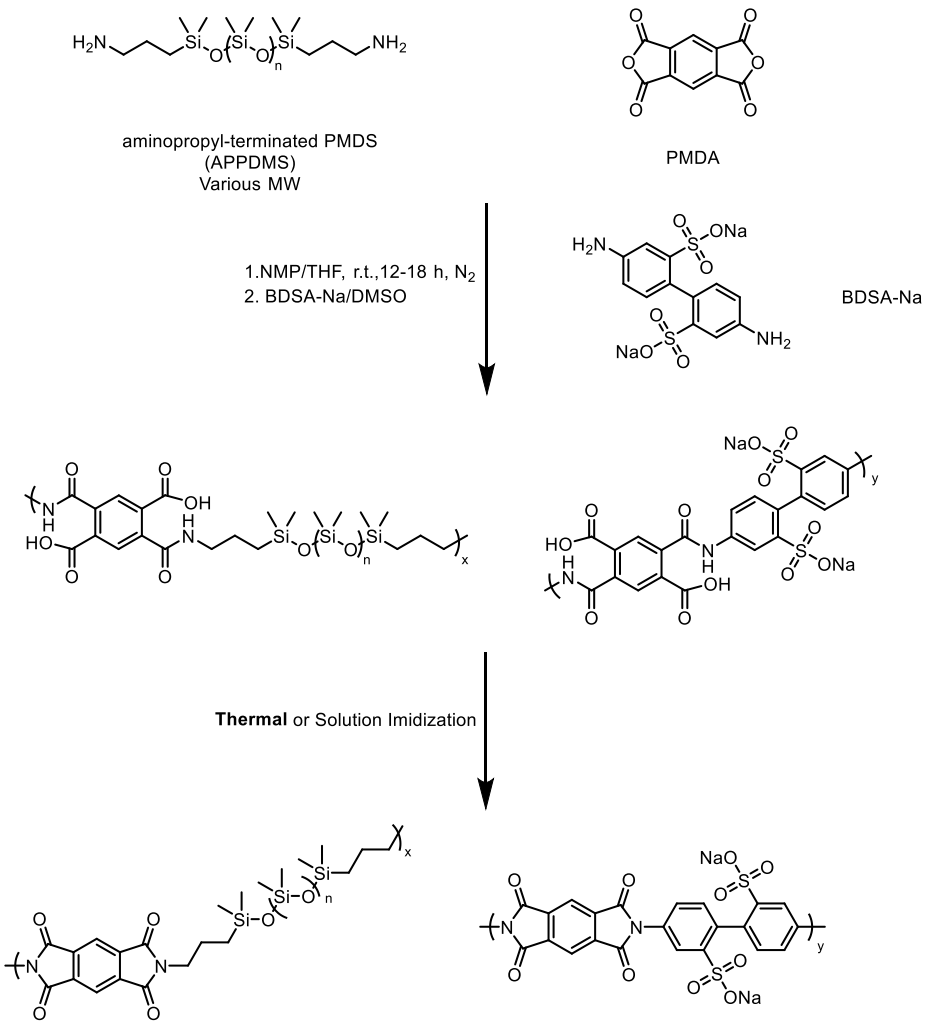

BDSA-Na was dissolved DMSO before slow addition to the free PMDA and PMDA-PDMS reaction solution. Despite increased solubility of the PMDA-PDMS oligomers in mixed solvent

systems (even with added DMSO on a small scale), the solution turned very cloudy/oily as the BDSA-Na/DMSO solution was added, indicating the immiscibility between the two components. To balance this, additional amounts of THF or NMP were added to the mixture, but this resulted in the precipitation of BDSA-Na from the solution. The main problem, in this case, amounts to the solubility of the BDSA-Na. BDSA-Na is only fully soluble in DMSO and water; it is minimally tolerant to mixed solvent systems like those here, but the balance is quite fragile. While many solvent ratios and methods of monomer addition, the results were unsuccessful. Many sulfonated polyimide-siloxanes have been synthesized, most traditionally using *m*-cresol as a solvent for the sulfonated diamine (BDSA), but BDSA-Na is also not soluble in this harsh organic solvent.

Synthesis of sPAA-PDMS using BDSA-MTPP monomer

In light of the immense solubility issues posed in the first method, the use of BDSA-MTPP allowed for adjustment of the synthetic route (**Scheme 2**). The increased non-polarity of BDSA-MTPP allows for dissolution in NMP, permitting the more efficient use of the THF/NMP co-solvent system while maintaining that the resulting polymer remains sulfonated with a moiety that shows promise for fire suppression. atPDMS, charged for 20 wt% incorporation, was treated as described above, with the addition of PDMA first followed by slow addition of BDSA-MTPP dissolved in the minimum amount of NMP. As the BDSA-MTPP was added to the free anhydride and PMDA-capped PDMS, a precipitate of what was presumably polymer formed in the seconds after addition. Subsequent careful additions of NMP restored homogeneity to the solution for the duration of the reaction. Overall, this reaction remained delicate in terms of reaction solution homogeneity; one must be cautious of extra solvent additions as this easily affected solubility of

the reagents. Many attempts failed (and continued to fail) to achieve homogeneity for the reaction duration.

Scheme 2. Synthetic route to sPAA-PDMS using BDSA-MTPP monomer

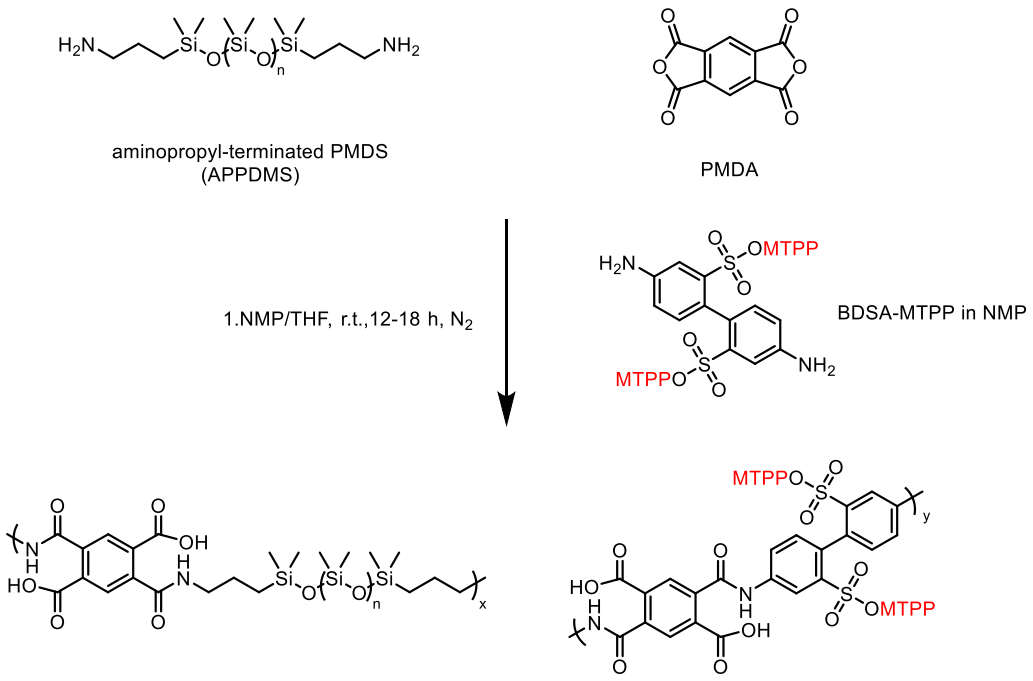

Following the successful reaction, isolated sPAA-PDMS afforded ^{1}H NMR analysis (**Figure 1**). The proton signals of the PDMS repeat unit appeared around 0.1 ppm, while the deshielded aromatic protons appear downfield between 8.5-7.25 ppm. Within this range were also the aromatic proton signals corresponding to phenyl groups of the methyltriphenylphosphonium cation. The methyl group of the MTPP appears at 3.2 ppm, and the PDMS propyl group proton appeared between 3.6-0.5 ppm, although in this case, the protons directly adjacent to the Si atom were difficult to discern.

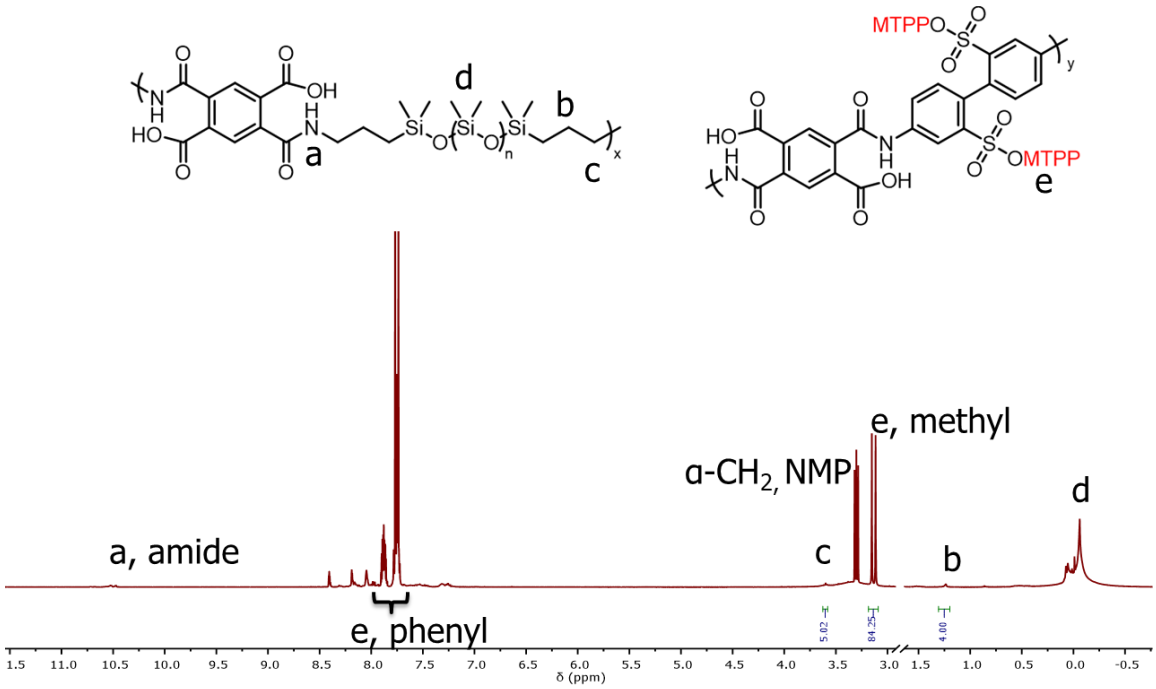

Figure 1. [1]H NMR spectrum of segmented sPI-PDMS copolymer with BDSA-MTPP (DMSO-d_6, 400 MHz)

[1]H NMR analysis also enabled weight percent PDMS incorporation into the sPI. The molecular weights of the PDMS block (calculated via [1]H NMR in **Figure S1**) and the polyimide block as well the peak areas and numbers of corresponding protons in the aromatic region versus the propyl group of the PDMS gave the following relationships (**Equations 1** and **2**) for wt% PDMS incorporation.[24] This example was charged for 20 wt% PDMS incorporation.

$$\frac{Polyimide\ block}{PDMS\ block} = \frac{\frac{Aromatic\ H\ Peak\ Area}{\#\ H\ per\ PI\ Block}}{\frac{b-H\ Peak\ Area}{\#\ H\ per\ PDMS\ block}} = \frac{\frac{505.03}{38}}{\frac{4}{4}} = 13.29 \quad \textbf{(1)}$$

The "b" proton signal of the PDMS propyl group acted as a reference peak in this case, as the α- carbon (bonded to the nitrogen atom) proton signal, which is most commonly used, was difficult to discern. Calculation of the block ratio enabled the further calculation of wt% PDMS incorporation.

$$Wt\%\ PDMS = \frac{M_n\ PDMS}{\frac{PI\ Block}{PDMS\ Block} \times (MW\ PI\ Repeat\ Unit) + M_n\ PDMS}$$

$$= \frac{1689.49}{13.29 \times 1093 + 1689.49} \times 100\% \approx 10\%$$

(2)

This sPAA-PDMS exhibited 10 wt% PDMS incorporation while the reaction was charged for 20 wt%, indicating the need for further optimization of this reaction. The elevated solubility difficulties of using sulfonated monomers and PDMS will continue to persist, however.

The sPAA-PDMS was naturally not soluble in water, but neutralization with DMAE converted the polymer into the poly(amic acid) salt) which enabled full water solubility. This suggests that these polymers with PDMS incorporation can be made water-soluble and proof of concept for further development of polyimide-based fire suppression foam formulations.

Synthesis of BDSA-matPDMS and corresponding sPAA-PDMS

The synthesis of a novel sulfonated diamine monomer containing monoammonium-terminated PDMS (matPDMS) counterions enabled an additional pathway to "segmented" spI-PDMS copolymers (**Scheme 3**). Simply, BDSA (in excess) in methanol was titrated with a matPDMS with slight heating until solids dissolved, indicating the formation of the ammonium sulfonate salt.

Vacuum filtration removed excess, unreacted BDSA and rotary-evaporation removed methanol to give a waxy, off-white product.

Scheme 3. Synthesis of BDSA-matPDMS using mono-amino terminated PDMS

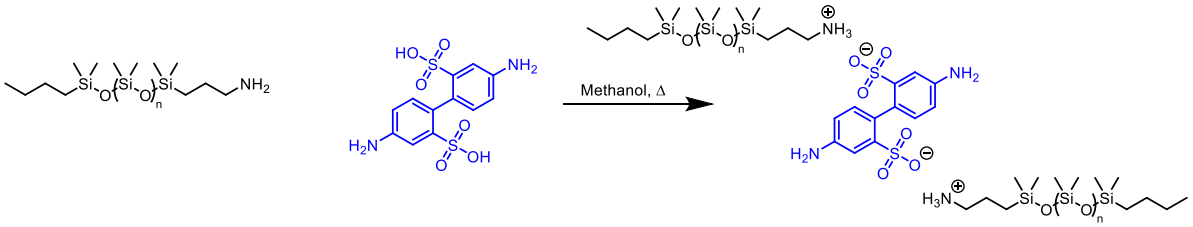

^{1}H NMR analysis assisted in structure confirmation of BDSA-matPDMS (**Figure 2**). The peaks associated with the matPDMS appear upfield, with five signals corresponding to the aminopropyl/ butyl end groups and one large peak corresponding to the backbone methyl peaks. The most deshielded protons are directly adjacent to the ammonium, appearing at 2.75 ppm, while those protons on the carbons adjacent to the Si appear at 0.5 ppm. The methyl group protons of the matPDMS butyl end group appear at 0.9 ppm. Further downfield are three peaks corresponding to the aromatic protons of the BDSA moiety. All of the peak integrations reasonably agree with the number of protons they represent. The aromatic peaks and those of the matPDMS most downfield appear quite broad. This broadness can be attributed to the less than optimal solubility in deuterated chloroform due to the vastly different polarities of the substituents. Deuterated methanol (CD_3OD) is suggested for future study.

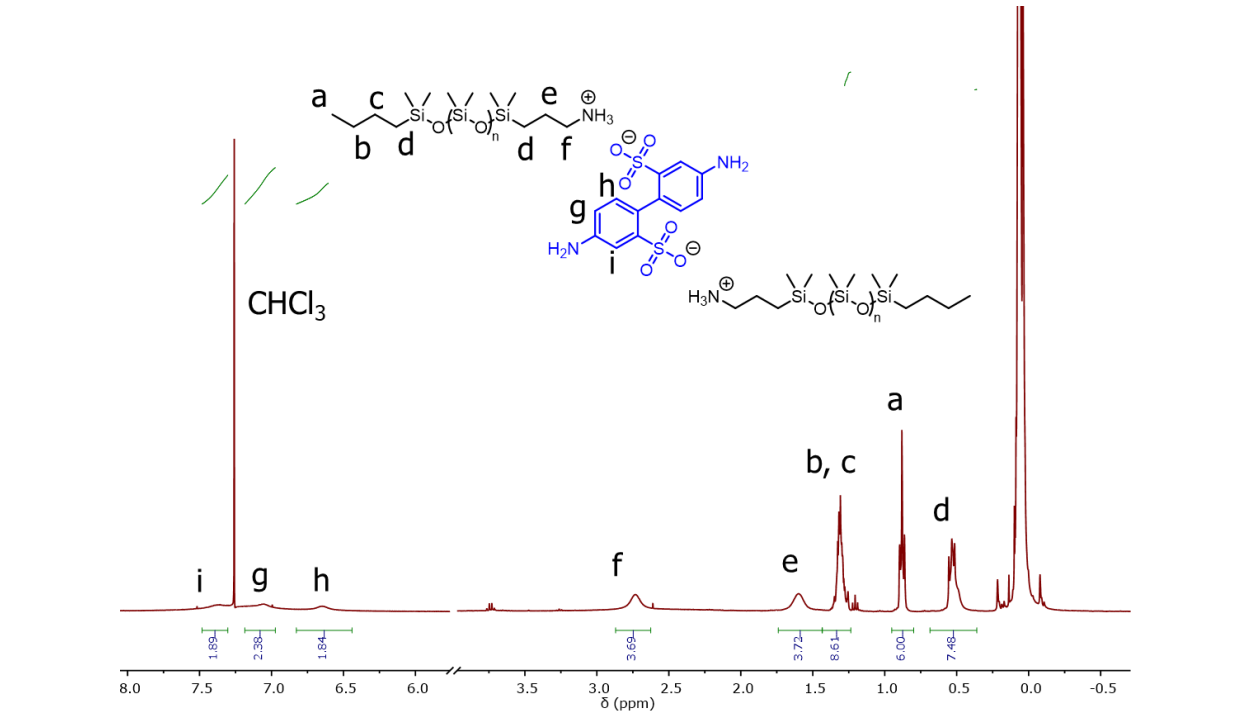

Figure 2. ^{1}H NMR spectra of BDSA-matPDMS ($CDCl_3$, 400 MHz)

As solubility optimization would be a significant barrier to overcome, BDSA-matPDMS was first copolymerized with ODA (and PMDA). **Scheme 4** shows this synthesis. Unlike most PDMS, BDSA-matPDMS seems to only be soluble in a mixture of THF: NMP (optimally 0.67:1). PMDA was added to the solution upon full dissolution of the diamines ODA and BDSA-matPDMS, charged for 10 wt% incorporation. Slight additions of THF mitigated minor reaction solution inhomogeneities within the first few minutes, after which the reaction remained homogeneous for its duration. Only very slight increases in viscosity were noticed.

Scheme 4. Synthesis of sPAA-PDMS with PMDA/ODA/BDSA-mATPDMS

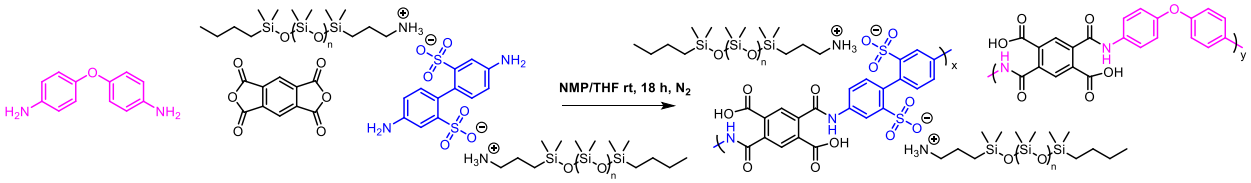

^{1}H NMR analysis again permitted the calculation of wt% siloxane incorporation. The NMR spectrum and calculations can be found in **Figure S3** and **Equation S3** in the Supporting Information. Although the reaction was charged with BDSA-matPDMS to afford 10wt% PDMS incorporation, it only achieved 3-3.5 wt% incorporation (taking into account aromatic peak overlap). In this case, low PDMS incorporation was more an attribute of lower monomer reactivity rater than solubility due to the electron-withdrawing groups (sulfonate) and bulky nature of BDSA-matPDMS.[25-26]

5.5. Conclusions

Siloxanes can greatly affect surface and solution behavior and have been successful components of aqueous firefighting foams. This preliminary study investigated the incorporation of PDMS into sPIs and sPAAs toward fire suppression foams, supplemental to our previous work. Inhibited by monomer solubility, attempts to incorporate PDMS into BDSA-Na containing polymers were unsuccessful. BDSA-MTPP, being more soluble and tolerant of the NMP/THF solvent system, enabled successful production of an sPI-PDMS segmented copolymer, although the calculated wt% PDMS incorporation was 10%. This suggested the need for further reaction and solubility optimization. Upon neutralization of the sPAA with DMAE to give an sPAAS, the polymer was fully water-soluble. An alternative route to PDMS incorporation into sPI/sPAA utilized a monoamino-terminated PDMS to neutralize BDSA, giving a novel sulfonated diamine monomer with an ionically linked PDMS moiety, BDSA-matPDMS. The BDSA-matPDMS was first copolymerized with ODA and PMDA, and though solubility posed less of an issue for this reaction, wt% PDMS incorporation was only approximately 3%. However, these minor successes

act as a proof of concept for segmented sPI-PDMS copolymers as a platform for the continued development of next-generation polymer-based surfactants for fire suppression.

5.6. References

1. Reisch, M. S. *C&EN Glob. Entep.* **2019**, *97*, 16-19.

2. Schaefer, T. H.; Dlugogorski, B. Z.; Kennedy, E. *J. Fire Safety Sci.* **2007**, *7*, 97-97.

3. Schaefer, T. H.; Dlugogorski, B. Z.; Kennedy, E. M. *Fire Technol.* **2008**, *44*, 297-309.

4. Hinnant, K. M.; Ursani, N.; Conroy, M.; Williams, B. A.; Ananth, R. Evaluating the Difference in Foam Degradation between Fluorinated and Fluorine-Free Foams for Improved Pool Fire Suppression. In *9th U.S. National Combustion Meeting, Central States Section of the Combustion Institute*, Cincinnati, OH, 2015; pp 1-10.

5. Williams, B.; Murray, T.; Butterworth, C.; Burger, Z. F., J.; Whitehurst, C.; Farley, J. Extinguishment and Burnback Tests of Fluorinated and Fluorine-Free Firefighting Foams with and without Film Formation. In *Signaling Research and Applications - A Technical Working Conference (SUPDET 2011)*, Orlando, FL, 2011; p 15.

6. Kambour, R. P.; Klopfer, H. J.; Smith, S. A. *J. Appl. Polym. Sci.* **1981**, *26*, 847-859.

7. Iji, M.; Serizawa, S. *Polym. Adv. Technol.* **1998**, *9*, 593-600.

8. Kumar, R.; Tyagi, R.; Parmar, V. S.; Samuelson, L. A.; Kumar, J.; Schoemann, A.; Westmoreland, P. R.; Watterson, A. C. *Adv. Mater.* **2004**, *16*, 1515-1520.

9. Nodera, A.; Kanai, T. *J. Appl. Polym. Sci.* **2006**, *100*, 565-575.

10. Mosurkal, R.; Tucci, V.; Samuelson, L. A.; Smith, K. D.; Westmoreland, P. R.; Parmar, V. S.; Kumar, J.; Watterson, A. C. Novel Organo-Siloxane Copolymers for Flame Retardant

Applications. In *Advances in Silicones and Silicone-Modified Materials*, American Chemical Society: 2010; Vol. 1051, pp 157-165.

11. Hill, R. M. Siloxane surfactants. In *Specialist Surfactants*, Robb, I. D., Ed. Springer Netherlands: Dordrecht, 1997; pp 143-168.

12. Yilgör, İ.; McGrath, J. E. Polysiloxane containing copolymers: A survey of recent developments. In *Polysiloxane Copolymers/Anionic Polymerization*, Springer Berlin Heidelberg: Berlin, Heidelberg, 1988; pp 1-86.

13. Bes, L.; Huan, K.; Haddleton, D. M.; Khoshdel, E. Surfactant Properties of Poly(dimethylsiloxane)-Containing Block Copolymers from Living Radical Polymerization. In *Synthesis and Properties of Silicones and Silicone-Modified Materials*, American Chemical Society: 2003; Vol. 838, pp 260-272.

14. Racles, C.; Cazacu, M.; Ioanid, A.; Vlad, A. *Macromol. Rapid. Commun.* **2008**, *29*, 1527-1531.

15. Hetzer, R. H.; Kümmerlen, F.; Wirz, K. A. I.; Blunk, D. Fire Testing a New Fluorine-Free AFFF Based on a Novel Class of Environmentally Sound High Performance Siloxane Surfactants. In *Fire Safety Science - Proceedings of the 11th International Symposium*, 2014; pp 1261–1270.

16. Hetzer, R. H.; Kummerlen, F. *SUPDET* **2016**.

17. Ananth, R.; Snow, A. W.; Hinnant, K. M.; Giles, S. L.; Farley, J. P. *Colloids Surf. A Physiochem. Eng. Asp.* **2019**, *579*, 123686.

18. Arnold, C. A.; Summers, J. D.; Chen, Y. P.; Bott, R. H.; Chen, D.; McGrath, J. E. *Polymer* **1989**, *30*, 986-995.

19. Tian, S. B.; Xu, G. *Polymer* **1995**, *36*, 1555-1558.

20. McGrath, J. E.; Dunson, D. L.; Mecham, S. J.; Hedrick, J. L. Synthesis and Characterization of Segmented Polyimide-Polyorganosiloxane Copolymers. In *Progress in Polyimide Chemistry I*, Kricheldorf, H. R., Ed. Springer Berlin Heidelberg: Berlin, Heidelberg, 1999; pp 61-105.

21. Zou, L.; Anthamatten, M. *J. Polym. Sci. A Polym. Chem.* **2007**, *45*, 3747-3758.

22. Zhang, S.; Li, J.; Huang, X.; Zhang, Y.; Zhang, Y. *Polym. J.* **2015**, *47*, 701-708.

23. Yilgör, İ.; McGrath, J. E. In *Polysiloxane containing copolymers: A survey of recent developments*, Berlin, Heidelberg, Springer Berlin Heidelberg: Berlin, Heidelberg, 1988; pp 1-86.

24. Pechar, T. W. Fabrication and Characterization of Polyimide-based Mixed Matrix Membranes for Gas Separations. Virginia Tech, 2004.

25. Hodgkin, J. H. *J. Polym. Sci. Polym. Chem. Ed.* **1976**, *14*, 409-431.

26. Ratta, V. Crystallization, Morphology, Thermal Stability and Adhesive Properties of Novel High Performance Semicrystalline Polyimides. Virginia Tech, 1999.

5.7. Supporting Information

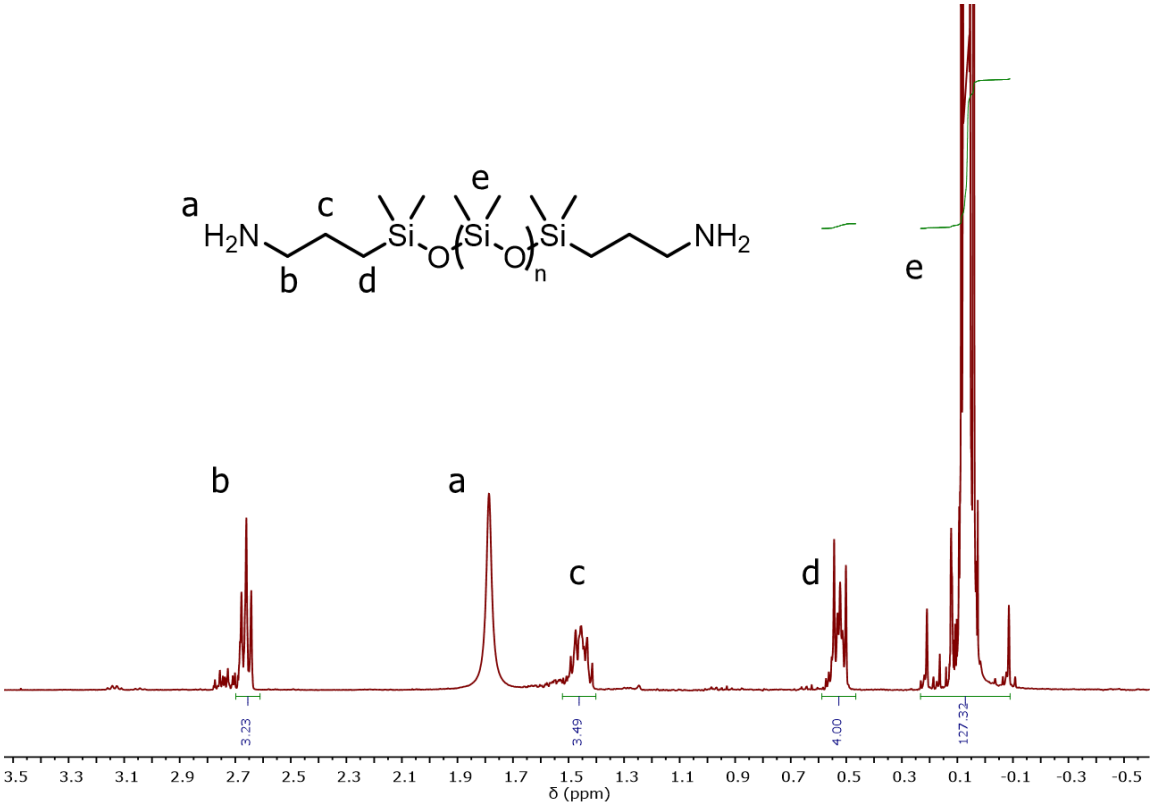

Figure S1. ^{1}H NMR of Gelest atPDMS ($CDCl_3$, 400 MHz)

Calculation of MW (M_n) atPDMS:

$$\frac{Peak\ area}{\#\ H} = \frac{127.32}{6} = 21.22$$

$$PDMS\ RU \times \frac{74.17\frac{g}{mol}}{RU} + 2(aminopropyl\ groups) =$$

$$21.22 \times 74.14 + 2(58.12) = 1689.49\ g/mol$$

(S1)

This is much larger than indicated on the manufacturer's label.

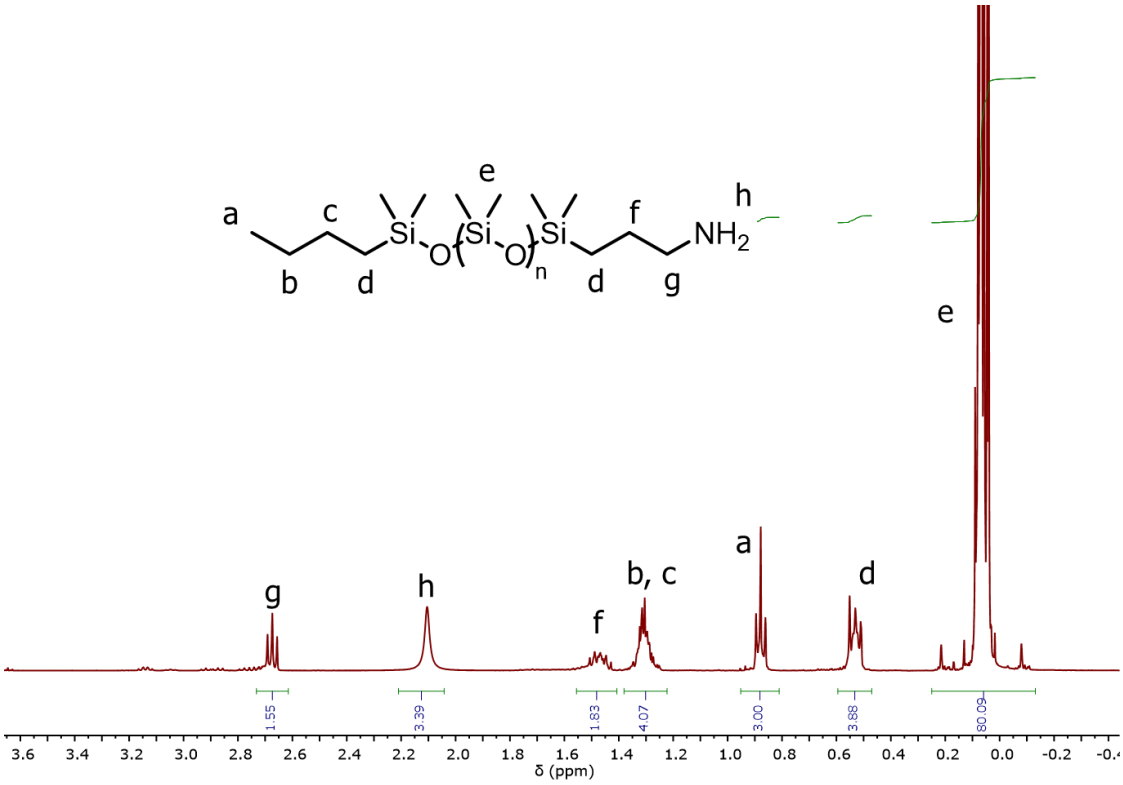

Figure S2. ^{1}H NMR of Gelest matPDMS ($CDCl_3$, 400 MHz)

Calculation of MW (M_n) matPDMS:

$$\frac{Peak\ area}{\#\ H} = \frac{80.09}{6} = 13.35$$

$$PDMS\ RU \times \frac{74.17\frac{g}{mol}}{RU} + (aminopropyl\ group + butyl\ group) =$$

$$13.35 \times 74.14 + (58.12 + 57.13) = 1105.02\ g/mol$$

(S2)

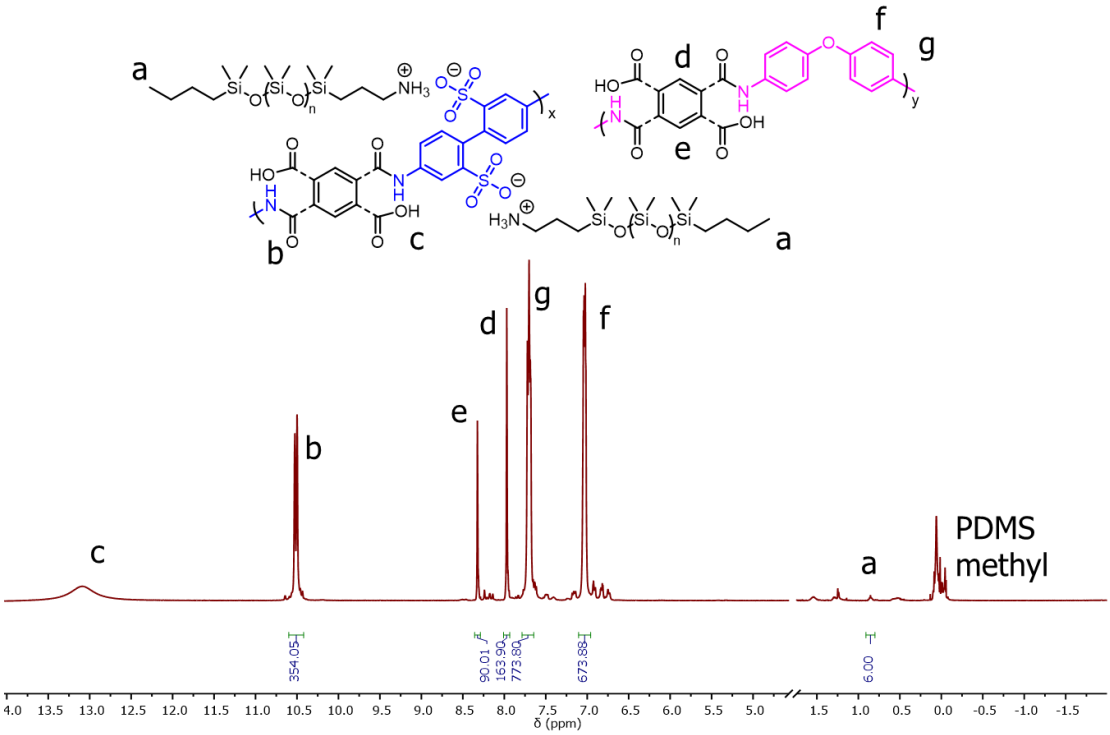

Figure S3. ^{1}H NMR of sPI-PDMS from BDSA-matPDMs/ODA (DMSO-d_6, 400 MHz)

Calculation of wt% PDMS incorporation for BDSA-matPDMS/ODA copolymer:

$$\frac{Polyimide\ block}{PDMS\ block} = \frac{\frac{Aromatic\ H\ Peak\ Area}{\#\ H\ per\ PI\ Block}}{\frac{a-H\ Peak\ Area}{\#\ H\ per\ PDMS\ block}} = \frac{\frac{1701.59}{10}}{\frac{6}{6}} = 170.16$$

$$Wt\%\ PDMS = \frac{M_n\ PDMS}{\frac{PI\ Block}{PDMS\ Block} \times (MW\ PI\ Repeat\ Unit) + M_n\ PDMS}$$

$$= \frac{2210.04}{170.16 \times 382.32 + 2210.04} \times 100\% \approx 3.3\% \quad \text{(S3)}$$

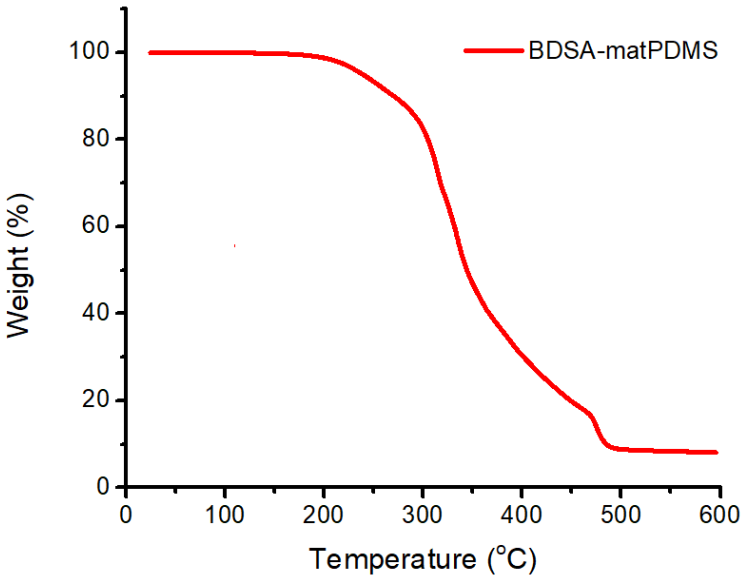

Figure S4. TGA thermogram of BDSA-matPDMS (10 °C/min ramp, N_2)

Chapter 6. Suggested Future Work

6.1. Foam solution property and structure characterization of sPI and sPAAS foam formulations

Arguably the most important aspects to the success of a fire suppression foam formulation are the foams' properties and behavior on a fuel surface. It would be greatly advantageous to systematically investigate how the preliminary formulations of sPI and sPAAS behave in their foam phase. Dynamic surface tension measurements will more adequately quantify foamability and foam stability and allow for direct comparisons between sPI and sPAAS with different surfactant concentrations. Measurement of static/equilibrium surface tension will elucidate the critical aggregation concentrations (CAC) and critical micelle concentrations (CMC), while (dynamic) interfacial tension measurements of the foam formulations on a fuel surface will inform spreading behavior and coefficients. Further systematic measurements of fuel vapor flux/ transport through foams will provide additional insight into polymer and foam structure-property relationships. All of the aforementioned characterizations can play a critical role in developing the next stages of sPI/sPAAS foams through more fundamental understanding and informed design.

6.2. Water-soluble, sulfonated polyimides and poly(amic acids) containing phosphine-oxide units for fire suppression foams

Phosphorous functionalized polymers are abundant in the flame retardant polymer literature. Researchers have studied phosphine-oxide-containing polyimides, and they are well known for their high thermal stability and flame retardant properties. Phosphine-oxides are most active and efficient in gas phase fire suppression and, as such, are prime candidates to explore in systems for liquid fuel fire suppression foams where gas-phase fire mechanisms are predominant. Phosphine-

oxide diamine monomers need to be synthesized, however, but in this way, they can also be quite modular. Incorporation of phosphine-oxide moieties into BDSA-Na based polyimides or poly(amic acid) salts through *co*-diamines (**Figure 1)** will enable their systematic evaluation as possible components of fire suppression foams. Percent incorporation will most importantly dictate water solubility. Soluble polymers will be accessed in foaming, drainage time, expansion ratio, suppression, and burnback time based on those experimental procedures developed by Jensen Hughes.

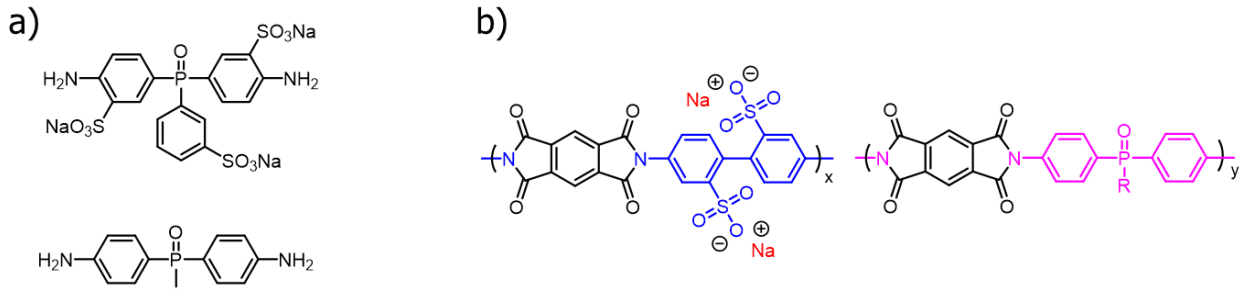

Figure 1. a) Possible variations of phosphine-oxide diamine monomers and b) structure of an sPI from BDSA-Na and phosphine-oxide monomer

6.3. Solution Rheology of water-soluble, wholly aromatic sulfonated poly(amid imide)s: bridging the gaps between polyimides and polyamides of similar nature

Recently poly(2,2'-benzidine-4,4'-disulfonyl terephthalamide) (PBDT) attracted much literature attention due to its extreme rigidity and double-helical structure brought on by strong interchain interactions, like H-bonding, pi-pi stacking, and others. Our recent studies revealed that although sPIs of similar structure are actually more flexible and less mesogenic; they still exhibit some intermolecular interactions as evidenced by solution rheology due in part to residual amide functionality. An investigation of similar poly(amide-imide)s (PAI) (**Figure 2)** would be a

fundamentally important study to elucidate their particular solution behavior and to coalesce structure-property relationships of three structural variations of the sulfonated polymer. Steady shear, continuous flow rheological experiments will determine viscosity vs. concentration scaling relationships, while polarized optical microscopy will evaluate any liquid crystalline behavior. Additionally, SANS of sPIs and sPAIs can give conformational information, complimentary to rheology. Furthermore, a systematic study of molecular weight dependence on scaling relationships would be greatly valued as the literature is not unified in this regard for polyelectrolytes.

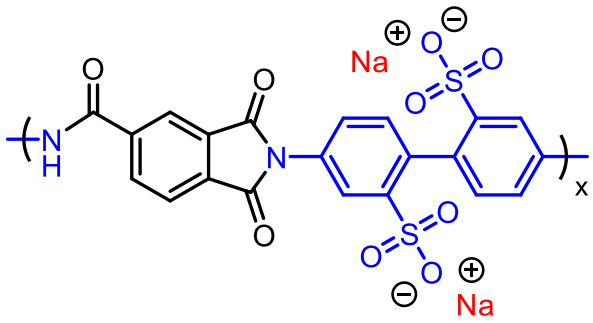

Figure 2. Structure of sulfonated poly(amide-imide)

6.4. Characterization of flame retardant properties of PMDA-ODA with BDSA-MTPP incorporation

Previous work in Chapter 4 explored thermal and physical properties of polyimides (PMDA-ODA) containing MTPP moieties via incorporation of a sulfonated diamine monomer, BDSA-MTPP. Phosphonium sulfonate moieties are expected to enhance the flame retardant properties of polymers. Polyimides containing less than 75 mol% BDSA-MTPP formed quite robust films and exhibited competitive thermal stability, with $T_{d,5\%}$ values of around 400 °C. These polymers also displayed higher residual weights than PMDA-ODA under both nitrogen and air atmosphere at

1000 °C. A systematic study of fire properties across compositions will enable quantification of flame retardant performance and comparison to other systems in the literature, like those described in Chapter 1. Limiting oxygen index, UL-94, and cone calorimetry experiments will give critical information on combustion, flammability and dripping, and heat release rates. Py-GCMS and surface analysis (i.e., XPS, EDS) can also be valuable in determining gas phase or condensed phase mechanisms of action.